To the Graduate Council:

I am submitting herewith a thesis written by Jochen Hurlebaus entitled "An Individual Based Model for Phytoplankton Assemblages with Application to *Skeletonema Costatum*". I have examined the final copy of this thesis for form and content and recommend that it be accepted in partial fulfillment of the requirements for the degree of Master of Science, with a major in Mathematics.

Thomas G. Hallam, Major Professor

We have read this thesis and recommend its acceptance:

Louis J. Gross

Mark Kot

Walker O. Smith, Jr.

Accepted for the Council:

Associate Vice Chancellor and

Dean of The Graduate School

AN INDIVIDUAL-BASED MODEL FOR PHYTOPLANKTON ASSEMBLAGES WITH APPLICATION TO *SKELETONEMA COSTATUM*

A Thesis

Presented for the

Master of Science

Degree

The University of Tennessee, Knoxville

Jochen Hurlebaus

August 1997

Dedication

This thesis is dedicated to my parents

Mr. Klaus Hurlebaus

and

Mrs. Gisela Hurlebaus

who gave me all imaginable opportunities for my education.

Acknowledgements

I thank Prof. Thomas G. Hallam and Prof. Walker O. Smith Jr. for their support of my work, as well as Prof. Louis J. Gross and Prof. Mark Kot, who were part of my committee. Special thanks go also to Prof. Suzanne Lenhardt who introduced me to the program in Mathematical Ecology and helped me with my application as a foreign graduate student at the University of Tennessee. Of great help were always the people working in the mathematics departmental office with their superior knowledge and friendliness.

I also want to mention here the Center of International Education and the International House staff that helped me with many formal and informal things that were new for me as a foreigner.

I also thank the Federal Republic of Germany for providing funding for my study for the first six months as well as travel expenses, and the Department of Mathematics for providing a teaching assistantship for me.

Abstract

In this study a mathematical model for phytoplankton assemblages is developed. A detailed physiological model on the individual cell level focuses on nutrient and energy flows in the system. Flows of nutrients, production of storage, and growth are modeled independently. This allows uncoupled dynamics of storage and structure pools in a cell. A population of zooplankton grazing on the phytoplankton cells is part of the model. Grazing and sinking determine the losses of phytoplankton cells. Euler's and Runge-Kutta's Method for numerical solutions of systems of ordinary differential equations were implemented in a computer code written in C. The code was used to perform simulations of a population of the diatom *Skeletonema costatum* under various environmental conditions. Simulations were usually performed for 5-25 days in a homogeneous environment with equally distributed cells. Additional simulations included two species simulations to investigate species competition and dominance. Dynamical behavior of the system showed realistic patterns. Growth of cells was either limited through nutrient or energy shortage. The uncoupling of storage and structure production resulted in changes in cell composition, and allowed to detect indirect effects of nutrient or energy limitations. In simulations of two competing species the model showed effects of cell growth and composition that cannot be explained with less detailed models.

Contents

List of Figures

List of Tables

1 Introduction

Nearly all of the primary production in the ocean is performed by phytoplankton assemblages. Composition of these assemblages can vary in many aspects such as number and population size of different species, total density, and growth rate. Dynamic behavior of these phytoplankton assemblages is a result of many factors including changes in temperature, light availability, and nutrient concentrations as well as the abundance of zooplankton.

A complete description of a dynamic phytoplankton community via a mathematical model is complex or may even be impossible. The model introduced in this thesis focuses on what are considered to be the most influential factors for species development. The individual based community model represents inhomogeneous populations of different species. Computer simulations are used with the goal to find an explanation of some of the dynamics in phytoplankton assemblages over a short time period.

1.1 Structure

This thesis is divided into 7 chapters. Chapter 3 to 7 contain the mathematical model and results, as well as a discussion and conclusions. Chapter 2 is a review of phytoplankton ecology. Readers with sufficient background in marine biology might skip Chapter 2, whereas for others Chapter 2 will help to understand the structure of the model. Appendix A shows

an alternative population model. Appendix B and C contain summaries of the parameters, variables, and equations used in the model.

1.2 Literature

As usual literature is cited in the text were used. However, I want to mention some books that helped me throughout my work:

- Falkowski and Woodhead's *Primary Production and Biogeochemical Cycles in the Sea* [15] is an excellent collection of recent articles.
- Kirk's *Light & Photosynthesis in Aquatic Ecosystems* [25] gives a detailed description of the photosynthetic processes in the water.
- S.A.L.M. Kooijman's book [29] *Dynamic Energy Budgets in Biological Systems* helped especially for the individual model and for energy considerations.
- Lalli and Parson's *Biological Oceanography: An Introduction* [32].

2 Phytoplankton Ecology and Model Design

This chapter is a summary of the phytoplankton ecology needed for construction of a mathematical model. More details can be found, for example, in *Algal Physiology and Biochemistry* [45], Barker [3], Falkowski and Woodhead [15], Kirk [25], Krogmann and Powers [30], Lalli and Parsons [32], and Round [43].

2.1 History of Marine Biology

The first evidence of human interest in marine biology is probably that of Aristotle who catalogued 180 marine animal species in the fourth century B.C. This might have been the beginning of oceanic research, which cover 70% of the earth's surface. After crossing the oceans became possible, interest and knowledge in their biology increased rapidly. Many expeditions in the 19th century had significant impacts on the understanding of marine ecosystems. These expeditions continued into the 20th century and continue today, still adding significant new knowledge or replacing older assumptions and theories with newer ones. New methods for the measurement of chemical compounds and improved optical instruments like electron microscopes helped to find more accurate information about physiological details of marine animals and plants. However, many questions remain to be solved. Mathematical models for the simulation of phytoplankton assemblages, which make use of computer-technology of increasing quality and quantity, have become an important part of

the research in marine biology.

The model in this thesis follows an individual-based approach to simulate phytoplankton growth. Individual-based models are qualitatively different from aggregated population models because they allow the simulation of nonhomogeneous populations and a detailed description of the individual on a physiological basis.

2.2 Phytoplankton

Phytoplankton is the collective expression for various types of unicellular algae that compose the major part of the autotrophic organisms in the ocean. The size of phytoplankton cells varies from 0.5 to 200μm. The model focuses on autotrophic species common in many places of the world (e.g. diatoms, coccolithophorids and dinoflagellates). An autotrophic cell builds organic material and obtains all energy from photosynthesis. The intent has been to include the most important environmental and physiological factors influencing species development.

Figure 2.1 shows the basic pathways of nutrients and energy between cell and environment. Figure 2.2 shows the underlying structure of the mathematical model.

2.3 Abiotic and Biotic Environment

Physical and chemical constraints of the environment on autotrophic cells include light, temperature, and currents. Biotic constraints are the speed of reactions and processes in the cell such as cell-growth or reproduction. These constraints determine the growth dy-

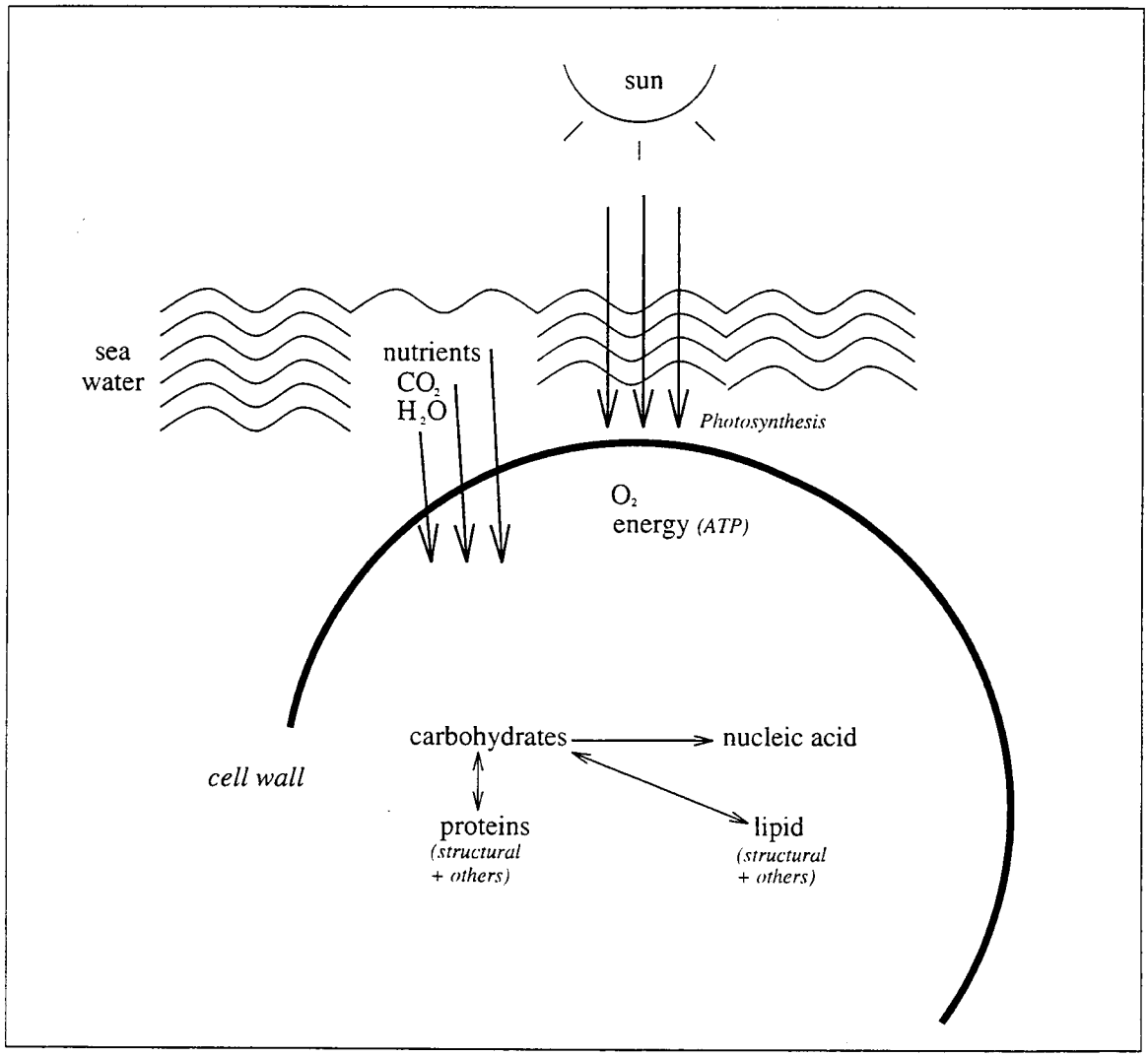

Figure 2.1: Major pathways of autotrophic unicellular algae.

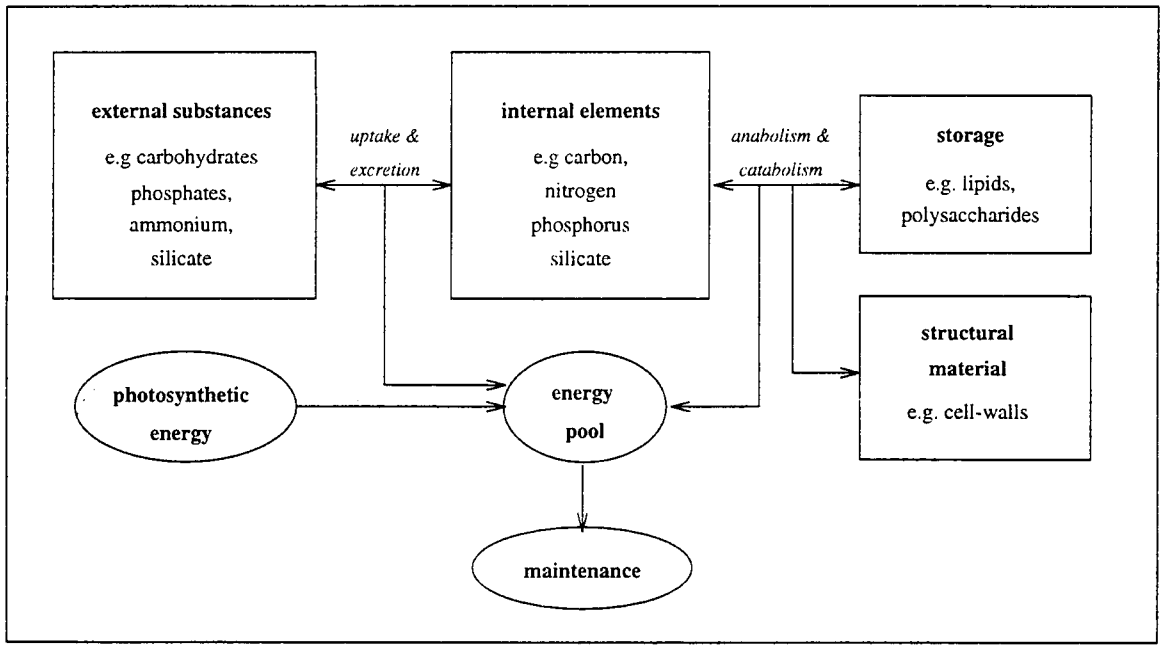

Figure 2.2: Underlying structure of the mathematical model.

namics of populations.

Two kinds of growth dynamics are distinguished for algal cells. Figure 2.3 shows the growth-rates of a cell population. On the left hand side of the graph, the population growth rate is high. After the population grows at this high rate r for a certain time, abiotic constraints will become growth limiting and, finally, the growth rate will approach zero and the population density will reach the carrying capacity K. This zero growth situation with the population at a carrying capacity is called K-selected. r-selected species are usually found in fast changing environments (changing temperature, irradiance, nutrient concentrations etc.) whereas K-selected species life-histories occur under predictable, stable environmental conditions. Therefore, K-selection occurs in tropical waters, especially where temperature,

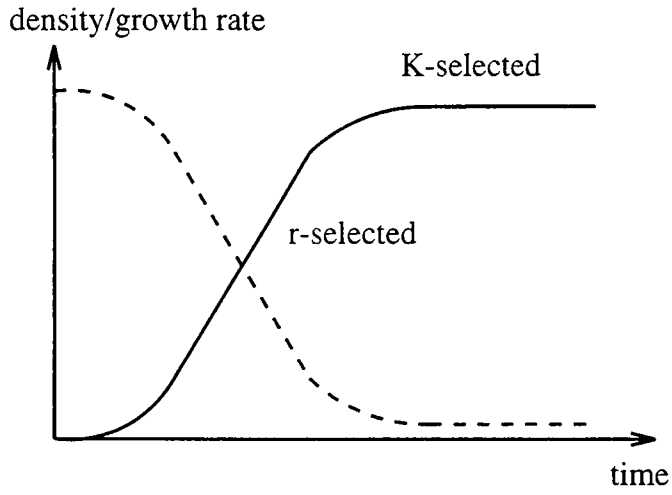

Figure 2.3: The two different growth dynamics of phytoplankton assemblages. Solid line: population density. Dashed line: growth rate.

nutrient-concentrations and irradiance are relatively constant. In contrast, in polar regions, these abiotic factors change significantly over time. As a result, in tropical oceanic waters the total population size of phytoplankton is usually rather constant over the year. In temperate latitudes, a spring and an autumn bloom usually occur, whereas in polar regions only a single summer bloom of phytoplankton is likely. However, r-selected life-histories can also be found in coastal waters of the tropics under appropriate environmental conditions.

2.4 Abiotic Constraints

2.4.1 Irradiance

Photosynthesis is the major energy source of the cell for autotrophic species. Irradiance and efficiency of light capture depend on various abiotic and biotic factors. In order to estimate the available internal energy of a cell due to photosynthesis, it is necessary to model these processes as accurately as possible. For simulations of an existing ecosystem, a combination with a meteorological and geographical database is necessary in order to obtain realistic results. Some factors influencing irradiance are discussed here.

Irradiance

- Seasonality: In tropical regions irradiance does not vary significantly over the year. However, temperate regions in winter have a significantly lower irradiance which decreases to zero as the pole is approached. In summer in polar regions 24 hour photoperiods occur, but from 20° to 0°, the surface reflection in calm water ranges from 10% to 100% (Kirk [25]) because the angle of the incoming light is small if measured relative to the surface of the water.
- Meteorological factors: Irradiance during sunny and partly cloudy days is not very different. On overcast days, irradiance can be reduced by more than 50% (Kirk [25]). Wind produces waves that are able to decrease or increase reflection especially at low solar altitude.
- Light spectrum: Light of different wavelengths is supplied in different quantities. If an estimation of photosynthesis is desired, it is helpful to measure irradiance in quanta per

$(m^2\ s\ nm)$. Pigment composition of the cell determines the probability of capturing a quantum of a specific wavelength.

- Absorption: Irradiance on the surface of the water is often measured in experiments. Absorption in the water plays a major role reducing irradiance for cells at greater depths by increasing amounts. Absorption is influenced by the presence of dissolved organic matter, phytoplankton density and composition, particulate organic detritus and amount of inorganic particles (Kirk [26, p.12]). Absorption processes are rather complicated and even the measurement of irradiance at a certain depth of the water is problematic. Kirk provides a detailed description of the absorption [25].

  A description of the complex irradiance-function with all its dependencies is far beyond the scope of this thesis. A mathematical approximation of the underwater field is possible only if parameter values for a specific area are available (Kirk [26, p.22]). Measurements provide an easier approach and data are available for many areas under various conditions.

The most constant and predictable irradiance conditions can surely be expected in laboratory-experiments. Duration of day and night periods as well as intensity, angle, and wavelength can be fixed. This provides good conditions for parameter estimations.

2.4.2 Seawater

Water composition around a phytoplankton cell influences the cell development. The major elements found in sea-water are present in ionic form. The ten major constituents (Chloride, Sodium, Sulphate, Magnesium, Calcium, Potassium, Bicarbonate, Bromide, Borate and Strontium) make up about 99.9% of all dissolved substances (Lalli and Parsons [32, p.32]),

and these concentrations are almost constant over time. Therefore, the composition of seawater is constant (with a few exceptions like estuaries). Concentrations of nutrients and other substances that are far more important for phytoplankton growth may vary rapidly over time, but their total concentration remains low compared to other ionic components. Therefore, nutrient concentrations do not influence the chemistry of the sea-water but are important for phytoplankton growth.

Temperature of sea-water depends on irradiance, season (especially in temperate and polar latitudes), and inflow (rivers). Temperature may also change due to upwelling, currents, or mixing. In general, temperature changes are slow over time compared to the dynamics of phytoplankton cells, which allows temperature to be considered as a constant parameter for short term simulations of phytoplankton growth.

2.5 Biotic Constraints

Biotic constraints determine the speed of the chemical and biological processes, including photosynthetic efficiency, speed of nutrient uptake, and speed of biosynthesis of storage and structural materials.

2.5.1 Photosynthesis

It is well-known that photosynthesis increases with increasing irradiance until it reaches some P_{max} and then decreases during photoinhibition. The light-photosynthesis relation under abundant nutrient conditions is shown in Figure 2.4. P_{max} is the maximum photosynthetic rate, E_d the irradiance, and E_k the irradiance where the line of initial photosynthetic

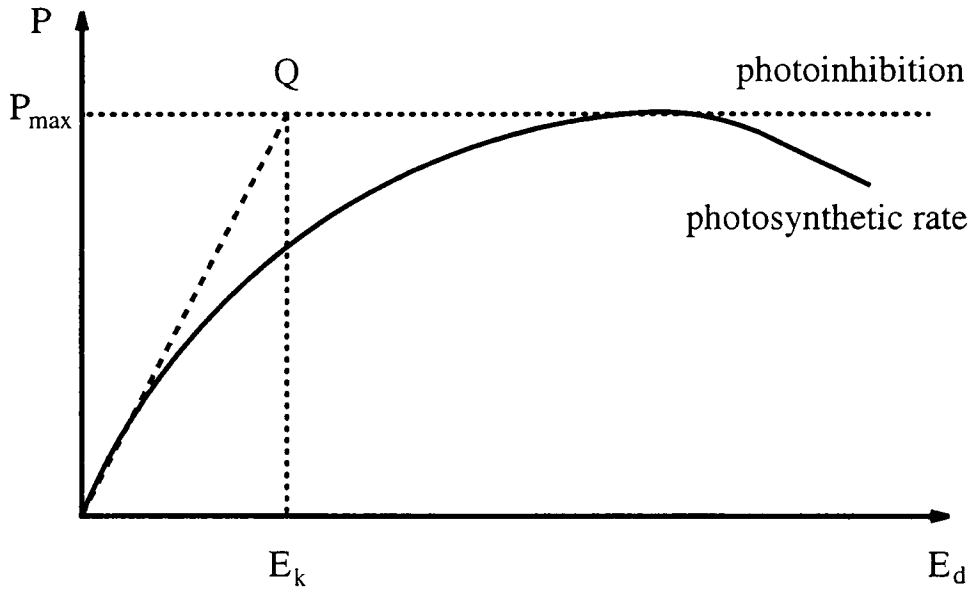

Figure 2.4: Photosynthesis as a function of irradiance: qualitative behavior under nutrient abundant conditions (arbitrary units). Q is the point where the line of initial photosynthetic increase intersects the maximum photosynthetic line.

increase intersects the maximum photosynthetic line.

The chemical process of photosynthesis is called the reductive pentose cycle and is considered to be the principal path of CO_2 fixation in algae. The major energy currency in cells is adenosine 5'-triphosphate (ATP). The overall equation for photosynthesis is

$$CO_2 + 2H_2O \xrightarrow{8\,h\nu} (CH_2O) + H_2O + O_2$$

The complete process of photosynthesis and carbon incorporation can be divided into the light reactions and the dark reactions.

The Light Reactions

The processes of light absorption in photosynthesis are called the light reactions of photosynthesis. In eucaryotes and cyanobacteria there are accessory pigments for light absorption:

- Chlorophyll a is ubiquitous to aerobic photosynthesis and can be found in all species.
- Carotenoids are a major component in diatoms.
- Phycobilins absorb a large fraction of the irradiance in cyanobacteria where chlorophyll b is not present. Different kinds of phycobilins can be found in different species.

The pigments are located on so called antennas. The purpose of the antennas is to catch as much light quanta as possible by increasing the effective cross-sectional absorption.

Eucaryotic cells have two kinds of antennas with pigments:

- Photosystem I: absorbs longer wavelength light ($\geq$ 680 nm)
- Photosystem II: absorbs shorter wavelength light ($\leq$ 680 nm)

Photosystem I can operate independently in cyclic photophosphorylation whereas Photosystem II can only operate in combination with Photosystem I in the noncyclic photophosphorylation. During the noncyclic photophosphorylation $NADP^+$ is reduced to NADPH and therefore has to be available in order for Photosystem II to be active.

During the light reactions electrons are transported from H_2O to $NADP^+$ using light energy and from NADPH to O_2 which results in the production of energy in form of ATP.

The basic reaction for ATP production during photosynthesis is:

$$NADP + H_2O \longrightarrow \frac{1}{2}O_2 + NADPH_2 \tag{2.1}$$

This reaction requires 4 photons and results in the production of 2 ATP from ADP and elementary phosphorus.

The Dark Reactions

In the dark reactions three ATP and two $NADPH_2$ are used to reduce one CO_2 and use it to synthesize carbohydrate:

$$CO_2 + 2\,NADPH_2 \rightarrow (CH_2O) + H_2O + 2\,NADP \tag{2.2}$$

ATP is oxydized into ADP and elementary phosphorus.

Because in the dark reactions energy is needed for incorporation of CO_2 it takes 10-12 quanta of light energy to reduce and incorporate one molecule of CO_2 and produce 2 ATP.

Efficiency of Photosynthesis

If a model for autotroph unicellular algae including irradiance dependency is constructed, the efficiency of photosynthesis is a crucial parameter. As mentioned above, the chemical reactions involved in photosynthesis allow the calculation of a theoretical yield in number

of ATP per quanta of light. However, the cycle does not operate with 100% efficiency.

The efficiency of photosynthesis is frequently measured in production of O_2 per quantum. The reduction of one mole of CO_2 to carbohydrate with concomitant O_2 formation requires about 112 kilocalories. One Einstein (= mole) of red light contains about 42 kilocalories. This would imply minimum required energy of 2.7 quanta red light per molecule of CO_2 or O_2 (Vennesland [47]).

Equations 2.1 and 2.2 implement a need of 10-12 quanta of light energy for reduction plus incorporation of one molecule of CO_2. The net gain in this calculation is 2 ATP (Prescott et al [41, page 166]). These theoretical values are neither achieved in experiments nor confirmed from measurements in the field, because light capturing by cells is influenced by other factors:

Cross-sections of photosynthesis: Functional or optical cross-sections of phytoplankton photosynthesis is measured in dimensions of area per unit of compound. It is a measure of the probability that light harvesting systems absorb light. If the pigments are extracted from the cell, they show a higher light-absorption probability than if the pigments are part of a cell (Dubinsky [13, p.31]). Measurements therefore have to be done with intact phytoplankton cells.

The cross-section of a cell is not constant over time. During low irradiance, chlorophyll a concentrations were found to increase which cause a decrease of the cross section due to shading between the light-harvesting entities in the interior of the cell (Dubinsky [13, p.35]). During nutrient limitation (especially nitrogen) the cell may not be able to produce chlorophyll a or other pigments. This increases the cross section which decreases limitation of photosynthesis due to nutrient depletion. Shape and size of cells are other influences on

the cross-section. Quantum yield of photosynthesis can be estimated if the cross-section is known.

An estimation of photosynthesis from irradiance and concentration of nutrients (nitrogen, phosphorus and iron) is achieved for this model. It is now generally accepted that the yield of the reaction for oxygen evolution is $0.125\frac{O_2}{\text{quanta}}$ (Falkowski [14, p.54]). This maximum value for the reaction (P_{max} in Figure 2.5 on page 11) is then influenced by the cross-section and nutrient availability. Figure 2.5 shows an observation made for the dependency of P_{max} on the nitrogen availability for three different species of phytoplankton (Experiments by Kolber et al [27]).

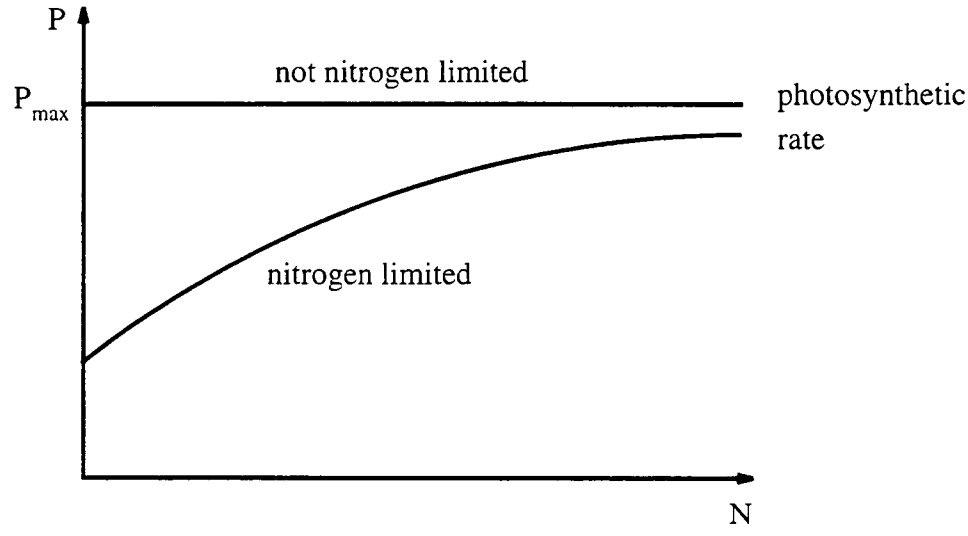

Figure 2.5: Nitrogen dependence of photosynthesis (arbitrary units).

P_{max} can also be calculated as the ratio of concentration of photosynthetic units to their turnover time. This relatively new approach seems to yield a more accurate estimation of P_{max}. However, few experiments have as yet been completed (Falkowski [14][p.61]).

2.6 Structure and Storage

Dependent on abiotic and biotic constraints, phytoplankton cells incorporate storage and structural materials. The common understanding is that during light periods phytoplankton cells produce storage and structural materials if nutrients and energy are sufficient. During dark periods some of the storage can be metabolized during respiration (CO_2 production) which results in energy production (see Section 2.7 Respiration). This energy is used for maintenance and production of structure in dark periods.

Carbohydrates are some of the most common molecules found in different parts of the cell such as cell walls and storage pools. Lipids are considered in the model as storage materials, and proteins as structural materials.

2.6.1 Carbohydrates

Carbohydrates play functional and structural roles and can be found in almost all parts of the cell. Carbohydrates include a huge variety of molecules of very different molecular weights (from less than 100 to over 1 million). The two basic forms are distinguished:

- monosaccharides: 3-9 carbons, at least one group from carbonyl function.

- polysaccharides: condensation of smaller carbohydrates (monosaccharides) through acetal linkages.

Basic constituents of carbohydrates are carbon, hydrogen and oxygen as well as phosphorus, sulfur and nitrogen.

Different kinds of carbohydrates are of importance for the cell:

- Structural materials: polymeric carbohydrates are the major components of the cell-walls, complex carbohydrates are found in membranes and nucleic acids.
- Energy utilization: simpler carbohydrates are utilized for energy production in the cell.
- Source of components: monocarbohydrate constituents are synthesized because they are components of many of the cofactors required in metabolic processes.
- Reserve materials: carbohydrates are synthesized as reserve materials and provide the cell with energy if needed. Sugars, starch and glucan are the most commonly used reserve carbohydrates.

Autotrophic cells derive their carbon mainly from photosynthesis. Additionally, uptake and breakdown of more complex carbohydrates may result in energy gain and may also influence the nitrogen and phosphorus interior nutrient pools. Utilization of these molecules depends on the species and environmental conditions. For most species and conditions, however, the additional energy gain is not significant.

2.6.2 Energy Pathways

The following pathways are important for breakdown of polysaccharides and lipids and, therefore, are important especially during respiration in the dark. They are also part of the uptake path of carbohydrates which plays, however, a minor role in most phytoplankton species.

Reserve polymers such as glucose, glycogen, starch, poly-β-hydroxybutrate are anabolized and catabolized. Lipids and proteins are also catabolized for energy production. Catabolism of these substances is mainly through the following pathways that are the most important processes for energy generation from storage materials in the cell.

- Glycolytic Pathway or Embden-Meyerhof Pathway: This way of glucose breakdown (Glycolysis) is very important for energy production. It is the most common way of conversion of hexoses to pyruvate. The so called substrate-level phosphorylation consists of two parts. In part one, ATP is consumed to break down glucose to Fructose 1,6 - biphosphate. In part two, ATP is produced during the breakdown of 1,6-biphosphate to pyruvate. The overall reaction for the process is

  $$\text{Glucose} + 2\ \text{ADP} + 2\ \text{P}_i + 2\ \text{NAD}^+ \rightarrow 2\ \text{Pyruvate} + 2\ \text{ATP} + 2\ \text{NADH} + 2\ \text{H}^+$$

  so that the total energy production from one glucose molecule is two ATP for the conversion to pyruvate.

- The pentose phosphate or hexose monophosphate pathway: This pathway is important not only for ATP production but also for NADPH production as source of electrons for reduction of molecules during biosynthesis and as source of products used to synthesize aromatic acids, nucleic acids and in photosynthesis. It is more often of greater

importance in biosynthesis than as an energy source. The total reaction is

$$\text{Glucose 6-Phosphate} + 12\ NADP^+ + 7\ H_2O \rightarrow 6\ CO_2 + 12\ NADPH + 12\ H^+ + P_i$$

- Pyruvate produced during glucose breakdown enters the so called TCA cycle for further breakdown and energy production. This cycle transforms pyruvate to CO_2 aerobically. It is the second stage of glucose catabolism. The TCA cycle however is also of importance for the catabolism of other carbohydrates as well as lipids and amino acids. During the catabolic process of these materials an intermediate product of the cycle (acetylcoenzyme A; acetyl-CoA) arises that can enter the TCA cycle. The cycle provides energy and produces carbon skeletons for use in biosynthesis.

  For glucose the glycolytic pathway and the TCA cycle produce four ATP for each glucose molecule oxidized to CO_2.

- The Electron Transport Chain is yet another step of catabolism of glucose or reserve materials. The process yields considerable more energy than the first two steps of glucose breakdown.

  During the process electrons are transferred from donors (NADH, $FADH_2$) to acceptors (O_2) and eventually O_2 and H^+ are combined to H_2O. When a pair of electrons passes from NADH to a atom of O_2, three ATP are synthesized whereas if the two electrons come from $FADH_2$ only two ATP are produced. These are maximum ATP yields for ideal conditions.

2.6.3 Glucans

Glucans are frequently used as storage materials. The amount of starch in algae is generally under 3% of the dry weight. However, under 'abnormal' conditions such as nutrient limitation the amount can be much larger.

Constitution and structure: Complete acid or enzymatic hydrolysis of $(1 \rightarrow 4)$-α-D-Glucan produces in most cases glucose. The glucose can then enter the catabolic pathway for glucose. $(1 \rightarrow 3)$-β-D-Glucan is found in many algae. For the diatom *Skeletonema costatum* it was shown to be a storage polysaccharide. In coccolithophoridae a complex heteropolysaccharide has been found. The composition of reserve glucans is species specific and therefore not discussed here.

2.6.4 Lipids

Lipid is taken up by some species but is more frequently synthesized in the cell as a storage material. Triglycerides or triacylglycerols, esters of glycerol and fatty acids, are common lipids used as energy sources.

Details about lipid synthesis and catabolism are omitted. Catabolism of lipids involves some of the processes mentioned above. Only composition and metabolic energy costs of lipids are considered to be of importance for the storage and growth dynamics of the cells.

2.6.5 Proteins

Proteins are important parts of all autotrophic cells. They are considered to be structural materials; however, when energy is needed, some proteins can be catabolized. Proteins are polymers of amino acids joined by peptide (amide) bonds. Peptides normally are referred to as amino acids with lower molecular weights whereas polypeptides or proteins are huge polymers of many amino acids. A table of amino acids occurring in proteins can be found e.g. in Barker [3, p.56]. The average protein of biochemical interest is usually an albumin

or a globulin (Barker [3, p.126]). Catabolism of proteins also involves some of the processes mentioned above. The composition of proteins and other structural materials is addressed in the section about certain species.

2.7 Respiration

As already discussed, respiration, the metabolism of storage materials, is an important process in phytoplankton cells. This section explains what determines the need and amount of respiration. During dark periods, respiration provides energy for growth, and during light periods it can provide molecules needed for anabolism. The fact that respiration also occurs during the light periods influences measurements of photosynthetic rates.

Respiration accounts for only about 10% of the photosynthetic rate under normal conditions. However, higher rates have been reported (Geider [16, p.333]). Under nutrient-limited conditions respiration can be $> 50\%$ of the photosynthetic rate.

In models respiration offers a control for phytoplankton growth. In many models not including respiration, sinking rates and grazing rates are unrealistically high in order to maintain a reasonable growth rate.

The amount of respiration depends on many factors. Often it is assumed that respiration has two components: a constant maintenance metabolic rate, and a variable rate associated with cell synthesis activities.

$$r = \mu_0 + \xi\mu$$

where μ_0 is the maintenance metabolic rate, ξ is the cost of synthesis and μ is the growth rate. Maintenance metabolic rate includes turnover of macromolecules, volume regulation and maintenance of solute gradients.

The different components of respiration are:

- Protein turnover: Protein turnover is costly. The minimum cost, based on cleavage and resynthesis, of the peptide bond is 0.25g glucose per g protein (Geider [16, p.340]). This equals 80% of the costs of protein synthesis from glucose and ammonium. Total respiration cost for turnover depend on composition of the cell.
- Cost of Biosynthesis: Biosynthesis and nutrient transport require energy. The cost of synthesis depends on the biochemical composition of the biomass and the redox state of the nitrogen source. Also the costs for synthesis of storage or structural materials is not considered to be part of maintenance but instead the needed energy is provided from the energy pool during biosynthesis.

Respiration cannot supply sufficient energy for maximum growth of cells. However, respiration is important to provide basic molecules for lipid, protein, carbohydrates and nucleic acid synthesis (Geider [16, p.341]). Respiration rates have been found to be proportional to protein synthesis or ammonium assimilation and differ for various nitrogen supplies.

One unsolved question is what happens during winter if phytoplankton cells remain in deep, cold water. Obviously no energy can be provided from the environment or from storage (over a long time period) but still the cells can survive, come to the surface in spring and grow and reproduce. What enables the near zero-maintenance state of the cell is yet unsolved.

2.7.1 Amount of Respiration

Respiration rates seem to be best estimated if the asymptotic value of respiration after prolonged darkness (20-30 hours) is measured or a plot of growth rate versus irradiance is extrapolated to $E_0 = 0$. Both approaches yield similar results. Using the latter approach, a maintenance metabolic rate of < 0.002 to 0.1 per day has been estimated (Geider [16, p.340]).

Evaluation of dark respiration: It is useful to obtain absolute rates of dark respiration in units of grams CO_2 evolved per gram cell carbon per hour. Biomass specific respiration rates range from $< 0.01h^{-1}$ to $0.005h^{-1}$. For single species, respiration is often linearly related to growth. The following relationships have been found (see Geider [16]):

- under limiting light conditions and high nutrient conditions, low growth-rates and respiration rates have been reported.
- under saturated light and limiting nutrients a direct correlation between growth rate and respiration has been found during low growth rates.
- under saturated light and limiting nutrients independence or inverse correlation between growth rate and respiration has been found during high growth rates.

Possible regulators of dark respiration are supply of substrate for glycolysis itself, transport of organic acids across mitochondrial membranes, TCA cycle and mitochondiral electron transport.

Substrate supply: Respiration depends on available substrate. Higher irradiance may yield higher respiration because more substrate is available. This has been shown by light-dark

experiments where dark respiration was dependent on light availability during the light period; saturating light conditions yielded increased respiration rates.

Skeletonema costatum (Varum et al [46]) accumulated 50% glucans (of total cellular carbon) during light period (of 6-18 hours) and 42% to 89% of these storage materials were metabolized during darkness (see also Lancelot and Mathot, 1985). Experiments by Laws et al. (1987) showed a 60% reduction in non-protein ^{14}C during darkness, 14% of which ended up in the protein fraction (Geider [16, p.351]).

Nutrient Status: Source of nitrogen influenced respiration in many cases. In nitrogen limited cultures, supply of nitrate or ammonium increased the respiration rate. It is not clear if this is an indirect effect because more nitrogen increases the substrate levels and therefore respiration.

Glycolysis, oxidative pentose phophate pathway, and TCA cycle are essential biosynthetic pathways leading to lipids, proteins, and nucleic acids. An estimated 0.1-0.15 carbon atoms are lost as CO_2 per unit carbon incorporated from glucose into cell material from essential biosynthetic reactions involving operation of the complete TCA cycle (Geider [16, p.347]). Under nitrogen limitation, nitrogen limited the protein synthesis.

Resistant respiration rates: The energetic costs of maintenance and growth are often converted to a respiration rate by assuming the maximum permissible efficiency for mitochondiral transport of $ATP/CO_2 = ATP/O_2 = 6$ (Geider [16, p.348]. Continuation of respiration, however, is also possible with $ATP/CO_2 < 6$ if energy conserving steps of the mitochondrial electron transport chain are bypassed.

Mitochondrial respiration in the dark: Respiration during the light period can be different

from dark respiration. However, some investigators report no changes between light and dark periods (See Geider [16] for a detailed discussion).

2.8 Nutrient Limitation

Nitrogen and phosphorus are essential for cell development. In addition, some species require other nutrients (e.g. silicate for diatom growth and calcium for coccolithophorids). Iron has received attention in recent years and is now considered to be a limiting factor in many phytoplankton communities. The reason for this development was the inability to accurately measure iron concentrations in the water until recently (Martin [35, p.123]).

2.8.1 Diffusion Limitation of Nutrient Transport

When nutrient concentrations are low, a cell taking up nutrients creates a zero-concentration of nutrients around itself (Chisholm [7, p.225]). Considering nitrogen in a cell (total number of elements), small cells have better chances of reproduction because they reach requirements more rapidly. Therefore, small cells might have advantages over large cells in nutrient limited waters. This phenomena may be a major factor in regulating the size of phytoplankton crops in nutrient rich oceanic zones where a trace nutrient (e.g. iron) is limiting.

2.8.2 Iron

It is believed that distribution of Fe (iron) in the open ocean occurs through deposition of Fe-rich atmospheric dust. In coastal waters and areas with a high dust-input, Fe-concentrations

are frequently significantly higher than in other areas. This often coexists with low concentrations of other nutrients (Martin [35, p.124]). C:Fe ratios are a matter of discussion, and ratios between 10,000:1 and 100,000:1 have been estimated (Martin [35, p.127]).

One possible scenario supporting the iron-dust theory is the discovery that glacial atmospheric CO_2 was lower than those in the interglacials. One hypothesis states that the 10-20% higher dust input in the system increased phytoplankton production (via Fe) which decreased CO_2 in the atmosphere.

2.8.3 Nitrogen

Nitrogen is essential for cell-growth and also for production of photosynthetic pigments. As mentioned in the section on photosynthesis, nitrogen influences the maximum photosynthetic rate P_{max}.

The main nitrogen sources for unicellular algae are nitrate (NO_3^-) and ammonium (NH_4^+). Nitrate is reduced to ammonium in the cell which results in oxygen production. Nitrate reduction requires energy. Ammonium is the material used for metabolism.

Assimilatory Nitrate Reduction consists of two reactions, nitrate reduction

$$NO_3^- + NADH + H+ \longrightarrow NO_2^- + NAD^+ + H_2O \tag{2.3}$$

and nitrite reduction

$$NO_2^- + 6e^- + 2H^+NH_2OH \longrightarrow NH_3 \tag{2.4}$$

Many experiments have shown that NADH has to be present whereas NADPH cannot be the electron donor for the reaction. Some experiments, however, show that in some species nitrate reductase takes also place if only NADPH is present. During the nitrite reductase NADPH can be the electron donor for many species.

Nitrogen is also needed for synthesis of carbohydrates, proteins and other structural materials. The role of nitrate depends on the species. Some species use nitrate only if ammonium is depleted, others use nitrate in considerable amounts even during times of high ammonium concentration in the water.

2.8.4 Phosphorus

Phosphorus, as part of the main energy currency ATP, is a very important part of the cell. Phosphorus is taken up in form of orthophosphates and in organic and inorganic combinations. Especially when orthophosphates are depleted, other phosphorus sources become important. Different species are able to use different inorganic or organic phosphorus combinations.

Normally little phosphate-phosphorus is available. However in polluted waters, phosphate could be high which can then influence production. Phosphorus is needed not only as part of the ATP molecules but is also part of many lipids and structural materials.

2.8.5 Silicification and Calcification

Mineralization is present in some species of algae. Silicification and calcification are the most common forms of mineralization. Both processes are needed for production of some form of cell-wall or other skeletal structures. Siliceous structures are found in diatoms, silicoflagellates, and in some species of Chrysophyceae, Chlorophyceae, Phaeophyceae and Xanthophyceae. Mostly these structures consist of hydrated amorphous silica, $SiO_2.nH_2O$. Silicon is an absolute requirement for the growth of diatoms.

Crystalline calcium carbonate occurs naturally as calcite and as aragonite (e.g. in coccolithophorids). The processes and the importance of mineralization are species specific and will be addressed later.

3 Individual Model Development

Chapter 2 presented the general structure and flows of a model applicable to many different species of autotroph unicellular algae. In this chapter mathematical expressions for the flows of the individual-based model are presented. This chapter is kept as general as possible, however, some of the derivations require assumptions that are only reasonable for a few or even a single species. It should be noted here that the computer code for the model consists of objects containing the mathematical expressions which allows an easy change of some or all mathematical expressions without rewriting the whole code.

In this chapter ϕ_e is used to represent one of the substances uptaken by the cell: CO_2 (carbon dioxide), FE (iron), AM (ammonium), NI (nitrate), OP (orthophosphate), OR (other phosphate). Calcium and silicate are included as nutrients for coccolithophorids and diatoms, respectively. Most of the parameters used in this section are species specific. Tables of all variables and parameters as well as abbreviations and units can be found in Appendix B.

Figure 3.1 gives an overview of the flows considered in the individual cell model.

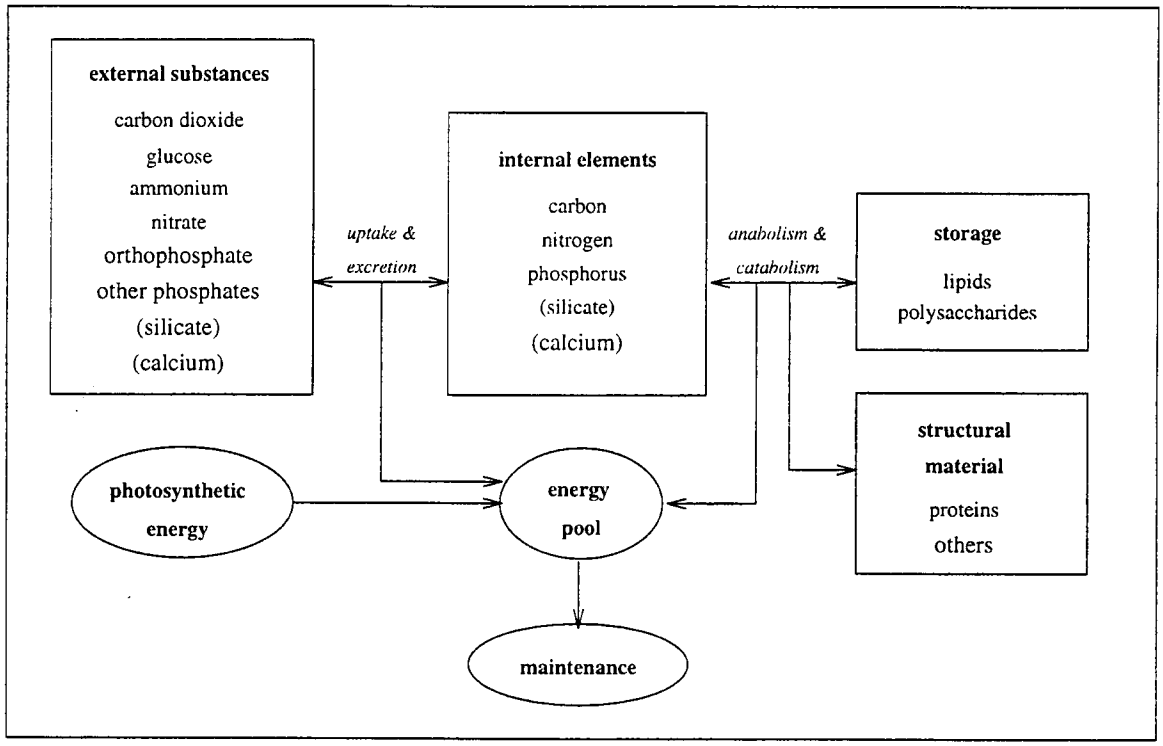

Figure 3.1: Flow diagram of the individual model

3.1 Aqueous Environment

The Sections 3.1.1 and 3.1.2 describe the flows of substances from the ambient water into the cell. The substances pass through the cell-membrane via active transport.

3.1.1 Active Transport

Uptake and incorporation of CO_2 into the phytoplankton cell is assumed governed by the photosynthetic rate. Uptake of iron, ammonium, nitrate, orthophosphate and other phos-

phate is assumed to depend on external concentration and the time needed to transport one molecule across the cell-membrane. This transport-time depends on temperature and thickness of the cell-membrane as described below.

The approach follows the idea of parallel processing of various molecules (de Groot [12]). The uptake of each substance is limited by the minimal uptake-time for one molecule of the substance. Because parallel processing is assumed, uptake of a single substance is independent from uptake of the other substances. The following assumption is made: Under optimal conditions (i.e. high substrate concentrations, optimal light and temperature conditions) substances are taken up such that the Redfield-ratio (see Section 3.1.2) is maintained in the interior of the cell.

In contrast to de Groot, who included the time of biosynthesis in the model, only arrival- and transport-time are considered because incorporation into storage and structure is modeled separately. The limitation for molecules of one substance is (minimal uptake-time)/(actual uptake-time). Minimal uptake-time is the time needed for uptake under optimal environmental conditions. Hence, the limitation is

$$\frac{t_{\phi,min}}{t_\phi} \tag{3.1}$$

where

$t_{\phi,min}$ (s): minimal uptake-time for one molecule of substance ϕ in seconds.

t_ϕ (s): actual uptake-time consisting of arrival- and transport-time for one molecule of type ϕ in seconds.

This can also be written as:

$$\frac{t_{\phi,min}}{\frac{a}{v(T)} + \tau(\phi_e)} \tag{3.2}$$

where

a (cm): distance or thickness of cell-membrane

$\tau(\phi_e)$ (s): function for arrival-time of one molecule as a function of external concentration level

$v(T)$ $(\frac{cm}{s})$: transport velocity as a function of temperature

ϕ_e $(\frac{\mu\, mol}{cm^3})$: external concentration of substance ϕ in molecules per cm^3

For one limiting nutrient, O'Neill et al [36] assumes that the waiting time (time until arrival of one molecule at the processor) is inversely proportional to the nutrient concentration. The same relationship is assumed here between substance concentration and waiting-time:

$$\tau(\phi) = \frac{c_{\phi_e}}{\phi_e} \tag{3.3}$$

where c_ϕ $(\frac{s}{cm^3})$ is a proportionality constant.

If arrival-times of molecules of one substance are assumed to be Poisson distributed, the same inverse proportionality is achieved.

The actual uptake term for substance ϕ_e does not involve $t_{\phi,min}$ and is defined as

$$\rho_{up,\phi_e} = \begin{cases} \frac{1}{\frac{a}{v(T)} + \tau(\phi_e)}\, n_{\phi,A}\, A & \text{for } \phi_e > 0 \\ 0 & \text{for } \phi_e = 0 \end{cases} \tag{3.4}$$

where

ρ_{up,ϕ_e} ($\frac{\mu\, mol}{s}$): uptake of molecules ϕ_e.

$n_{\phi,A}$ ($\frac{1}{cm^2}$): number of processors for substance ϕ_e molecules per surface area A

A (cm^2): efficient surface area for substance uptake (not necessarily equal surface area of individual for all species).

Equation 3.4 gives the number of $\mu\, mol$ of substance ϕ uptaken per second. The definition of the function in 3.4 includes a continous extension to the interval $[0, \infty]$. For the uptake of silicate and calcium the same dynamics are assumed.

The above formulation of nutrient uptake does not depend on internal nutrient concentrations. However, excretion of nutrients limits the internal concentrations and therefore internal nutrient pools do not grow without limit.

3.1.2 The Redfield Ratio

Under optimal conditions, the abundance of the elements C, N and P in autotrophic cells is often in the following ratio:

$$C : N : P = 106 : 16 : 1$$

which is the well known Redfield-ratio. Because of its fundamental importance, 106 C-molecules, 16 N-molecules and 1 P-molecule will be called 'a fundamental set of nutrients' in the following. It is assumed that nutrients are taken up according to this ratio only under optimal environmental conditions. Conditions that yield a maximum growth rate of a species are considered to be optimal.

3.2 Storage and Growth Dynamics

Nutrients in cytoplasm are used during anabolism for maintenance, growth and incorporation into storage. The energy needed for anabolism comes either from photosynthesis or from catabolism of reserves. Under low light conditions catabolism usually increases to provide energy for maintenance and growth. Catabolism of proteins appears to occur only under extreme energy limitation.

The physiological background of storage and growth dynamics in phytoplankton is not fully understood, but sufficient data are available so that a function indicating dependence on light and nutrient availability can be determined. Various papers report a favored polysaccharide production during light periods and a favored protein production during dark periods (e.g. Barlow [4], Harding et al [22], Konopka [28], Lancelot and Mathot [33]). This is, however, not a general result.

In the model internal storage materials are lipids and polysaccharides. Nitrogen is assumed to be essential only for protein and some structural material production, phosphorus is needed for lipid, protein and some structural material synthesis. During the dark period, polysaccharide catabolism not only provides energy for protein synthesis but also basic carbon molecules, lipid catabolism provides phosphorus in addition.

A variety of polysaccharides, lipids, proteins and other structural material can be found in different species. Mostly, however, one specific species synthesizes only a few types of these materials. It is assumed that each species or ecotype synthesizes some 'typical' molecules of storage and structural materials. For the model only the composition of the materials is important (i.e., how many molecules of C, N and P and how much ATP is needed to

produce one molecule of polysaccharide, lipid and protein plus other structural material).

Following Kooijman's approach of a Dynamical Energy Budget (see Kooijman [29]) the energy pool $\bar{E}$ determines the actual storage and growth dynamics of the individual. The energy in $\bar{E}$ is derived from photosynthesis, decomposition of substances and catabolism of polysaccharides and lipids.

3.2.1 Polysaccharide Incorporation

For the production of polysaccharides only carbon and energy are needed. The number of polysaccharide molecules in the storage compartment is assumed to follow the dynamical equation

$$\frac{dm_{Ps}}{dt} = \rho_{st,Ps} = m_{0,Ps} f_{Ps}(\bar{E}, C_i) - g_{Ps} \tag{3.5}$$

where

m_{Ps} (μ**mol**): reserve polysaccharides

$\rho_{st,Ps}$ ($\frac{\mu\mathbf{mol}}{s}$): flux of polysaccharide molecules into storage.

$m_{0,Ps}$ ($\frac{\mu\mathbf{mol}}{s}$): polysaccharide molecules fixed during anabolism per time.

$f_{Ps}(\bar{E}, C_i, N_i)$, **nd.**: functional response to internal energy, carbon and nitrogen pools for production of polysaccharide molecules.

$\bar{E}$ (μ**mol**): energy pool in μmol ATP.

C_i (μ**mol**): internal nutrient in μmol C .

g_{Ps} ($\frac{\mu\mathbf{mol}}{s}$): catabolic rate of polysaccharides (e.g. a function of available energy in the energy pool and polysaccharides in storage compartment).

The first term of Equation 3.5 stands for the anabolism and the second for the catabolism of polysaccharides. Anabolism is considered to depend on available energy and carbon availability only. Catabolism depends on a function g_{P_s} which can be created following experiments (see Lancelot and Mathot [33]). The function g_{P_s} can depend on many variables. A possible formulation is given in Chapter 5. The energy gained through catabolism is transferred to the energy pool whereas the freed nutrients go back to the internal nutrient pools. Catabolism provides energy and carbon for protein production.

3.2.2 Lipid Incorporation

Lipids are produced in presence of carbon, phosphorus and energy. Catabolism of lipids during light and dark periods is important for some species. The anabolism and catabolism of lipid molecules is assumed to follow the equation

$$\frac{dm_{Lp}}{dt} = \rho_{st,Lp} = m_{0,Lp} f_{Lp}(\bar{E}, C_i, P_i) - g_{Lp} \tag{3.6}$$

where

m_{Lp} (μ**mol**): reserve lipids.

$\rho_{st,Lp}$ ($\frac{\mu\mathbf{mol}}{s}$): flux of lipid molecules into storage.

$m_{0,Lp}$ ($\frac{\mu\mathbf{mol}}{s}$): lipid molecules fixed during anabolism per time.

$f_{Lp}(\bar{E}, C_i, P_i)$, **nd.**: functional response to internal energy, carbon and phosphorus pools for production of lipid molecules.

N_i (μ**mol**): internal nutrient N in μmol.

P_i (μ**mol**): internal nutrient P in μmol.

g_{Lp} ($\frac{\mu \text{mol}}{s}$): catabolic rate of lipids (e.g. a function of available energy in the energy pool and lipid in storage compartment).

Lipid anabolism is represented by the first term of Equation 3.6 and depends on nutrient availability and energy. Catabolism is represented by the second term of Equation 3.6 and can depend on many variables. A possible form for g_{Lp} is given in Chapter 5.

3.2.3 Protein Incorporation and Structure

A major part of cellular structural material is protein and in the text structural materials are sometimes just referred to as proteins. Proteins are produced during the light period and the dark period. Catabolism of proteins is possible under extreme energy limitations (e.g. Cook [9] or Handa [21]) and is included in the model. Protein production determines growth characteristics of the individual. It is assumed that growth has highest priority after maintenance. During the light period, energy for anabolism comes from the photosynthesis and catabolism of reserves, whereas at night the only energy source is the reserve (polysaccharides and lipids). Protein production is determined by carbon, iron, nitrogen, and phosphorus availability and by energy production through photosynthesis and catabolism of reserve products (energy pool).

Other structural materials are also produced such as those employed for cell-membrane construction. Equation 3.7 is assumed to include not just proteins but also the other structural materials.

The dynamics for production of proteins and other structural materials are assumed to

follow the equation

$$\frac{m_{Pr}}{dt} = \rho_{st,Pr} = m_{0,Pr} f_{Pr}(\bar{E}, C_i, F_i, N_i, P_i) - g_{Pr} \tag{3.7}$$

where

m_{Pr} (μ**mol**): Protein or structural material in the cell measured in μmol.

$\rho_{st,Pr}$ ($\frac{\mu\textbf{mol}}{s}$): flux of protein and other structural molecules.

$m_{0,Pr}$ ($\frac{\mu\textbf{mol}}{s}$): fixation of proteins and other structural molecules per time.

$f_{Pr}(\bar{E}, C_i, F_i, N_i, P_i)$, **nd.**: functional response for protein and structure production.

g_{Pr} ($\frac{\mu\textbf{mol}}{s}$): catabolic rate of proteins.

The function g_{Pr}, similar to the functions g_{Ps} and g_{Lp}, can only be determined from experimental data. A possible formulation is given in Chapter 5.

3.2.4 The Functional Response f

There is a physiological difference between simple uptake of substances as described in Section 3.1.1 and incorporation of nutrients into structure or reserves (polysaccharides and lipids). Whereas simple uptake was assumed to be a parallel process independent for each substance, for incorporation there is a different assumption: if a molecule of one type is ready to process, the processor has to wait for one or several molecules of the other nutrient in order to be able to complete one molecule of a polysaccharide, lipid or protein (see De Groot [12]). Because incorporation of nutrients (or building of molecules) requires energy, energy is included in the functional response terms. Energy is included via the number of ATP molecules. One approach (Henson and Hallam [24]) considering a sequence of tasks

to be completed for building one molecule is used here.

Composition of molecules is normalized to one C molecule. Assuming that a new molecule of material ϕ_s (where ϕ_s = Ps, Lp or Pr) can be completed after one C molecule and k N molecules arrive at the processor and l ATP molecules are available to form the molecule the completion of the molecule takes a fixed amount of time with the time needed for the completion of one molecule of ϕ_s expressed as

$$t_{\phi_s} = max(t_{w,C}, k\, t_{w,N}, l\, t_{w,ATP}) + t_{\phi_s,b} \tag{3.8}$$

where

t_{ϕ_s} (s): time for completion of one molecule of polysaccharides

t_{w,ϕ_i} (s): waiting-time (time until arrival) for a molecule of type ϕ_i

$t_{\phi_s,b}$ (s): building-time for one molecule of material ϕ_s

As in Section 3.1.1, the waiting-time is assumed to be inversely proportional to the nutrient availability, where here the absolute nutrient concentration is chosen,

$$t_{w,\phi_i} = \frac{c'_{\phi_i}}{\phi_i} \tag{3.9}$$

where

c'_{ϕ_i} (s): proportionality constant.

ϕ_i (μmol): internal nutrient in μmol.

The building-time is expressed as the reciprocal of the maximal reaction rate $I_{m,Ps}$. Assuming Poisson distributed arrival-times for each of the nutrients yields a very complicated

expression for the functional response. In contrast, the Liebig model assumes the process-rate to be proportional to the most limiting nutrient (O'Neill et al [36]). Following this approach, the functional responses take the form

$$f_{Ps}(\bar{E}, C_i, N_i) = \frac{1}{max(\frac{c'_{C_i}}{C_i}, k_{ATP,Ps}\frac{c'_{\bar{E}}}{\bar{E}}) + \frac{1}{I_{m,Ps}}} \tag{3.10}$$

and

$$f_{Lp}(\bar{E}, C_i, P_i) = \frac{1}{max(\frac{c'_{C_i}}{C_i}, k_{P,Lp}\frac{c'_{P_i}}{P_i}, k_{ATP,Lp}\frac{c'_{\bar{E}}}{\bar{E}}) + \frac{1}{I_{m,Lp}}} \tag{3.11}$$

and

$$f_{Pr}(\bar{E}, C_i, F_i, N_i, P_i) = \frac{1}{max(\frac{c'_{C_i}}{C_i}, k_{F,Pr}\frac{c'_{F_i}}{F_i}, k_{N,Pr}\frac{c'_{N_i}}{N_i}, k_{P,Pr}\frac{c'_{P_i}}{P_i}, k_{ATP,Pr}\frac{c'_{\bar{E}}}{\bar{E}}) + \frac{1}{I_{m,Pr}}} \tag{3.12}$$

where

k_{ϕ_i,ϕ_s}, $(\frac{\mu\mathbf{mol}}{s})$: constant relating number of molecules of type ϕ_i needed for production of one molecule of material ϕ_s.

I_{m,ϕ_s}, **nd.** : measure for maximum reaction rate for production of a molecule ϕ_s.

If species like coccolithophorids and diatoms are considered, the amount of calcium and silicate, respectively, is included in the functional response. A similar expression results for these species. Also iron can be included as a factor because it changes enzymatic rates which influences protein synthesis.

3.3 Energy Pool

The energy pool includes energy provided from photosynthesis and from catabolism of reserve products. It is used for maintenance and growth.

$$\frac{d\bar{E}}{dt} = \rho_{st,ATP} + \rho_{up,ATP} - \rho_{ma,ATP} \tag{3.13}$$

where

$\bar{E}$ (μ**mol**): energy in μmol ATP available in the cell.

$\rho_{st,ATP}$ ($\frac{\mu\mathbf{mol}}{s}$): amount of ATP produced/used for storage catabolism and anabolism (negative or positive number).

$\rho_{up,ATP}$ ($\frac{\mu\mathbf{mol}}{s}$): amount of ATP produced/used during uptake of materials from water, including photosynthetic energy.

$\rho_{ma,ATP}$ ($\frac{\mu\mathbf{mol}}{s}$): amount of ATP used during maintenance per second.

Therefore $\rho_{*,ATP}$ are energy fluxes whose specific forms are introduced in Section 3.9.

In addition, it is assumed that a certain fraction of the internal carbon pool is respired (dependent only on the internal carbon concentration). This process is included to account for the CO_2 production of phytoplankton cells during light and dark periods. The process results in energy production.

$$\rho_{ex,C} = j_{ex,C} C_i \tag{3.14}$$

where $j_{ex,C}$ (s^{-1}) is the fraction of free carbon molecules respirated per second.

Production of one ATP molecule requires 3 P elements. Therefore energy production results in a decrease of available phosphorus, whereas use of energy results in an increase of the available phosphorus. The following term is included in the phosphorus pool for some of the simulations

$$-3\ [\rho_{st,ATP} + \rho_{up,ATP} - \rho_{ma,ATP}] \tag{3.15}$$

3.4 Photosynthesis

Due to the complexity of light availability and light capturing by phytoplankton cells, combined with the importance of photosynthetic energy, modeling of photosynthesis is difficult. The process and its dependencies on abiotic and biotic factors have been discussed in Chapter 2. In this section a mathematical formulation of the photosynthetic rate in a water-column is derived.

Figure 2.4 in Chapter 2 shows a irradiance-photosynthesis curve. For low irradiances, the relationship is linear. Often the value for E_k, the intersection of the continued line of the linear relation and the maximum photosynthetic rate, is measured. Kirk [25, p.283] gives the following expression (assuming that the capturing of photons is Poisson distributed):

$$L_{max}[1 - e^{\frac{-E_d}{E_k}}] \tag{3.16}$$

where L_{max} $(\frac{\mu molC}{cm^2 s})$ is the maximum photosynthetic rate and E_d $(\frac{\mu mol}{m^2 s})$ is the light irradiance.

The maximum photosynthetic rate is, however, not constant. Dependence on nutrient

availability has been reported from many experiments (Falkowski [14, p.55p]). Therefore L_{max} is expressed as a hyperbolic function of the form

$$L = [\frac{L_\beta}{M + L_\alpha} + (1 - L_\beta)]\, L_{max} \tag{3.17}$$

where L_α and L_β are nondimensional constants. M represents the nutrient dependency. If photosynthesis depends on external concentration of nitrate and phosphorus, M has the form

$$M = \max(c_1 N I_e, c_2 O P_e)$$

where c_1 (μmol) and c_2 (μmol) are constants. M can also be a function of internal nutrient concentrations.

In another set of simulations Equation 3.17 was replaced by the similar function

$$L = [1 - \frac{L_\beta}{N_i + L_\alpha}]\frac{1}{1 + \frac{L_P}{P_i}} L_{max} \tag{3.18}$$

where L_P (μmol) is a constant. If Equation 3.18 is used, the photosynthetic rate is a function of internal nitrogen and phosphorus concentration.

The irradiance E_d in Equation 3.16 is not a constant. Incoming light quanta are absorbed by water and phytoplankton. Kirk [25, p.129] describes irradiance as a function of depth as

$$E_d(z) = E_d(0) e^{-K_d z}$$

where $E_d(0)$ $(\frac{\mu mol}{m^2 s})$ is the irradiance just below the surface, z (m) is the depth and K_d $(\frac{1}{m})$ is a measure for the absorption of light in the water. In the model K_d is assumed to be a

function of the phytoplankton density but constant with depth. It is assumed that

$$K_d = K_s + \delta K_p$$

where K_s $(\frac{1}{m})$ is the absorption coefficient due to seawater alone, K_p $(\frac{1}{m})$ is the absorption coefficient due to phytoplankton, and δ $(\#)$ is the total phytoplankton density. Therefore the overall equation for photosynthetic rate is

$$L(z, \delta, E_d(0)) = [\frac{L_\beta}{M + L_\alpha} + (1 - L_\beta)]\, L_{max}\, [1 - e^{\frac{-E_d(0)e^{-(K_s+\delta K_p)z}}{E_k}}] \tag{3.19}$$

or, if Equation 3.18 is used,

$$L(z, \delta, E_d(0)) = [1 - \frac{L_\beta}{N_i + L_\alpha}]\frac{1}{1 + \frac{L_P}{P_i}}\, L_{max}\, [1 - e^{\frac{-E_d(0)e^{-(K_s+\delta K_p)z}}{E_k}}] \tag{3.20}$$

Figure 3.2 shows a three dimensional graph of Equation 3.16 for different depth and irradiance.

The model has, however, no spatial dimensions. It is assumed here that phytoplankton cells are distributed equally over a depth of z_0. The value z_0 might be the maximum depth where photosynthesis is still possible. It could also represent the depth of an upwelling surface layer. This choice makes the model more realistic for upwelling areas where the phytoplankton concentration is less depth dependent.

Equation 3.20 (or 3.19, respectively) has to be integrated over the depth z_0. On the first glance integration of this equation might seem a difficult task. However, using the substitution

$$u = \frac{-E_d(0)}{E_k} e^{-(K_s+\delta K_p)z}$$

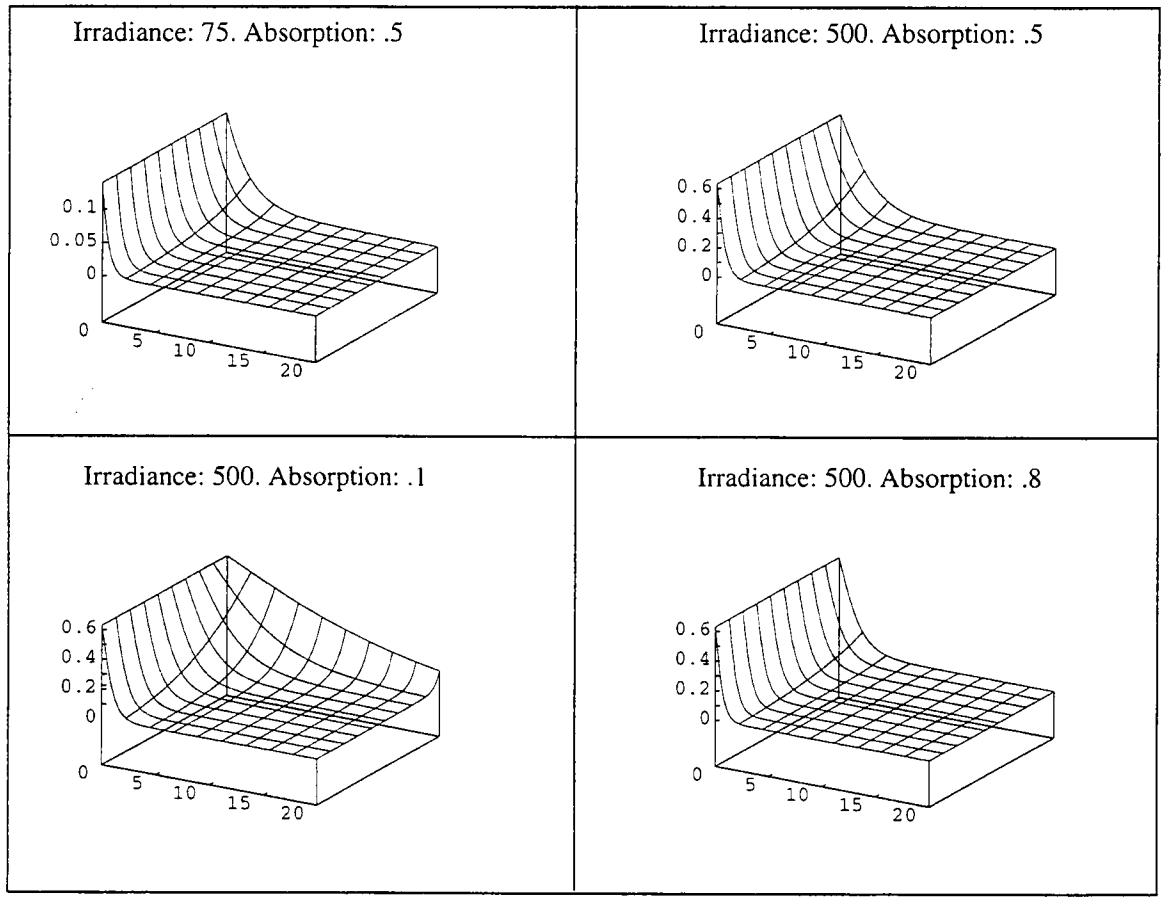

Figure 3.2: Photosynthetic rate as a function of depth and phytoplankton density for different irradiance and absorption coefficients. Irradiance in μmol $s^{-1}\,m^{-2}$. Vertical axis: photosynthetic rate, horizontal axis 0-20: depth in m, third axis: cell density, decreasing from left to right.

the integration reduces to the form

$$n \int_0^{z_0} \frac{e^u}{ku} du$$

where $n = [\frac{L_\beta}{M+L_\alpha} + (1 - L_\beta)]L_{max}$ (or $n = [1 - \frac{L_\beta}{N_i+L_\alpha}]\frac{1}{1+\frac{L_P}{P_i}}L_{max}$, respectively) and $k = -(K_s + \delta K_p)$ are constants. Using the series representation of the exponential function, one can calculate

$$\bar{L}(\delta, E_d(0) = -\frac{n}{k} \sum_{j=0}^{\infty} \left(-\frac{E_d(0)}{E_k}\right)^j \frac{(e^{kz_0} - 1)^j}{j\, j!} \tag{3.21}$$

An approximate calculation of the photosynthetic rate over a surface layer with depth z_0 via Equation 3.21 is possible. Kirk [25, p.278p] gives values for E_k for different species and locations, all of them being ≥ 0.5. Therefore inclusion of the first five terms of the sums in Equation 3.21 should give a sufficient approximation for $\bar{L}(\delta, E_d(0))$.

Figure 3.3 shows the photosynthetic rate and the average photosynthetic rate as a function of cell density and irradiance. Cell density seems to be a small factor except if densities are extremely high. Irradiance and depth, however, play a significant role. The shape of the various graphs is not very different, however, a look at the scale reveals the huge differences in the photosynthetic rate.

The surface irradiance $E_d(0)$ is time dependent. Values can either be obtained from a meteorological database or can be approximated. A good approximation for sunny or partly cloudy days is

$$E_d(0,t) = E_{d,max} sin(\frac{\pi t}{D}) \tag{3.22}$$

where D (h) is the daylength (Platt et al [40]).

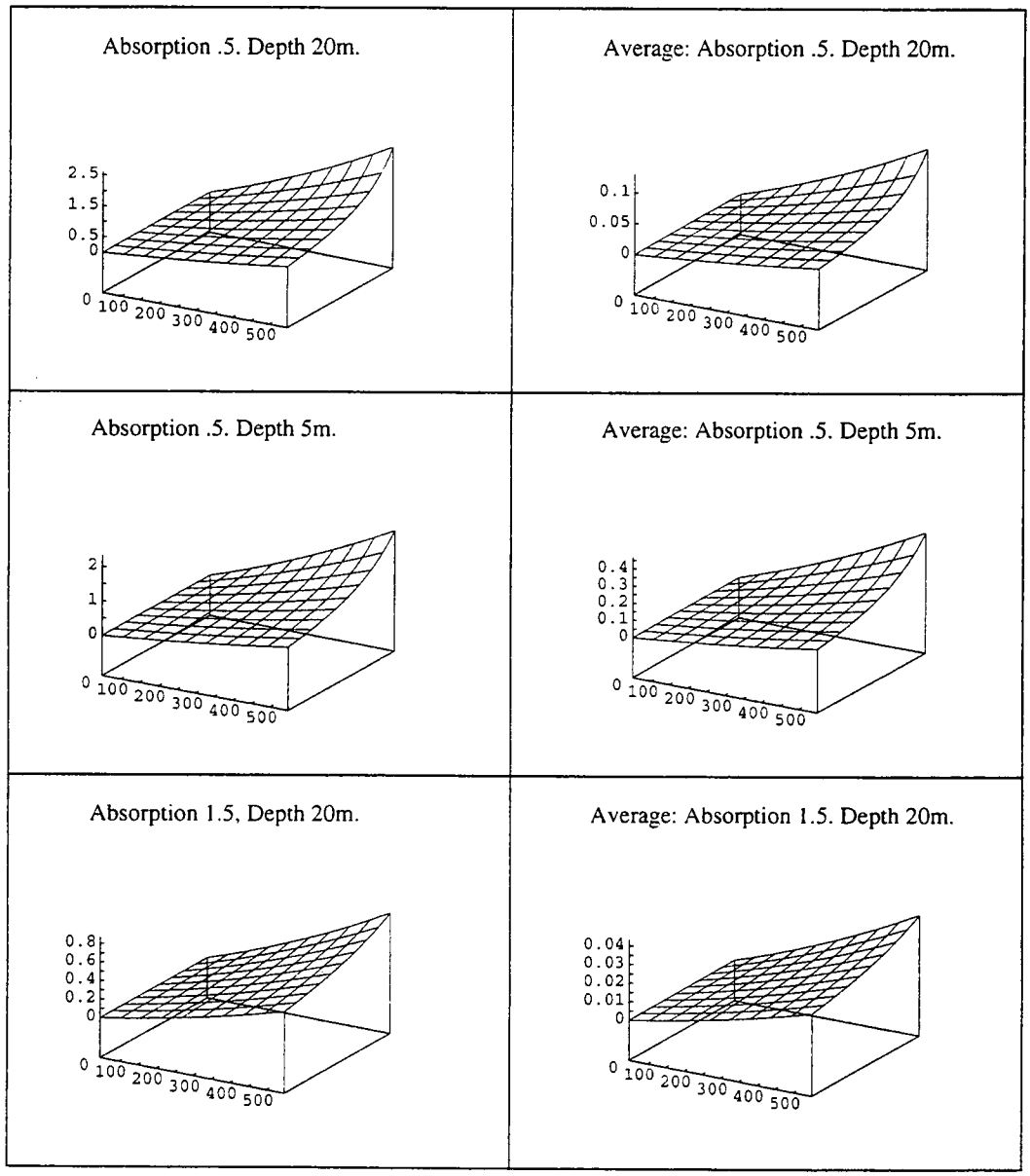

Figure 3.3: Total (left column) and average (right column) photosynthetic rate for a certain depth as a function of irradiance at the surface and phytoplankton density. Shapes are similar, whereas scales are very different. Vertical axis: photosynthetic rate, horizontal axis 0-500: irradiance in μmol $s^{-1}\, m^{-2}$, other horizontal axis: cell density, decreasing from left to right.

As mentioned before, CO_2 uptake is assumed to be determined by photosynthesis. Therefore, CO_2 cannot be a limiting factor in contrast to irradiance. The CO_2 uptake flux is

$$\rho_{up,C} = L(I)A \tag{3.23}$$

$$\rho_{up,ATP} = L(I)\mu_{C,ATP}A \tag{3.24}$$

assumed to be where $\mu_{C,ATP}$ (nd.) is a measure for the number of ATP gained from incorporation of one C element during photosynthesis. This is also a measure for the efficiency of photosynthesis.

3.5 Maintenance

Maintenance is the most basic and most important process in the cell. If maintenance requirements cannot be fulfilled, the individual cannot grow and reproduce. The energy required for maintenance is proportional to the volume of the cell (a cell of double volume has twice as many proteins to turn over, see e.g. Kooijman [29, page 76p]). Maintenance costs are described by the simple equation

$$\dot{M} = M_0(m_{Ps} + m_{Lp} + m_{Pr}) \tag{3.25}$$

where where M_0 ($\frac{1}{\mu mol}$) is the maintenance cost per μmol in number of ATP molecules per volume. This assumes the same maintenance cost per $/mumol$ of storage and structural material. M_0 could, however, also be different for storage and proteins.

3.6 Excretion

Algae excrete different substances. The reasons for excretion are not really known but probable are waste removal, excess nutrients being transported, or diffusion due to concentration differences. Extracellular products are soluble substances liberated from healthy cells. Typical substances are:

- Carbohydrates: A considerable fraction of the photoassimilated carbon (1%- 50%) may be released in form of simple and complex polysaccharides such as glucose, galactose or mannose.
- Nitrogeneous substances: amino acids and peptides are released but normally do not represent a large fraction of the extracellular products.
- Organic Acids: Glycolic acid is excreted in a considerable amount by some species.
- Phosphates: Inorganic phosphates are released particularly when inorganic phosphorus is abundant. At the end of blooms, organic phosphorus is released in considerable amounts.
- Lipid: only small amounts of lipids are released.
- Auto-inhibitors and Antibiotics (limit growth of excreting cell or growth of other species)
- Toxins (especially during blooms)

For more details and tables summarizing the released extracellular carbohydrates and organic acids see Hellebust [23, page 839p]. Many studies and experiments have been carried out to find what determines the excretion of substances by healthy cells but no complete answer has been found. Intracellular products play a role as well as environmental conditions. Excretion by different species depends on different parameters.

Excretion is modeled here as part of the active transport. A high internal concentration of nutrients yields an excretion of substances. Internal concentration is measured as a fraction of the structural material and a maximum possible concentration in the internal is assumed.

$$\rho_{ex,\phi_i} = j_{\phi_i} \frac{\phi_i}{m_{Pr}} \tag{3.26}$$

where j_* $(\mu\ mol)$ is a constant determined from maximum concentration of element * in the cell.

3.7 Reproduction

Reproduction occurs when the structural material of the cell has doubled. Simple division of protein, structural material, and reserves is assumed. The two new cells are therefore identical in all respects.

3.8 The Temperature dependence $v(T)$

For the dependency of physiological rates on temperature, Arrhenius proposed the following description (see e.g. Glasstone et al [18]):

$$s(T^K) = s(T_1^K)\exp(\frac{T_A^K}{T_1^K} - \frac{T_A^K}{T^K}) = s(T_1^K)\exp(\frac{T_A^K}{T_1^K T^K}(T^K - T_1^K)) \tag{3.27}$$

where

$s(T)$ $(\frac{cm}{s})$: rate of a physiological process, here velocity of nutrient transport

$s(T_1^K)$ $(\frac{cm}{s})$: constant

T^K (K): absolute temperature

T_1^K (K): chosen reference temperature

T_A^K (K): Arrhenius temperature

This function is used for the transport velocity of nutrients through the cell-membrane, i.e. $v(T-278) = s(T^K)$. The values $s(T_1^K)$ and T_A^K for different species can be found in the literature. The function can also be used to describe the influence of temperature on production of storage products and on growth.

3.9 Transition Matrices

This section summarizes the calculations for the mass and energy-fluxes $\rho_{*,*}$. Dealing with several different macromolecules containing several of the internal nutrients, a matrix representation of the mass and energy flows proves to be very helpful.

3.9.1 Transition-Uptake-Matrix

The following molecules are considered: CO_2, iron, ammonium, nitrate, orthophosphate and other phosphorus combinations. CO_2 is assumed to be abundant and its actual mass uptake flux is determined by the light availability. Mass uptake fluxes for the other molecules are governed by the equation given in Section 3.1.1. Nitrate needs to be reduced to ammonium before it can be used. These energy losses and gains are included in the transition-uptake matrix. The following mass uptake flux vector can be determined by the equations given

in Section 3.1.1 and Section 3.4.

$$\rho_{up,m} = \begin{bmatrix} \rho_{up,CO_2} \\ \rho_{up,FE} \\ \rho_{up,AM} \\ \rho_{up,NI} \\ \rho_{up,OP} \\ \rho_{up,OR} \end{bmatrix}$$

where $\rho_{up,\phi}$ $[\frac{\mu \text{mol}}{s}]$ represents the uptake of molecules of substance ϕ. A simple matrix multiplication can provide the changes in the internal nutrient pools (elementary iron, carbon, nitrogen and phosphorus) and the energy pool.

$$T_{up} * \rho_{up,m} =$$

$$\begin{bmatrix} \mu_{C,CO_2} & \mu_{C,FE} & \mu_{C,AM} & \mu_{C,NI} & \mu_{C,OP} & \mu_{C,OR} \\ \mu_{N,CO_2} & \mu_{N,FE} & \mu_{N,AM} & \mu_{N,NI} & \mu_{N,OP} & \mu_{N,OR} \\ \mu_{P,CO_2} & \mu_{P,FE} & \mu_{P,AM} & \mu_{P,NI} & \mu_{P,OP} & \mu_{P,OR} \\ \mu_{ATP,CO_2} & \mu_{ATP,FE} & \mu_{ATP,AM} & \mu_{ATP,NI} & \mu_{ATP,OP} & \mu_{ATP,OR} \end{bmatrix} \begin{bmatrix} \rho_{up,CO_2} \\ \rho_{up,FE} \\ \rho_{up,AM} \\ \rho_{up,NI} \\ \rho_{up,OP} \\ \rho_{up,OR} \end{bmatrix} =$$

$$\begin{bmatrix} \rho_{up,C} \\ \rho_{up,F} \\ \rho_{up,N} \\ \rho_{up,P} \\ \rho_{up,ATP} \end{bmatrix} = \rho_{up,e} \qquad (3.28)$$

where

T_{up}: Transition-Uptake-Matrix.

$\rho_{up,e}$ ($\frac{\mu mol}{s}$): uptake of the elementary products and ATP.

μ_{ϕ_i,ϕ_e}, **nd** : number of ϕ_i-molecules in a ϕ_e-molecule.

μ_{ATP,ϕ_e}, **nd** : number of ATP molecules produced or used by reduction of one ϕ_e-molecule.

Determination of the elements in the Transition-Uptake-Matrix should not cause any problems because the chemical composition of the substances is well known.

3.9.2 Transition-Storage-Matrix

Synthesis of polysaccharides, lipids and proteins requires carbon, iron, nitrogen and phosphorus, as well as energy. The reverse process (catabolism) adds these products to the internal pools. Assuming that the mass-fluxes between internal nutrient compartments and storage compartments as well as structural compartment are known, the following matrix representation will be helpful.

$$T_{st} * \rho_{st,m} = \begin{bmatrix} \mu_{C,Ps} & \mu_{C,Lp} & \mu_{C,Pr} \\ \mu_{F,Ps} & \mu_{F,Lp} & \mu_{F,Pr} \\ \mu_{N,Ps} & \mu_{N,Lp} & \mu_{N,Pr} \\ \mu_{P,Ps} & \mu_{P,Lp} & \mu_{P,Pr} \\ \mu_{ATP,Ps} & \mu_{ATP,Lp} & \mu_{ATP,Pr} \end{bmatrix} \begin{bmatrix} \rho_{st,Ps} \\ \rho_{st,Lp} \\ \rho_{st,Pr} \end{bmatrix} = \begin{bmatrix} \rho_{st,C} \\ \rho_{st,F} \\ \rho_{st,N} \\ \rho_{st,P} \\ \rho_{st,ATP} \end{bmatrix} = \rho_{st,e} \qquad (3.29)$$

where

T_{st}: Transition-Storage-Matrix

$\rho_{st,e}$ ($\frac{\mu mol}{s}$): transition in or from storage of the elementary products and ATP.

μ_{ϕ_i,ϕ_s}, **nd:** number of ϕ_i-molecules in a typical/average ϕ_s-storage-molecule.

μ_{ATP,ϕ_s}, **nd:** number of ATP molecules used by production of one ϕ_s- molecule or gained during catabolism.

Inclusion of additional nutrients like calcium and silicate increase the dimension of the matrix.

3.9.3 Invertibility

The question if the matrix multiplications in Sections 3.9.1 and 3.9.2 are left and right invertible can not be answered in general. However, there are necessary conditions for each of the matrices.

Transition-Uptake Inverse

The transition-uptake matrix T_{up} represents a linear operator from $\Re^6$ to $\Re^5$. Invertibility of this operator depends on its rank. The rank of the operator is equal to the column rank of the matrix.

1. If the column-rank$<$ 5: the operator is not invertible because it is not one to one.
2. If the column-rank$=$ 5: the operator is invertible, for each element in $\Re^5$ there exists a unique pre-image in $\Re^6$.
3. If the column-rank$>$ 5: the operator is invertible, but only for a subset of $\Re^5$.

Only in the second case can we calculate the fluxes $\rho_{up,\phi}$ where $\phi = CO_2$, FE, AM, NI, OP and OR from given fluxes ρ_{up,ϕ_i} where ϕ_i = C, N, P and ATP. However, it is unlikely that the transition-uptake-matrix $\boldsymbol{T}_{up}$ has exactly column-rank 5.

The result means that knowing the fluxes ρ_{up,ϕ_i} of the internal nutrient uptake usually is not sufficient to get information about the original uptake fluxes $\rho_{up,\phi}$. That is, the original uptake fluxes have to be considered, and should be measured in experiments.

Transition-Storage Inverse

The transition-storage matrix $\boldsymbol{T}_{st}$ represents a linear operator from $\Re^3$ to $\Re^5$. In this case, the row-rank of the operator is ≤ 3. That means the operator is invertible but only for a subset of $\Re^3$ except when the rank equals 3. Therefore, the power-fluxes ρ_{st,ϕ_s} for the storage products can be calculated from the mass-fluxes ρ_{st,ϕ_i} of the internal nutrients. However, there exist mass-fluxes for the internal nutrients that do not allow determination of corresponding power-fluxes.

The result implies that the power-fluxes ρ_{st,ϕ_s} of reserves and structure cannot be determined by independent mass-fluxes ρ_{st,ϕ_i}. That is, the power-fluxes are driving the system. In contrast to the transition- uptake matrix, a determination of the mass-fluxes could result in an insolvable situation.

3.10 Surface and Volume Calculations

The surface and volume of a cell are important for uptake and maintenance. A common assumption is isomorphism (for a more detailed discussion see e.g. Kooijman [29, page 22f]). Isomorphism means individuals keep their shape as they grow: if a cell has a length of l_1 and later a length of l_2 then surface area and volume are related by the factors $(\frac{l_1}{l_2})^2$ and $(\frac{l_1}{l_2})^3$ respectively.

If protein is assumed to determine the volume (i.e. internal nutrient pool and reserves neglected), the simple relation is

$$V = \frac{m_{Pr}}{\sigma_{Pr}} \tag{3.30}$$

where

m_{Pr} **(μmol)**: protein and structure in the cell.

σ_{Pr} ($\frac{\mu\mathbf{mol}}{cm^3}$): molecular density of protein and structure

The inclusion of reserves in volume calculation gives a more realistic model, but also a more complicated one. The equation then reads as

$$V = \frac{m_{Pr}}{\sigma_{Pr}} + \frac{m_{Lp}}{\sigma_{e,Lp}} + \frac{m_{Ps}}{\sigma_{e,Ps}} \tag{3.31}$$

where σ_{ϕ_s} ($\frac{1}{cm^3}$) is the molecular density of substance ϕ_s.

Surface area is assumed to be

$$A = (V)^{\frac{2}{3}} = \left[\frac{m_{Pr}}{\sigma_{Pr}} + \frac{m_{Lp}}{\sigma_{e,Lp}} + \frac{m_{Ps}}{\sigma_{e,Ps}}\right]^{\frac{2}{3}} \tag{3.32}$$

3.11 Summary

The two transition matrices introduced in Section 3.9 are easy means to calculate mass and energy fluxes. However, the problem is to determine the mass-fluxes. In particular, insufficient information exists about what drives the catabolism and anabolism of storage materials. Several experiments have shown that during poor light conditions, protein production increases and polysaccharides production decreases. One possible explanation is a lack of energy because more energy is needed to produce one molecule of a (typical) polysaccharide than for one molecule of protein. However, this does not explain why during nitrogen deficiency the same switch from polysaccharide to protein production occurs. During these periods, the cell uses perhaps more energy for the reduction of nitrite to ammonium to get a maximum of nitrogen supply and therefore chooses the cheaper protein production. These are speculations but show that available energy could be the most important factor in cell production.

For a summary of the equations, see Appendix C.

4 The Population Model

This chapter introduces a population model that includes sinking and grazing of single cells and no aggregation. For a population model including aggregation see Chapter A.

4.1 Species and Ecotypes

The individual model presented in Chapter 3 was developed to follow the dynamics of each cell independently. However, even with the fastest available computers, it would be very time consuming to model thousands of individual cells over long time periods. To reduce the number of calculations needed, one divides the population of each species into groups of ecotypes. Individuals in one ecotype have the same parameter values, i.e. at time of birth they have the same amount of structural and storage material and consequently grow according to the same dynamics.

The population models presented in this chapter and in Chapter A are population models for one species. To keep the number of indices on parameter values minimal, species dependence is not indicated on the parameters. If a sum over a species occurs in the formulas it is assumed that each species has its own set of parameters. A sum over ecotypes means a sum over all ecotypes of one species. Parameter values are different for different ecotypes of one species but this is not indicated in the formulas.

4.2 A McKendrick-Von Foerster Equation

It is assumed that the population is structured by mass of polysaccharides, lipids and proteins. Let $\delta(t, m_{Ps}, m_{Lp}, m_{Pr})$ be the density of cells with mass of polysaccharides m_{Ps}, mass of lipids m_{Lp} and mass of proteins m_{Pr} at time t. A Mc-Kendrick-Von Foerster equation for a population structured by three dynamic variables has the following form (see Hallam [20]):

$$\frac{\partial \delta}{dt} + \sum_{i=1}^{3} \frac{\partial}{\partial m_i}(\varphi_i(m)\delta) = -D\delta$$

where

$m = (m_1, m_2, m_3)$: vector of the three dynamic variables

$\varphi_i(m) = \frac{dm_i}{dt}$: derivative with respect to time of the dynamic variable m_i

D: death-rate.

Using the notation of the individual model, the equation takes the form

$$\begin{aligned} \frac{\partial \delta(t, m_{Ps}, m_{Lp}, m_{Pr})}{dt} &+ \frac{\partial}{\partial m_{Ps}}[\varphi_{Ps}(t, m_{Ps}, m_{Lp}, m_{Pr})\delta(t, m_{Ps}, m_{Lp}, m_{Pr})] \\ &+ \frac{\partial}{\partial m_{Lp}}[\varphi_{Lp}(t, m_{Ps}, m_{Lp}, m_{Pr})\delta(t, m_{Ps}, m_{Lp}, m_{Pr})] \\ &+ \frac{\partial}{\partial m_{Pr}}[\varphi_{Pr}(t, m_{Ps}, m_{Lp}, m_{Pr})\delta(t, m_{Ps}, m_{Lp}, m_{Pr})] \;=\; -D\delta \end{aligned} \tag{4.1}$$

The death-rate D is a constant in the simplest case or a function $D(m_{Ps}, m_{Lp}, m_{Pr})$ of the dynamical variables in a more complicated case. The functions $\varphi_*(m) = \frac{dm_*}{dt}$ (* stands for Ps, Lp or Pr) are part of the individual model. However, these functions are species specific (due to variation of processes and parameters) and therefore a Mc-Kendrick-Von

Foerster equation is needed for each ecotype separately.

Boundary Conditions: The boundary conditions of the model are determined by the birth equation. For the given individual model, reproduction occurs if the structural material has doubled in mass. Let the initial value of protein and structural material in a cell be $m_{Pr,0}$. Then, the death-rate $D = \infty$ if the structural mass m_{Pr} has the double value of the start value $m_{Pr,0}$. At this time two new cells with structural mass $m_{Pr,0}$, lipid mass $\frac{1}{2}m_{Lp}$, and polysaccharide mass $\frac{1}{2}m_{Ps}$, enter the population. The birth function can be written as

$$B(t) = \int_0^\infty \int_0^\infty 2\delta(t, m_{Ps}, m_{Lp}, 2m_{Pr,0}) dm_{Lp}\, dm_{Ps} \tag{4.2}$$

and the boundary conditions are

$$\delta(t, m_{Ps}, m_{Lp}, m_{Pr,0}) = 2\delta(t, 2m_{Ps}, 2m_{Lp}, 2m_{Pr,0}) \tag{4.3}$$

The value $m_{Pr,0}$ can be different for each ecotype.

4.3 Application to Individual Model

The McKendrick-Von Foerster Equation presented in Section 4.2 assumes the existence of partial derivatives of the density function $\delta(t, m_{Ps}, m_{Lp}, m_{Pr})$. However, the individual model does not allow calculation of a continuous density function. If calculated from the individual model, the density function δ is only nonzero for a finite number of sets of values for m_{Ps}, m_{Lp} and m_{Pr} - one set for each ecotype. Therefore, a modification of the equations of Section 4.2 is necessary.

Equation 4.1 takes the form

$$\delta(t+\triangle t,\ m_{Ps}+\rho_{st,Ps}\triangle t,\ m_{Lp}+\rho_{st,Lp}\triangle t,\ m_{Pr}+\rho_{st,Pr}\triangle t) \quad = \quad \delta(t, m_{Ps}, m_{Lp}, m_{Pr}) \\ -D(m_{Ps}, m_{Lp}, m_{Pr})\delta(t, m_{Ps}, m_{Lp}, m_{Pr})\triangle t \tag{4.4}$$

This equation is applicable to each set of values of m_{Ps}, m_{Lp} and m_{Pr} determined by the different ecotypes. For different ecotypes the values m_{Ps}, m_{Lp} and m_{Pr} are never all the same. Again $D = \infty$ is assumed for $m_{Pr} \geq 2m_{Pr,0}$ due to cell division.

Equation 4.2 for the birth process takes the form

$$B(t) = \sum_{ecotypes} 2\delta(t, m_{Ps}, m_{Lp}, 2m_{Pr,0}) \tag{4.5}$$

and Equation 4.3 for the boundary condition

$$\delta(t, m_{Ps}, m_{Lp}, m_{Pr,0}) = 2\delta(t, 2m_{Ps}, 2m_{Lp}, 2m_{Pr,0}) \tag{4.6}$$

does not change its form. However, it is important to remember here that the value $m_{Pr,0}$ is different for each ecotype.

4.4 Sinking

The component determining sinking is

$$\frac{x}{z}\delta(t, x) \tag{4.7}$$

where x (cm^3) is the volume of a cell, and z (m) is the depth of the surface layer. This formulation allows calculation of number of lost cells due to sinking for each ecotype. For

a derivation of this equation see Section A.2. The volumes x can be calculated from the known values of m_{Ps}, m_{Lp} and m_{Pr}, see Section 3.10.

4.5 Grazer Model

Grazing by zooplankton is one of the most important factors of population control for phytoplankton. Here, zooplankton is modeled in a very general way as one population grazing on phytoplankton. A dependence of grazing on the volume of the phytoplankton cells is included. The following dynamics for the zooplankton community are assumed:

$$\frac{dZ}{dt} = (MI)\ (AE)\frac{\sum_{species}\left[\sum_{ecotypes} q(x)\delta(t,x)\right]}{\sum_{species}\left[\sum_{ecotypes} q(x)\delta(t,x)\right] + \vartheta_p} Z - \theta\ Z^r \tag{4.8}$$

where

Z ($\frac{\#}{m^3}$): density of grazers.

r, **nd.**: constant, either 1 for a first order grazing process or 2 for a logistic representation.

(MI): maximum ingestion rate of grazer.

(AE): assimilation efficiency of grazer.

$q(x)$: probability an individual grazer ingests a cell of volume x.

ϑ_p: trophic response half saturation constant.

θ: constant mortality rate of grazer population.

As mentioned before, volume of the cells is calculated from the known values of m_{Ps}, m_{Lp} and m_{Pr}. Sum over ecotypes means sum over all volumes present at a certain time. The sum over all species is required in Equation 4.8 because the total population of phytoplankton determines the population change of the zooplankton.

The losses for each ecotype in number of cells are then

$$q(x)\delta(t,x) \quad . \tag{4.9}$$

4.6 Summary

If the equations are put together, Equation 4.4 takes the form

$$\begin{aligned}
&\delta(t+\triangle t,\ m_{Ps}+\rho_{st,Ps}\triangle t,\ m_{Lp}+\rho_{st,Lp}\triangle t,\ m_{Pr}+\rho_{st,Pr}\triangle t) \\
&\quad = \delta(t,m)+\left[-\frac{1}{z}V(m)\delta(t,m)-q(V(m_{Ps},m))\delta(t,m)-D(m)\delta(t,m)\right]\triangle t \\
&\quad = \delta(t,m)-\left[\frac{1}{z}V(m)+q(V(m))+D(m)\right]\delta(t,m)\triangle t
\end{aligned} \tag{4.10}$$

where m represents the vector (m_{Ps}, m_{Lp}, m_{Pr}). Here the death-rate D is still included because cells have to be removed due to division. Also there could be an additional loss of cells due to toxicant, currents, or other environmental effects. For the simulations in Chapter 6 no additional death term was used.

5 Model Analysis

5.1 Assumptions

In Chapter 3 the model for the individual was presented in a general way. Several functions were not specified because they are still a matter of scientific speculations. However, to analyze the model these functions have to be known. The following assumptions are made:

- Polysaccharide incorporation (Section 3.2.1): One possible formulation for the function g_{Ps} for catabolism is

$$g_{Ps}(\bar{E}, m_{Ps}) = \begin{cases} \kappa_{Ps,0} \frac{\frac{m_{Ps}}{\bar{E}}}{\kappa_{Ps} + \frac{m_{Ps}}{\bar{E}}} & \text{for } \bar{E} > 0 \\ \kappa_{Ps,0} & \text{for } \bar{E} = 0 \end{cases} \tag{5.1}$$

  where κ_{Ps} (nd) is a constant, and $\kappa_{Ps,0}$ ($\frac{\mu mol}{s}$) is the maximum rate of catabolism for polysaccharides. This formulation assumes an inverse proportionality to the energy in the energy pool and a functional response to the available polysaccharides in the storage compartment.

  Alternatively, for simulations where the mass balance for phosphorus was included, the function g_{Ps} was chosen as

$$g_{Ps}(\bar{E}, m_{Ps}, P) = \begin{cases} \kappa_{Ps,0} \frac{1}{(\kappa_{Ps,1} + \kappa_{Ps,2} \frac{\bar{E}}{m_{Ps}}) \frac{\kappa_{Ps,3}}{P_i}} & \text{for } \bar{E} > 0 \\ \kappa_{Ps,0} & \text{for } \bar{E} = 0 \end{cases} \tag{5.2}$$

where $\kappa_{Ps,*}$ (nd) are constants. This formulation includes the dependence on the internal phosphorus pool, because catabolism produces energy in form of ATP. ATP can, however, only be produced if phosphorus is present. Equation 5.2 is similar to Equation 5.1 in a way that it assumes high catabolism if energy in the cell is low or storage pool is large.

- Lipid incorporation (Section 3.2.2): For lipid incorporation, the same functions are used as for polysaccharide catabolism, with m_{Ps} replaced by m_{Lp}.
- Excretion (Section 3.6): Excretion has been modeled according to the equation:

$$\rho_{ex,*} = j_* \frac{\phi_i}{m_{Pr}} \tag{5.3}$$

where j_* is a proportionality constant for excretion of the element *.

See Appendix C for a summary of the model equations in the notation used so far as well as in the notation used in the computer code.

5.2 System of Equations and Solvability

The model equations form a system of over 10 coupled, nonlinear, ordinary differential equations coupled with one difference equation. Before aiming for a solution of the system of ordinary differential equations, the question of existence has to be answered. The existence theorem for a solution of a system of ordinary differential equations is (see Goldberg and Schwartz [19]):

THEOREM: Existence

Let $x' = f(t, x)$ be a system of ordinary differential equations and let $x(t_0) = x_0$ be the

initial value. If f is continuous on $|t - t_0| \leq T$ and $||x - x_0|| \leq R$, where T and R are constants, then there exists at least one solution of the system in the interval $[t, t_0]$.

It can be easily seen that all equations used in the model are continuous, the only exception being Function 4.10 for the population dynamics. This function is given in a discrete representation with time-step $\triangle t$.

The following observations can be made:

The discrete function for the phytoplankton populations 4.10 leads to discrete changes in the sums of total uptake and excretion of the substances in water. The grazer equation is also no longer continuous. This leads to jumps in the substance equations and therefore continuity is also lost in the individual model equations.

However, this loss of continuity does not effect the time intervals in between the time steps. In the time-intervals $[0, \triangle t)$, $(\triangle t, 2\triangle t)$ and so on, all functions of the model are continuous (including the population sizes δ which are constant) and therefore the existence theorem is applicable and guarantees existence of solutions in these intervals.

For uniqueness the functions f need also to fulfill a Lipschitz-condition. All functions in the model are differentiable (via continuous extensions) and therefore Lipschitz continuous in compact intervals. Therefore, uniqueness of the solution in the time intervals $[0, \triangle t)$, $(\triangle t, 2\triangle t)$ and so on follows.

5.3 Numerical Methods

An analytical solution of the nonlinear system of ODE's cannot be found easily - if at all. Therefore numerical methods have been used. There are many numerical methods providing different accuracy and requiring different amounts of work. As one can expect higher accuracy require more work. Some of the methods are

- The Euler Method: The Euler Method is one of the easiest methods for an approximation of a solution of a nonlinear system of ordinary differential equations. For each time-step the derivatives have to be evaluated once. The accuracy changes with the choice of the time-step.
- Multistep formulas: A multistep formula such as the Adams-Bashforth Method (see for example Conte and de Boor [8]) uses information about the solution at more than one point. It increases accuracy with little increase in the number of calculations to be done, if information of preceding time steps are stored in the memory.
- Runge-Kutta Method: Runge and Kutta invented a more sophisticated method for an approximate solution of systems of ordinary differential equations. The method is more accurate than the Euler method. A second order Runge-Kutta Method does requires approximately the double amount of work than the Euler Method.

Many other methods are available, but most of them require even more work. The results have been obtained using the simple Euler method or a second order Runge-Kutta Method.

Convergence of the Euler Method and the Runge-Kutta Method follows from the existence of a unique solution and the boundedness of the derivatives. Finding an optimal time step for the method is difficult. Because simulations obtained using different step-sizes showed no

differences in the qualitative behaviour of the model, no further attention has been paid to the time step. However, for a quantitative analysis of an experiment or a data set obtained from the field, the importance of the time step has to be examined carefully.

6 Results and Discussion

A mathematical model with an ecological application can be tested on data from experiments or from the field. Complex models such as this are very flexible and one can imagine that there exist parameters that fit the model to many real world data sets. The question, however, is if, after parameters are chosen for one species under certain conditions, the model is also applicable to other environmental conditions without changing parameters. In this case the model would be useful for prediction of growth and composition of phytoplankton assemblages under certain conditions.

First a summary of the results is given before some results of the individual simulations are presented. A discussion about sensitive parameters follows these results.

6.1 Method

The qualitative behavior of the model was tested with a computer code written in the language C. Simulations were performed on Sun SPARC Stations (different models). One version of the code makes use of the Euler Method, whereas another version uses the Runge-Kutta Method. The simulations performed with the Runge-Kutta Method include the mass balance for phosphorus (makes use of the alternative formulations for photosynthesis and catabolism given in the text). Table 6.1 summarizes the performed simulations. If not men-

Table 6.1: Performed simulations: conditions and results

Num	Conditions	L/M	Results
	one species simulations		
1	constant nutrient concentrations and irradiance; no catabolism	10d, E	steady growth/reproduction pattern after 2 d.
2	only initial nutrients; constant irradiance	5d, E	growth until nutrients depleted (3 d); then storage production only.
3	same as 2 with lower irradiance	5d, E	one reproduction only; steady state achieved after 2 d.
4	only initial nutrients; 12:12 day-night cycle	5d, E	reproduction usually during the day, storage shows night-day fluctuations.
5a/ 5b	only initial nutrients, 12:12 day-night cycle, low maintenance rate	10d/ 80d, E	growth until nutrients are depleted (9d), then accumulation of storage until maintenance of storage uses all produced energy (70 d).
5c/ 5d	same as 5a/5b with higher maintenance rate	10d/ 80d, E	growth until nutrients depleted (10 d), then steady day-night pattern; at night all storage catabolized and no ATP.
6a	constant nutrient input	250 d, E	steady pattern after 20 d.

Num = number of simulation; L/M = length of simulation in days (d) and numerical method used; E = Euler Method; RK = Runge-Kutta Method.

Table 6.1, continued

Num	Conditions	L/M	Results
6b	same as 6a, but no sinking and grazing	250d, E	steady pattern with increasing period.
7	only initial nutrients	14.5d, RK	growth slow after 5 days because phosphorus concentrations are low.
8	constant nutrient input	25d, RK	speed of growth, ATP and storage pools decrease with increase in time.
	multiple species simulations		
9a	two species, one does not need silicate, has smaller cells, and lower maintenance rate; constant nutrient input	1d, RK	similar growth patterns for both species.
9b	same with very low silicate input	37d, RK	only species without silicate requirement is able to grow; other species accumulates storage.
10	low phosphorus input, 18:6 day-night cycle with compared to other simulations low irradiance	59d, RK	smaller species grows much faster; both species cannot produce enough energy to accumulate storage (due to phosphorus limitation).

Num = number of simulation; L/M = length of simulation in days (d) and numerical method used; E = Euler Method; RK = Runge-Kutta Method.

tioned explicitly, all simulations included catabolism for polysaccharides and lipids, constant temperature, sinking, and grazing. Grazing was constant, independent of cell size of phytoplankton. The internal nutrients nitrate, phosphorus and silicate were modeled.

6.1.1 *Skeletonema costatum*

Parameters for the diatom *skeletonema costatum* were estimated for use in the simulations. This species is widely distributed. It is a well studied species and therefore much relevant literature can be found. References for the parameter values are mentioned in Appendix B.

To start simulations, data from experiments performed in laboratories under fixed irradiance and nutrient conditions were chosen. Many model parameters had to be estimated because not all parameters can be found in the literature or, if they can, they appear in different articles about experiments under very different conditions. It might therefore be better to choose few data sets for comparable conditions and estimate the missing parameters. If growth in the computer simulation follows growth measured in these experiments, one hopes that the model is also able to simulate experiments done under other environmental conditions.

6.2 Summary of Results

General comments for all simulations:

- The time step for the numerical method was chosen to be between 0.5 seconds for short term simulations (1-10 days) and up to 3 seconds for the very long simulations (up to

250 days). For most simulations, 1 second was chosen.

- Environment was assumed to be homogeneous, with cells distributed equally. No movement was assumed.
- Results of the simulations were written to data files. The figures shown have been created with Gnuplot and Xfig for Unix.
- The jumps visible in the graphs result from reproduction when all internal cell compartments are divided into half. Actual status of each compartment was printed out every 10-60 minutes for the short term simulations and every 1-3 hours for the long simulations. Therefore, some of the figures show corners that are actually fast but smooth changes in compartments (none of the equations has a singularity). However, some corners can also be the result of the numerical solution method (overshooting of limits).
- Temperature changes are often slow in the environment. Temperature was chosen to be constant for all simulations.
- Most of the figures are from simulations that include processes of catabolism, maintenance, respiration, and excretion. Simulations without these flows have been performed but yielded expected, nonmeaningful results (such as unlimited growth of internal storage pools, energy pool or nutrient pools).
- If maintenance requirements were higher than the energy gained through photosynthesis and catabolism, it was assumed that all growth processes (storage and structure) stop. Catabolism continues, however, providing additional energy for maintenenance.
- Losses of cells were due to sinking and a grazer population. Losses turned out to have little impact on the dynamic behavior of the individual cell. This was different for long term simulations when populations sizes were large.

Simulations of one species under constant nutrient conditions (constant concentrations or constant input per time) resulted in a steady pattern of population growth and storage production (Simulations (1) and (6b)). Simulations under different conditions showed promising results for all three focus points of the model (nutrient limitation, energy limitation, and species composition).

1. Nutrient limitation: In the simulations, low nutrient concentrations decreased the speed of growth or stopped growth completely (e.g. Simulations (2), (4), (5), (6b), (7), (8)). During times of high irradiance (during the day), nutrients were in almost all cases the limiting factor for speed of growth (e.g. Simulations (4), (5)). Low concentrations of specific nutrients only resulted in a change of storage composition. If, for example, phosphorus was the limiting nutrient, cells shifted their storage production to polysaccharides, a storage material that does not contain phosphorus (e.g. Simulation 2).
2. Energy limitation: Limited availability of energy resulted in a decrease in the growth rate or a complete stop of growth (e.g. Simulations (3), (4), (5), (6b)). Energy limitation occurred during the night and other times of low irradiance. Energy limitation also resulted in a decrease or total disappearance of storage materials through catabolism of these materials (e.g. Simulations (3), (4), (5), (6b)). During times of limited or zero growth but abundant energy, the cell is still able to produce storage materials. If maintenenance for storage is zero, this production is not limited. The inclusion of maintenance requirements for storage materials prevented extensive production of storage materials (e.g. Simulations (3), (6b)).
3. Species competition: During simulations with two species it was examined that growth of one species is not influenced by the other species under conditions where no nutrient is limiting (e.g. Simulation 9a). If one species required an additional nutrient for growth (silicate was used in the simulations) in contrary to the other, and supply of

this nutrient was limited, then this species was growing only slowly (e.g. Simulation 9b). Differences in speed of growth between two species could also be examined under phosphorus limitation. Smaller cells seemed to be less effected by phosphorus limitation than larger cells. Even though a higher maintenance rate per volume for the species with smaller cells was assumed, the smaller cells seem to be less energy limited than the larger cells (larger volume means finally higher maintenance requirements for larger species). Therefore, smaller cells outperform larger cells (Simulation 10).

The following sections show some of the individual results, including graphs and further comments.

6.3 Individual Results

This section shows some of the simulations in greater detail. The figures that belong to a simulation always show the absolute number of cells (per liter), and some of the internal and external pools (μmol per l). If a day-night cycle was used in a simulation, irradiance during the day was calculated according to the formula

$$E_d(0)sin(\frac{\pi t}{D}) \tag{6.1}$$

(Platt et al [40]), where $E_d(0)$ (μmol $s^{-1}\,m^{-2}$) is the maximum irradiance and D (h) is the daylength. Simulations were usually started at midnight.

6.3.1 Simulation (1), Unlimited Growth.

Simulation 1 (Figure 6.1) shows growth of *Skeletonema costatum* under constant environmental conditions. Nutrient levels and irradiance were constant (24 h irradiance of 77μmol $s^{-1}\,m^{-2}$). Catabolism was turned off for this simulation. Reproductive rate was 2.5 per day which is a realistic value for the given conditions. All jumps in the model are results of reproduction.

After the first three reproductions, all internal pools show a steady pattern, showing fast increase between the reproductions. All internal nutrient pools and the energy pool show constantly high values. It does not appear that one of the nutrients or energy are growth limiting. Maximum speed of biosynthesis seems to determine speed of growth in this simulation.

6.3.2 Simulation (2), Nutrient Limited Growth.

Simulation 2 (Figure 6.2) includes catabolism for both lipids and polysaccharides. Maintenance was assumed to depend on proteins, lipids, and polysaccharides. Light was constant at 77μmol $s^{-1}\,m^{-2}$. No nutrient input in the system except initial concentrations was assumed.

Results show a growth rate of 2.5 divisions per day before nutrients are depleted and growth stops. For the first 80 hours, the growth rate is similar to the growth rate in Simulation 1 with unlimited nutrient supply. However, division rate slows down slightly with increasing time. After 80 hours, nitrogen and phosphorus are depleted, because no input of these nutrients was assumed and growth stops. Silicate is almost depleted in the

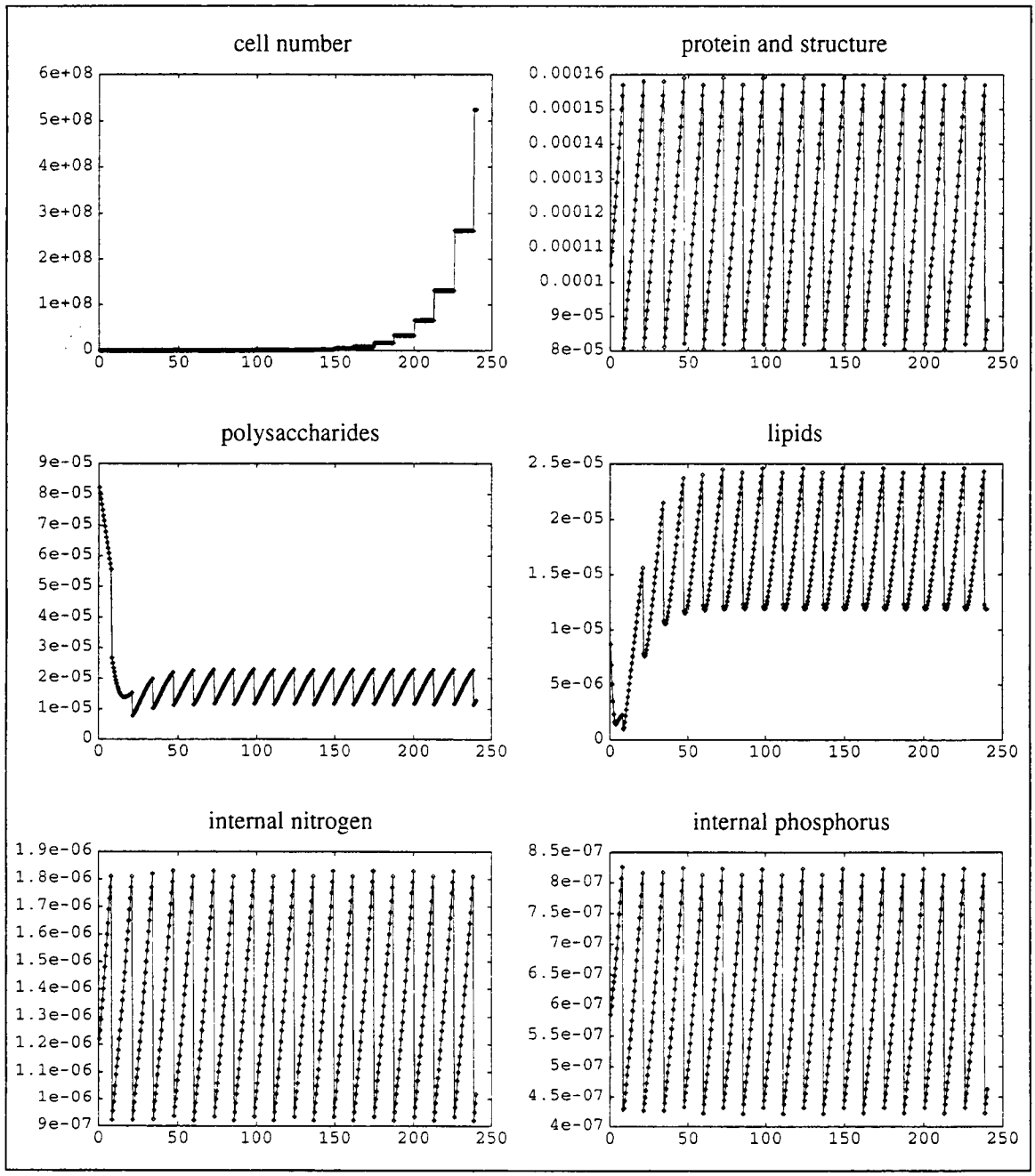

Figure 6.1: Simulation (1). Cell number in $\# \, l^{-1}$, internal pools in μmol, external concentrations in $\mu mol \, l^{-1}$, versus time in hours.

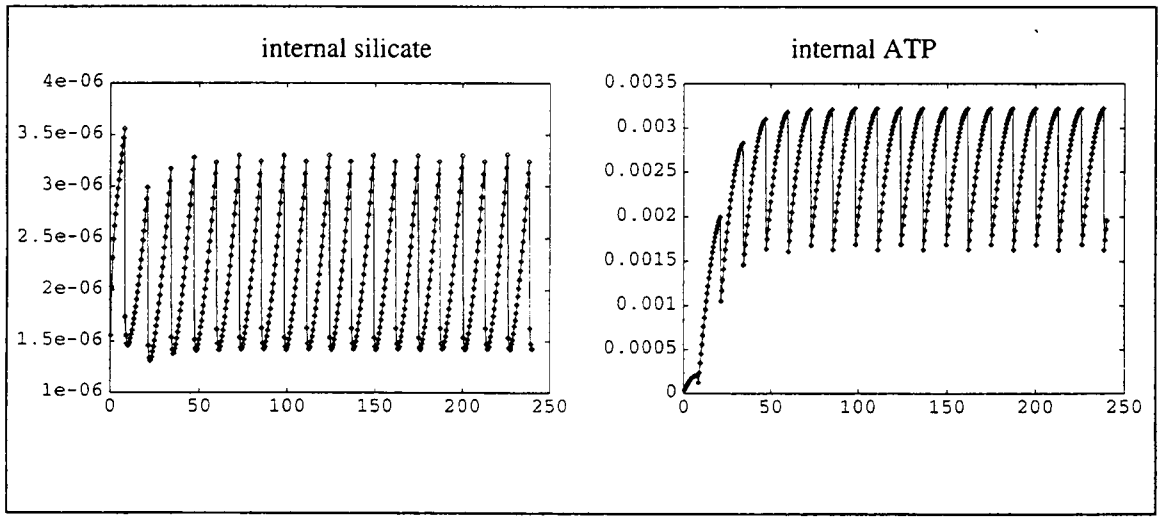

Figure 6.1, continued.

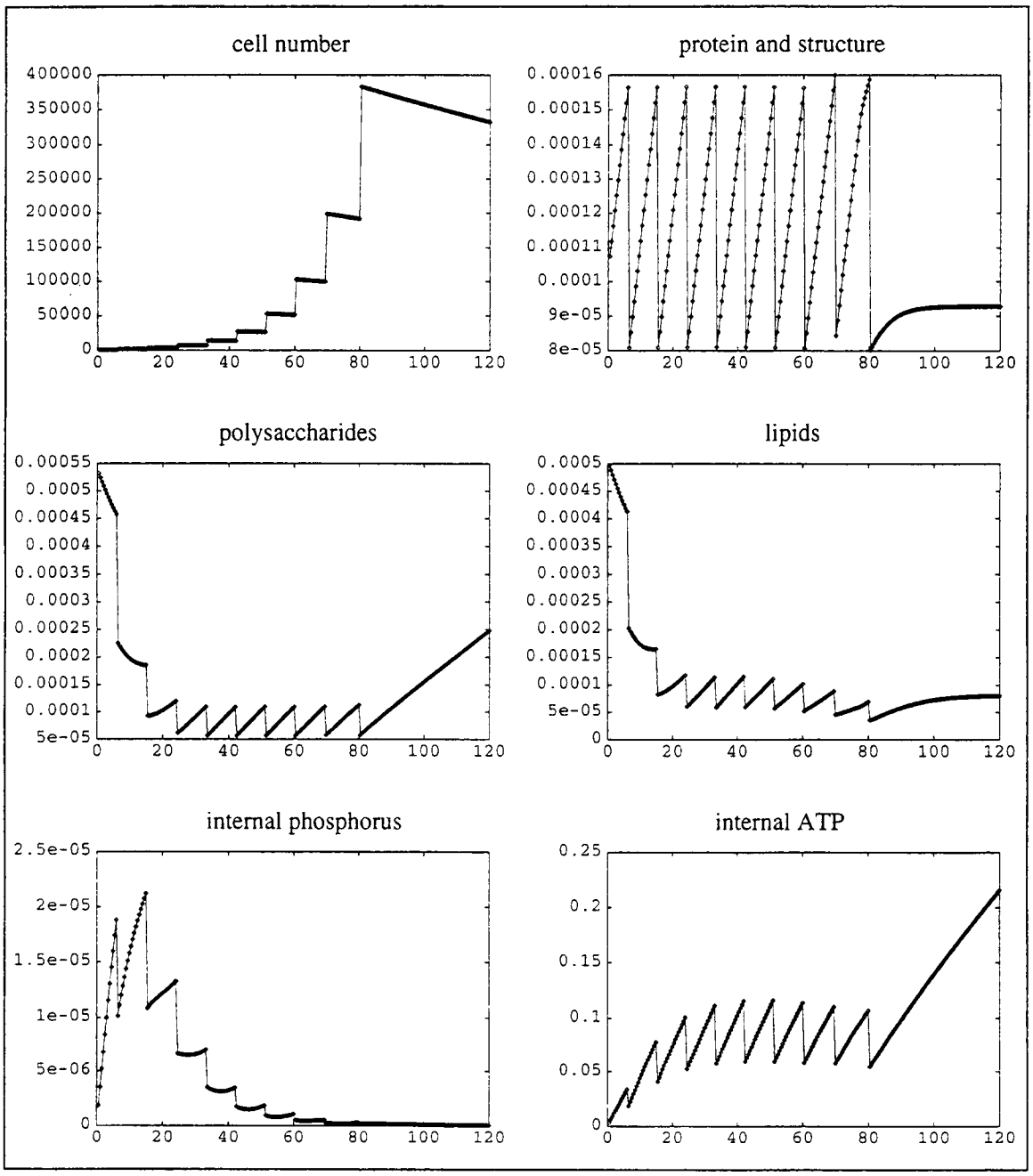

Figure 6.2: Simulation (2). Cell number in $\# \, l^{-1}$, other scales μmol, versus time in hours.

environment but still abundant in the cell. After reproduction stops, lipid concentration remains constant (phosphorus is depleted), polysaccharide concentration increases because enough energy from photosynthesis is available, even though photosynthesis is reduced by more than 50% due to nutrient depletion in the cell. Finally, however, maintenance costs of polysaccharides will exceed the available energy in the cell, stopping additional polysaccharide production.

6.3.3 Simulation (3), Low Irradiance

Simulation 3 (Figure 6.3) is under the same conditions as Simulation 2, but under constantly low irradiance of 17 μmol $s^{-1}\,m^{-2}$. The results show a total depletion of the storage compartments after 20 hours. The energy gained through catabolism was enough to yield one reproduction after 20 hours. Interior nitrogen, phosphorus, and silicate pools reach a steady state after growth stops, and as a result also external substance concentration remain constant for the rest of the simulation.

Examining details of the graph yields some interesting results. The ATP concentration in the cell remains zero for the first ten hours because maintenance costs are higher than yielded energy from catabolism and photosynthesis (gain from photosynthesis remains below maintenance requirements for the whole time period because of the low irradiance). After ten hours, however, storage pools are reduced significantly, which reduces the maintenance costs. Therefore, after approximately 10 hours, ATP yield is higher than maintenance requirements. ATP is invested into growth. After division, however, growth continues just for another 11 hours before ATP is depleted again. The reason is the depletion of storage material that provided the energy. The rest of the time maintenance for proteins is higher than ATP gained through the photosynthesis. Therefore the cell enters a steady state (no

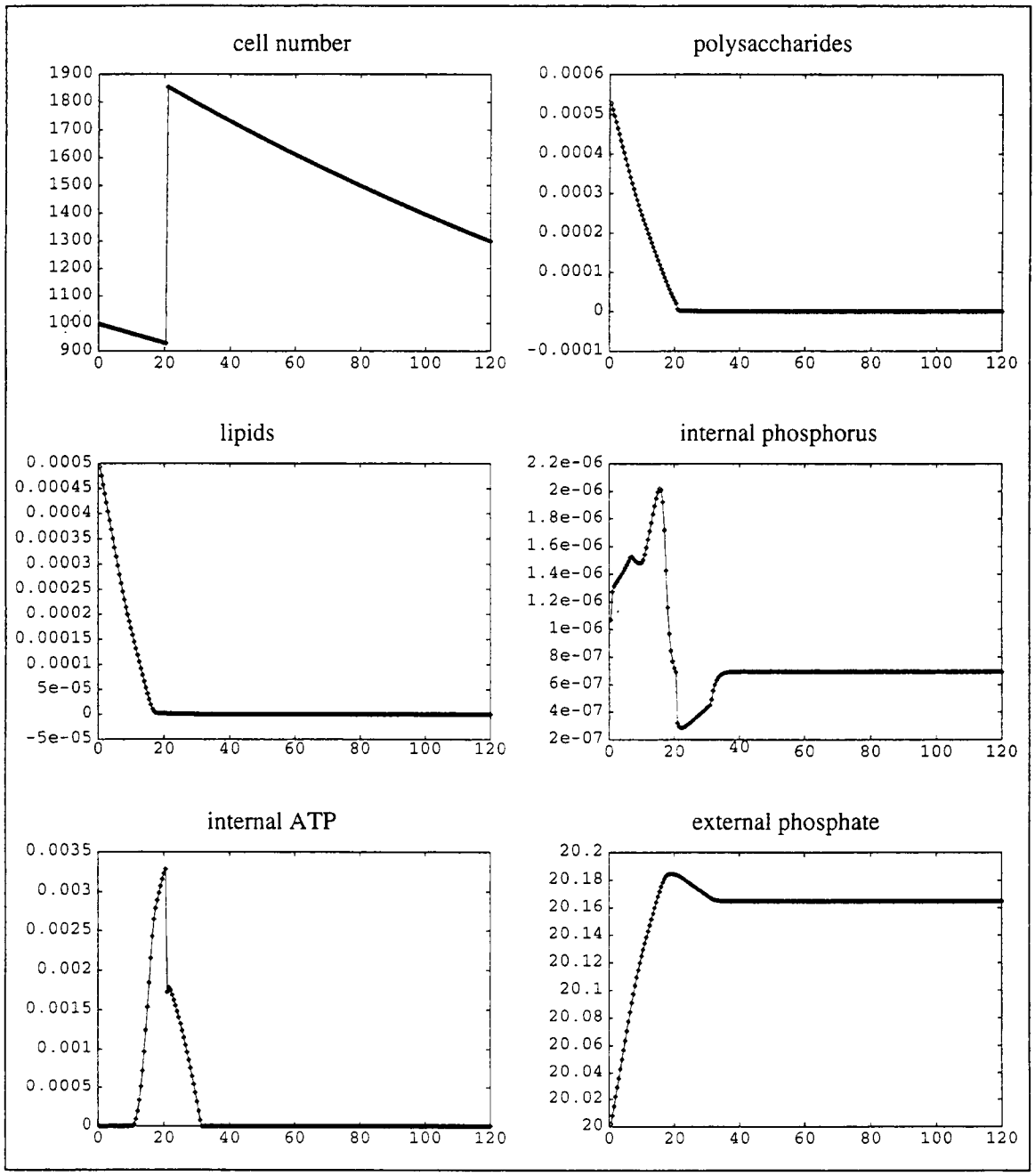

Figure 6.3: Simulation (3). Cell number in $\# \, l^{-1}$, internal pools in μmol, external pool in $\mu mol \, l^{-1}$, versus time in hours.

growth).

Looking at the external phosphate concentration, one recognizes that the concentration increases from the beginning of the simulation until about 20 hours (which is the time when reproduction takes place). Also, the internal phosphorus pool is on the rise. This is a result of the lipid catabolism that frees phosphorus from storage. Lipids start to get depleted before reproduction. This results in the sudden decrease of the internal phosphorus pool right before reproduction takes place. During this term even some phosphorus is taken back up from the environment. This uptake continues after reproduction until growth stops.

6.3.4 Simulation (4), Day-Night Cycle.

Simulation 4 (Figure 6.4) was for a 12:12 day-night cycle with a maximum irradiance of 277 μmol $s^{-1}\, m^{-2}$.

This simulation shows energy limited growth at night and nutrient limited growth during the day. In five days, 6 reproductions occurred (1.2 reproductions per day). The time between reproductions is not constant. Reproduction occurs normally during the day, on the third day 2 reproductions took place (one in the morning, one in the evening). Initial amounts of storage materials seemed to be high. High catabolism in the first and second night brought down the levels reducing maintenance requirements significantly. Polysaccharides and lipids show increase during the day, decrease at night. The energy gained at night is partially used for maintenance, but partially for growth as one can see the slow protein increase during the night.

Internal nitrogen, phosphorus, and silicate show increase at night until a maximum con-

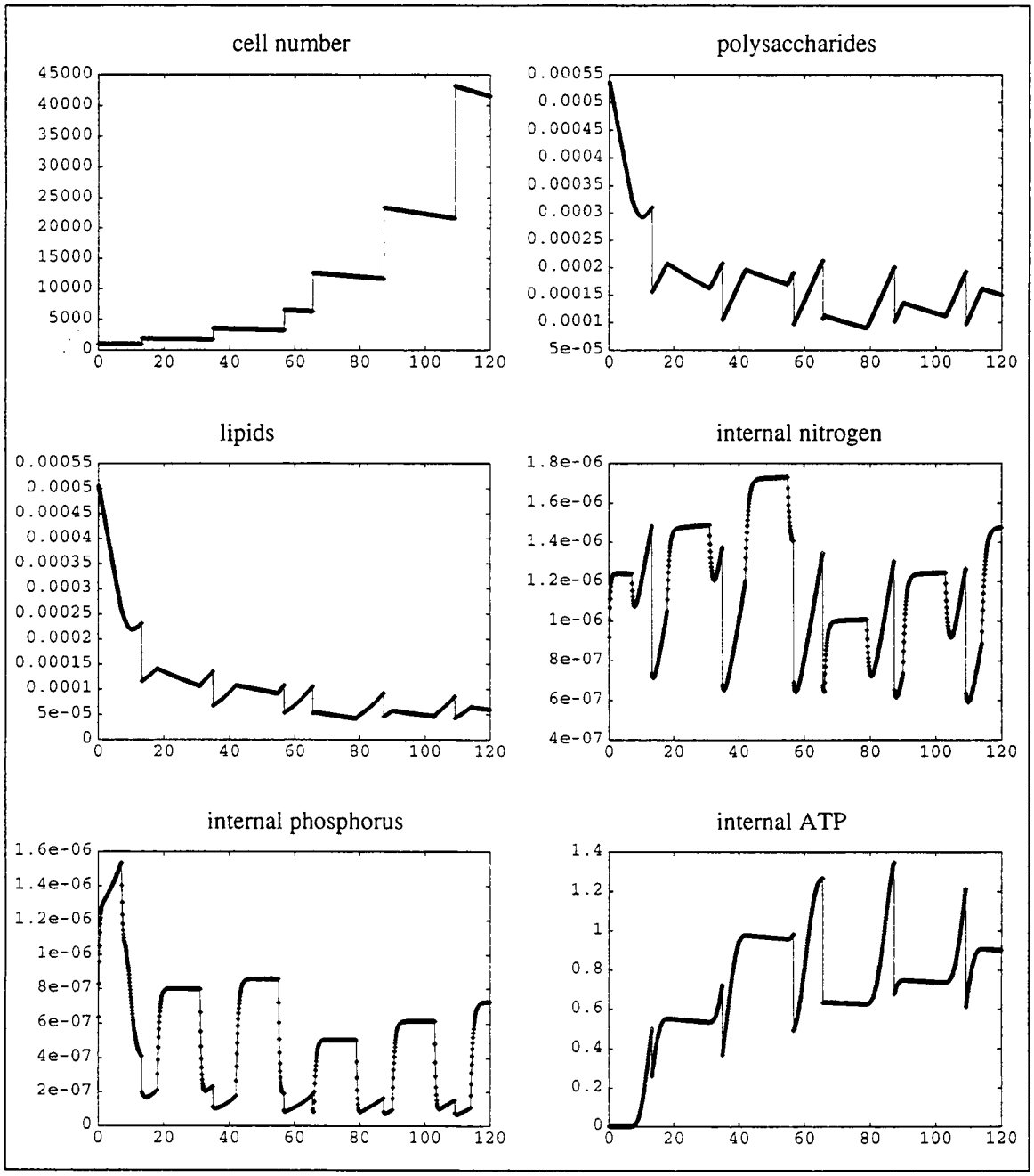

Figure 6.4: Simulation (4). Cell number in $\# \, l^{-1}$, other scales μmol, versus time in hours.

centration is reached. Again the graph for internal phosphorus shows a different behavior during times of lipid catabolism (especially during the first night). ATP concentrations are only low at the beginning when the high storage compartments

require maintenance energy. Later ATP remains at fairly high concentrations. External nutrients decrease but are still at high levels after five days.

6.3.5 Simulation (5a) to (5d), Low and High Maintenance Rate.

Simulations (5a) to (5d) (Figures 6.5 to 6.8) compare two different maintenance rates. Compared to Simulations (1) to (4), parameters for energy budgets were changed in order to get more realistic ATP levels in the cell. Simulations were with initial nutrient input only. A 12:12 day-night cycle with a maximum irradiance of 277 μmol s^{-1} m^{-2} was assumed. Simulations (5a) and (5b) are simulations for a low maintenance rate for 10 and 80 days, respectively. Simulations (5c) and (5d) are for the high maintenance rate for 10 and 80 days, respectively.

The two 80 days simulations show that growth continues for about 10 days before nitrogen depletion stops growth. Comparision of Simulations (5a) and (5c) shows that the species with the lower maintenance rate has one more reproduction after 9 days, showing already 9 reproductions compared to 8 for the species with higher maintenance rate. The reason is that a lower maintenance rate allows faster growth especially at night. A high maintenance rate can force a cell to catabolize all its storage at night and use it mainly for maintenance (Simulation (5c)), whereas a low maintenance rate allows a cell to use energy, gained through catabolism at night, for growth.

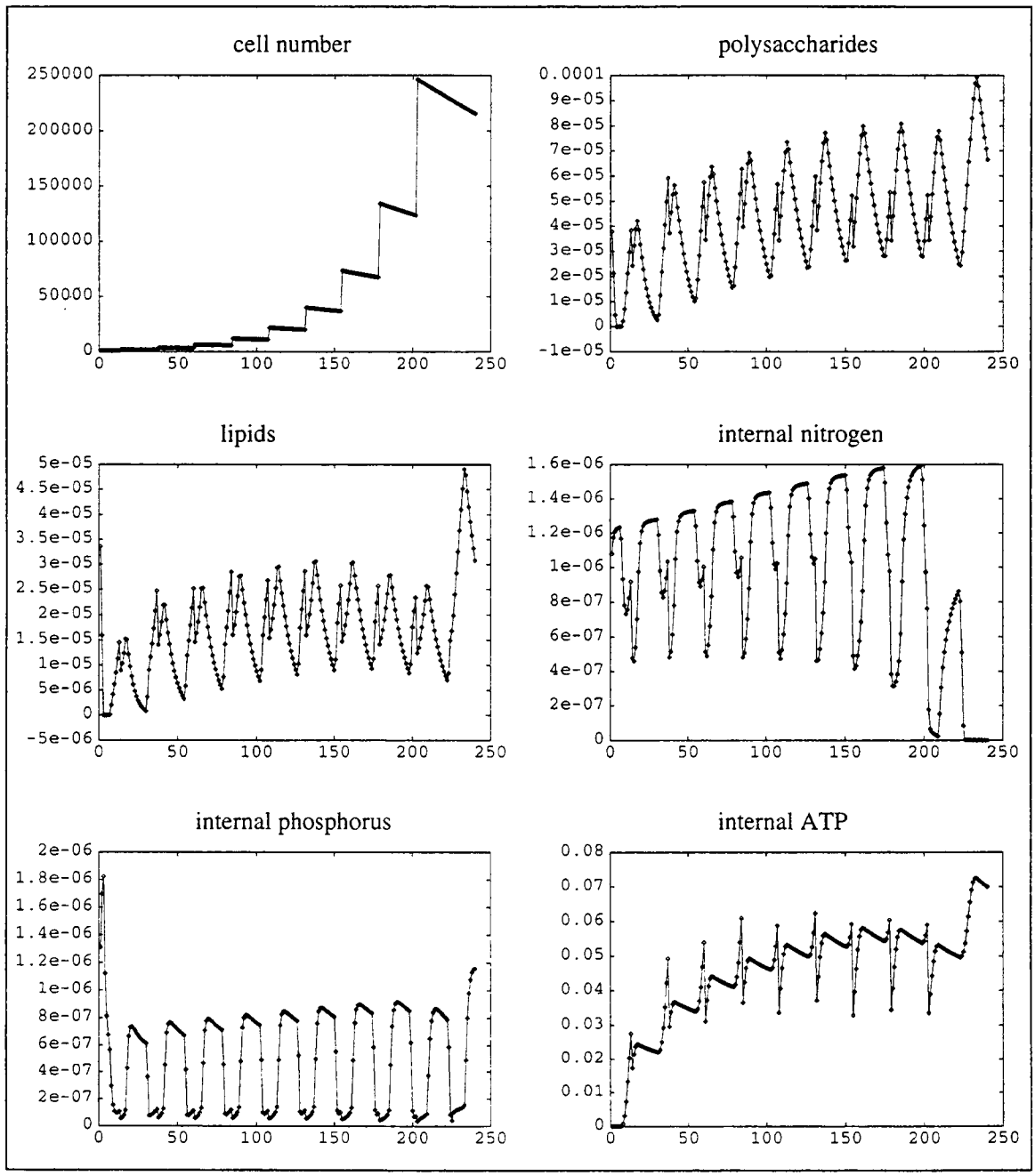

Figure 6.5: Simulation (5a). Cell number in $\# \, l^{-1}$, other scales μmol, versus time in hours.

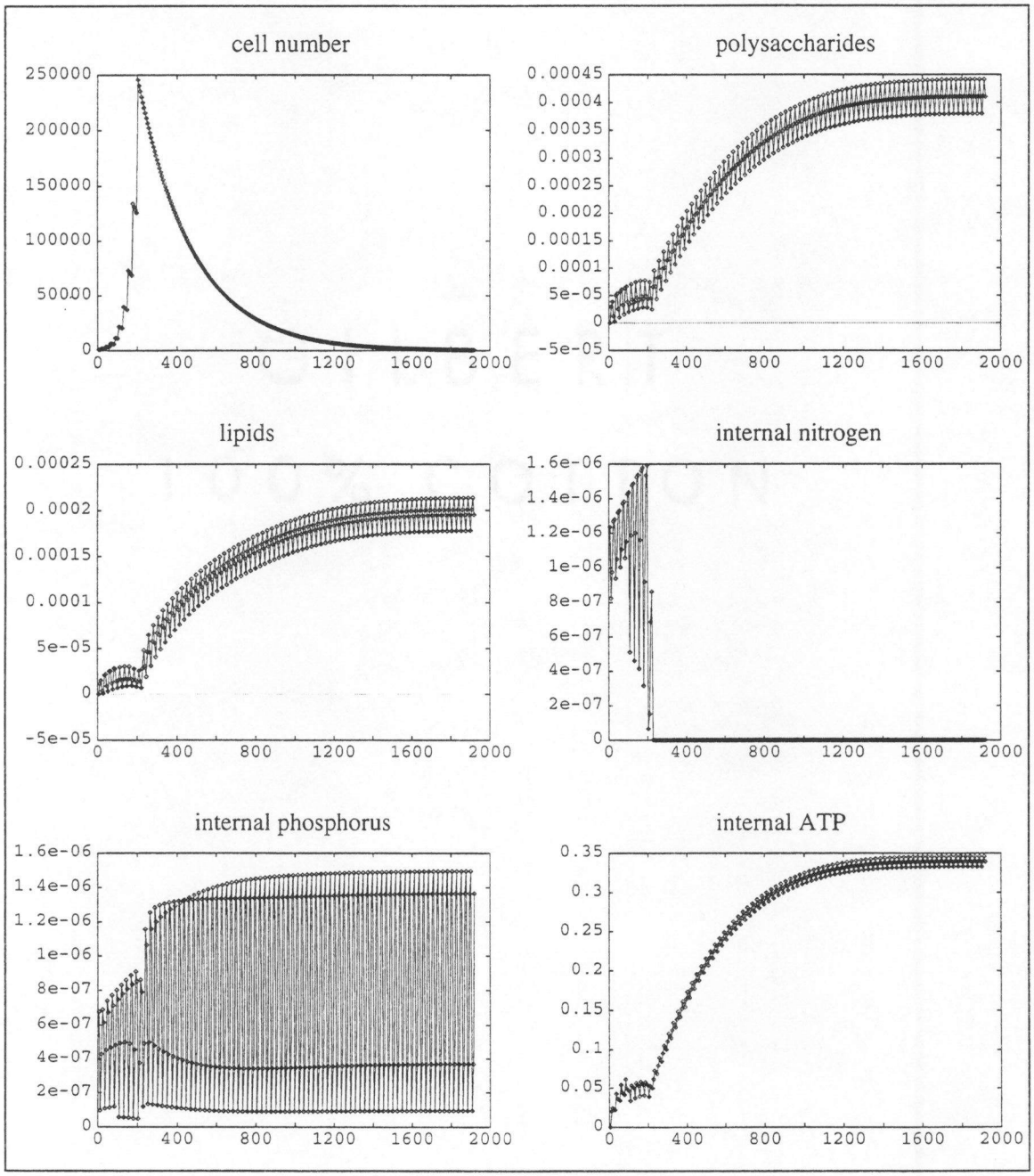

Figure 6.6: Simulation (5b). Cell number in $\#\ l^{-1}$, other scales μmol, versus time in hours.

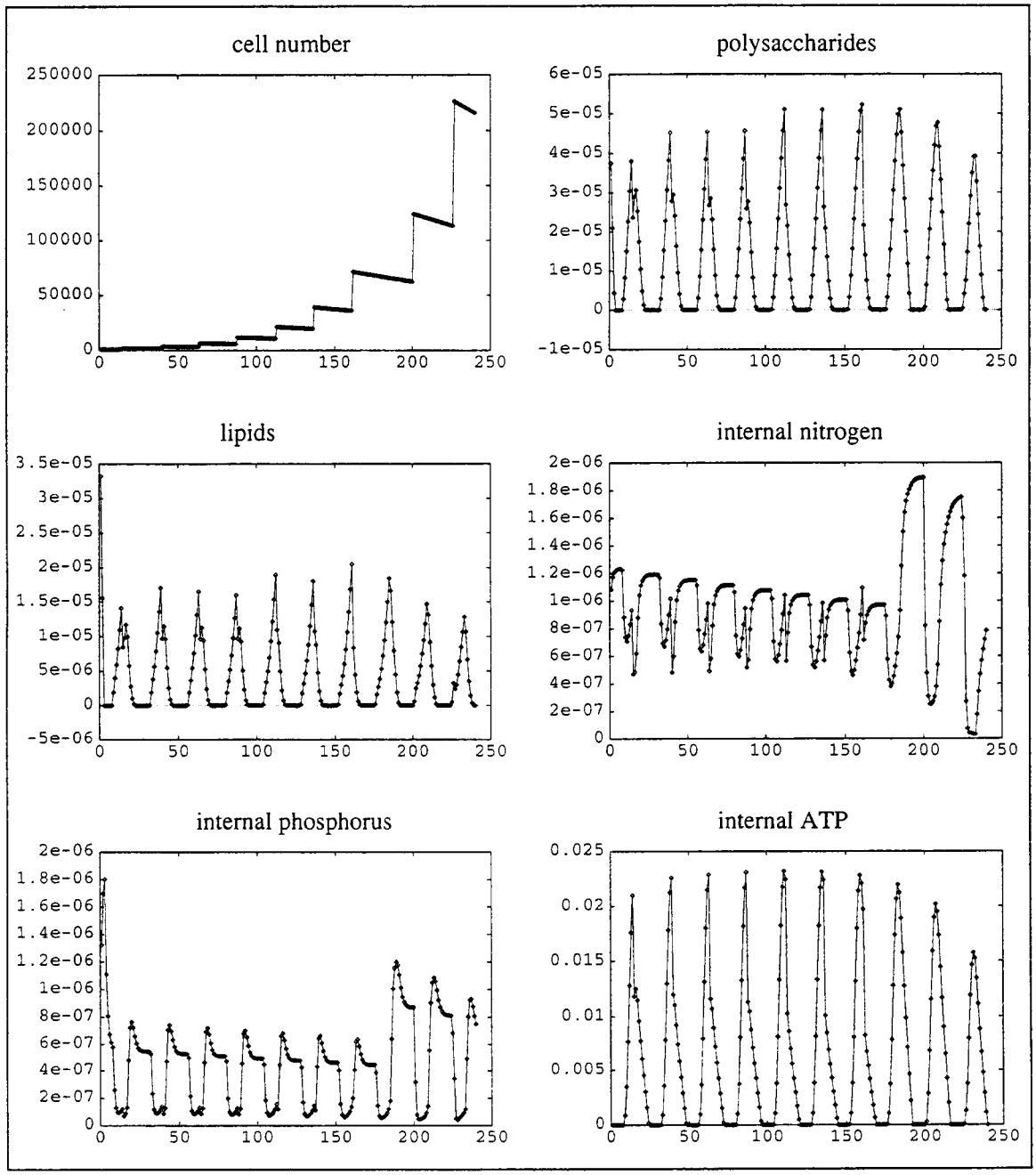

Figure 6.7: Simulation (5c). Cell number in $\# \, l^{-1}$, other scales μmol, versus time in hours.

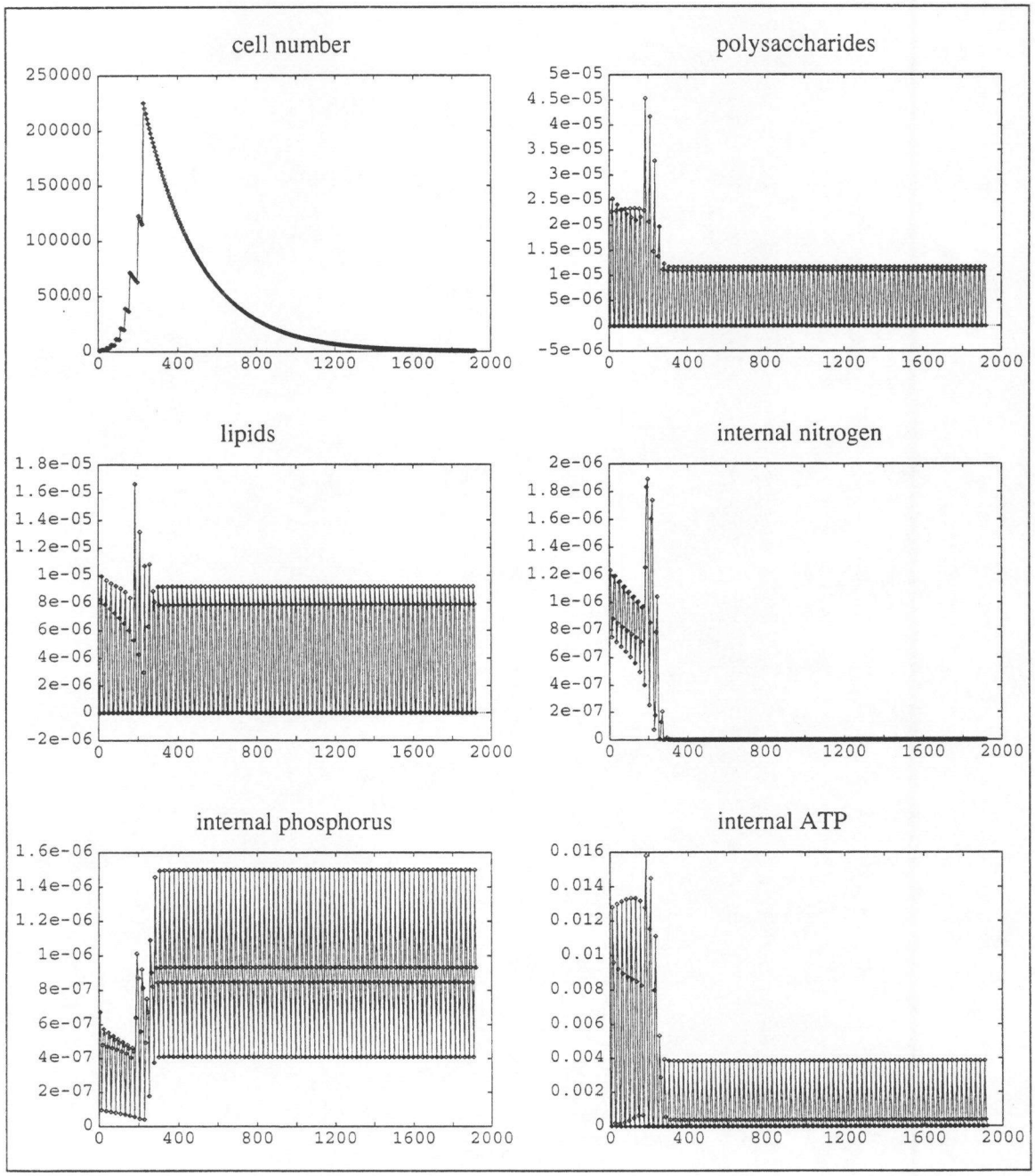

Figure 6.8: Simulation (5d). Cell number in $\# \, l^{-1}$, other scales μmol, versus time in hours.

After nitrogen is depleted, and growth stops, a high maintenance rate does not allow a cell to accumulate storage materials (Simulation (5d)). A low maintenance rate, however, allows a cell to store energy and nutrients through production of polysaccharides and lipids (Simulation (5b)). Finally, storage production stops also for the low maintenance rate because storage requires maintenance.

6.3.6 Simulation (6a) and (6b), Long Term Behavior.

The two Simulations (6a) and (6b) (Figures 6.9 and 6.10) were performed in order to test the model behavior over a long time period of 250 days. For these simulations, nutrients were supplied at constant rates during the entire time period. Simulation (6a) included a sinking and grazing term, whereas Simulation (6b) did not include any losses. Included losses in Simulation (6a) result in a steady pattern of population growth after ten days. If no losses are included, a repeating pattern also occurs after approximately 10 days. However, the times between reproductions are increasing because less nutrients are available for each cell after each reproduction. Simulation (6a) shows a stable population, Simulation (6b) a stable growth of a population.

6.3.7 Simulation 7, Nutrient Limited, Phosphorus Mass Balance

For Simulation 7 (Figure 6.11) the computer code based on Runge-Kutta's Method was used. This code includes the mass balance for phosphorus. Only initial nutrient input was assumed.

The figures show that phosphorus becomes a limiting factor of growth after approximately

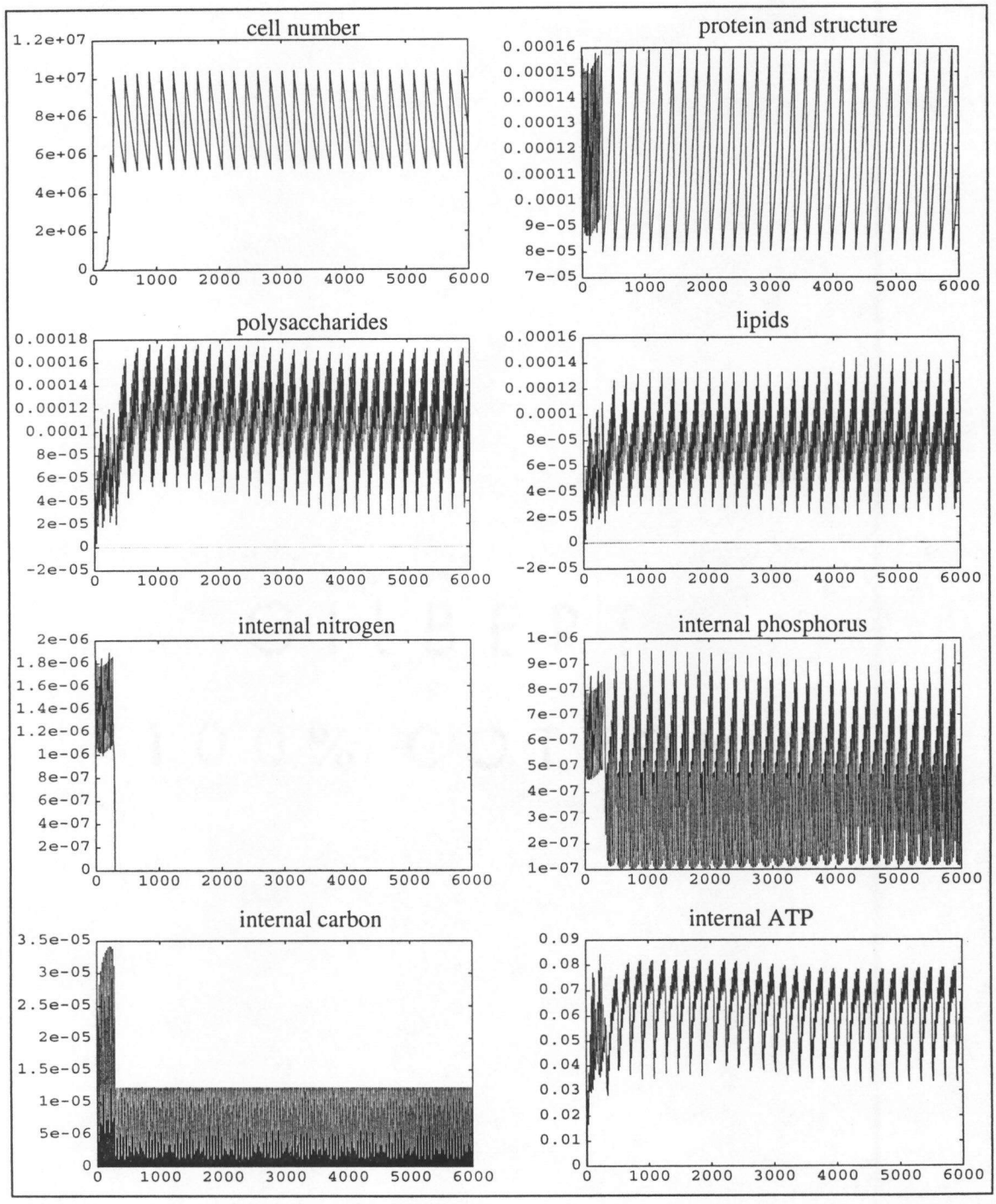

Figure 6.9: Simulation (6a). Cell number in $\# \, l^{-1}$, other scales μmol, versus time in hours.

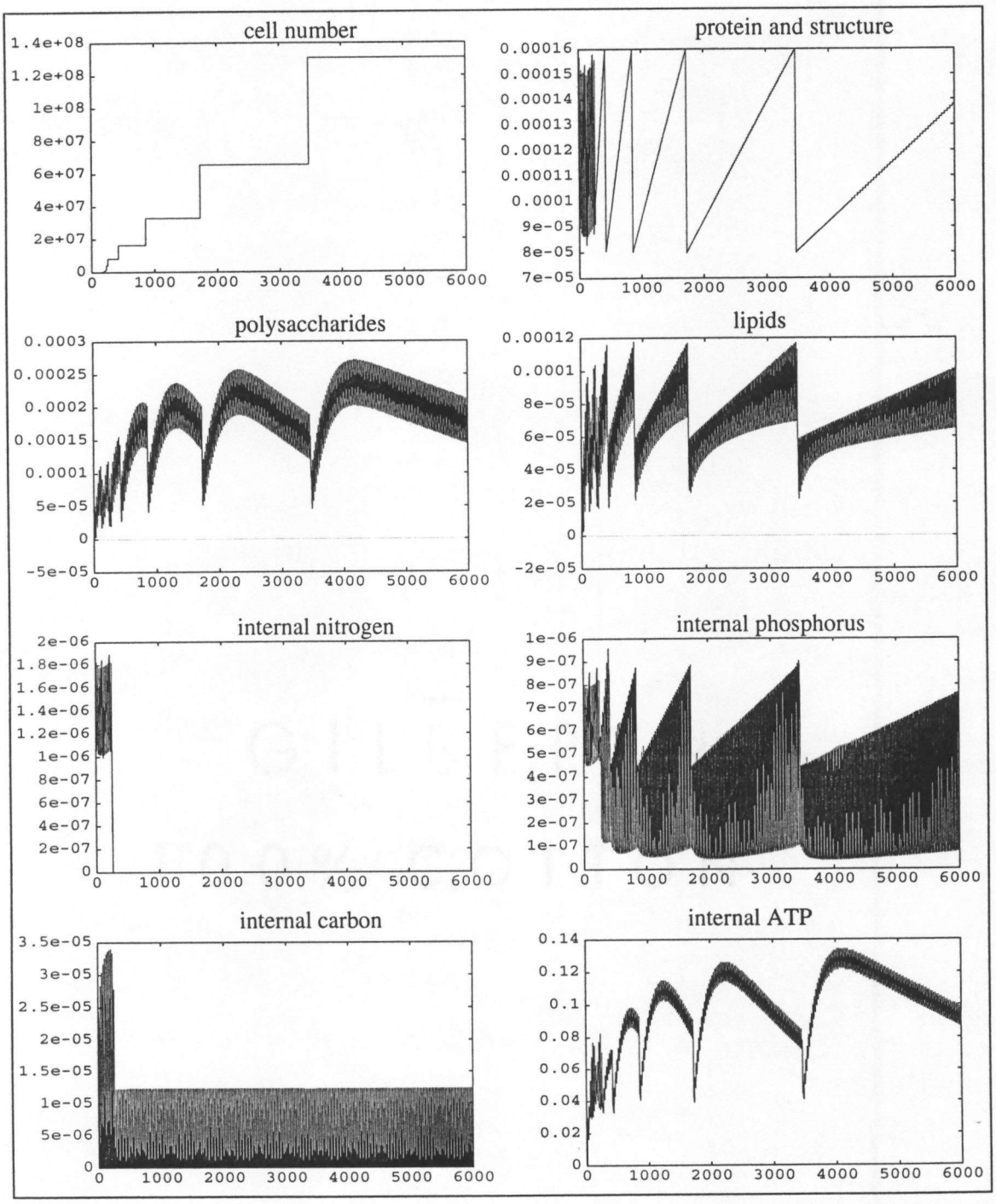

Figure 6.10: Simulation (6b). Cell number in # l^{-1}, other scales μmol, versus time in hours.

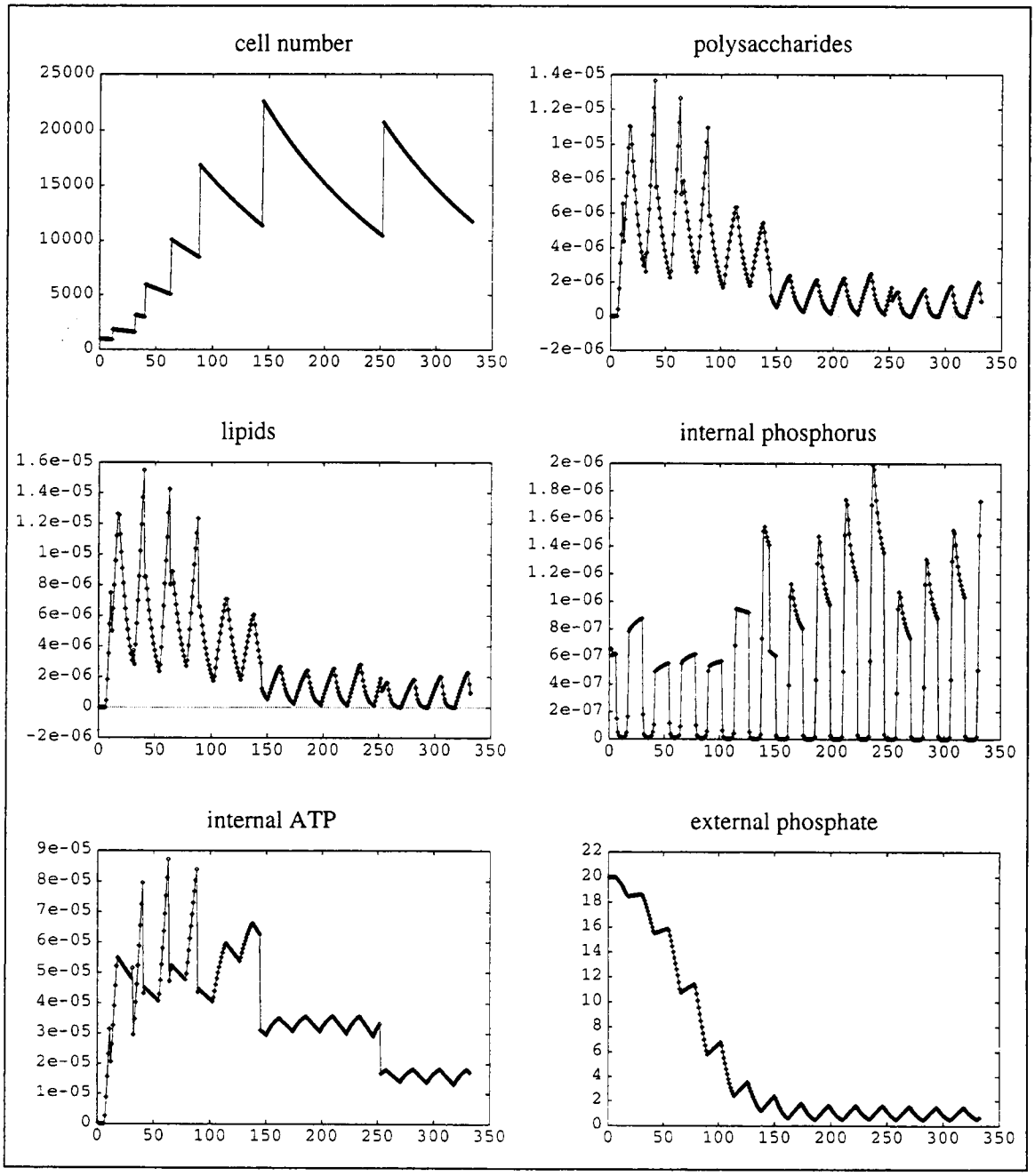

Figure 6.11: Simulation (7). Cell number in $\# \, l^{-1}$, internal pools in μmol, external pool in μmol l^{-1}, versus time in hours.

five days. Because no ATP can be produced without phosphorus, the internal ATP concentration also decreases. Therefore, no polysaccharides can be produced. This is a different result than the one obtained in Simulation 2, where polysaccharides could still be produced after phosphorus was depleted. This was possible in Simulation 2 because it did not include the mass balance for phosphorus.

6.3.8 Simulation 8, Constant Nutrient Inflow

Simulation 8 (Figure 6.12) was performed under the same conditions as Simulation 7 with constant nutrient input over the entire time. Length of the simulation was 25 days.

Results show an almost steady speed of growth. After 5 days, however, external phosphate concentration becomes low. However, growth does not stop. Instead, the cell produces much less storage during the day. External phosphate shows also high concentrations at night, because phosphorus is freed from lipids and from ATP.

6.3.9 Two Species Simulations

Simulation using Euler's method (figures not shown): Simulations are performed including two species with the same parameter files except that the one species needed silicate for growth, whereas the second species does not. All nutrient levels remained constant except silicate which had only an initial value and no additional input. The results showed what can be expected: both species grow with the same speed initially. After silicate becomes depleted, species one stopped growing whereas species two continued its growth.

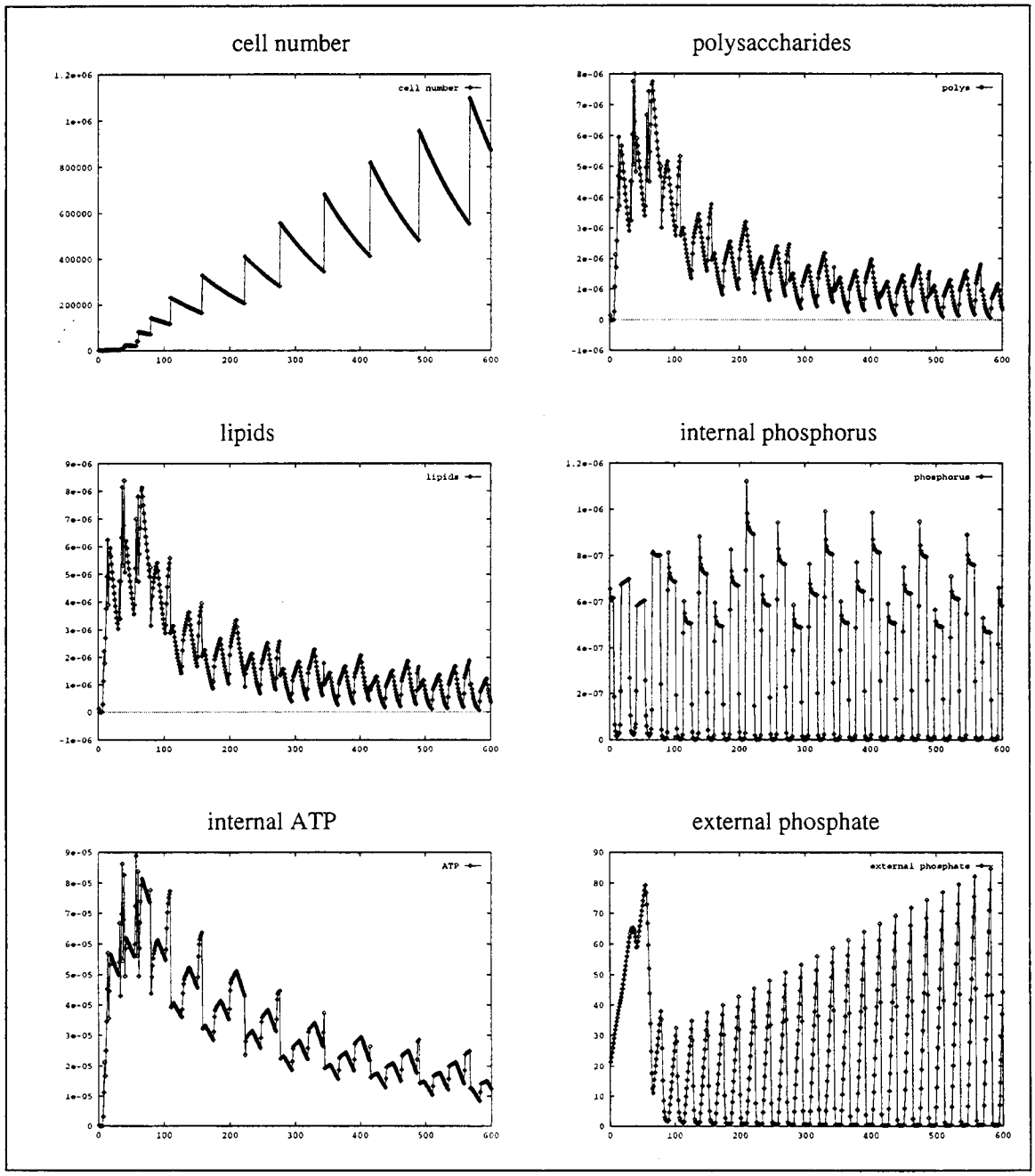

Figure 6.12: Simulation (8). Cell number in $\# \, l^{-1}$, internal pools in μmol, external pool in μmol l^{-1}, versus time in hours.

If the silicate level was held at a constant low concentration and all other nutrients had only initial values, differences in speed of growth could be recognized. Results showed growth of both species over the whole time period. However, the species depending on silicate grew at a much lower speed. The lower silicate level limits the growth of one species. The low silicate concentration determines the success of one species over the other.

Simulations using Runge-Kutta's method are shown in the following sections.

6.3.10 Simulation (9a) and (9b), Silicate Limited

Simulations (9a) and (9b) (Figures 6.13 and 6.14) were performed with the computer code using Runge-Kutta's method and including the mass balance for phosphorus. In each simulation, two species, each divided into two ecotypes, were simulated. Species one required silicate for growth, species two did not. In addition, species two consisted of smaller cells (lower minimal structural material), and had higher maintenance requirements. Simulation 9a assumed high nutrient inputs over the entire time period, whereas simulation 9b assumed high nutrient inputs for phosphate and nitrite but extremely low silicate input.

Results of 9a show fast growing species. Species two (smaller cells) grow faster than species one. In Simulation 9b, species one can only reproduce ones after 25 days, at a time when the species is almost extinct. Even though growth is not possible for these cells, storage production is high. Species two grows fast until phosphorus becomes limiting. The cells can still grow at a slower rate, lipids can, however, only produced in low amount. In contrast, cells accumulate storage in form of polysaccharides.

These simulations show success of one species over another if species have different re-

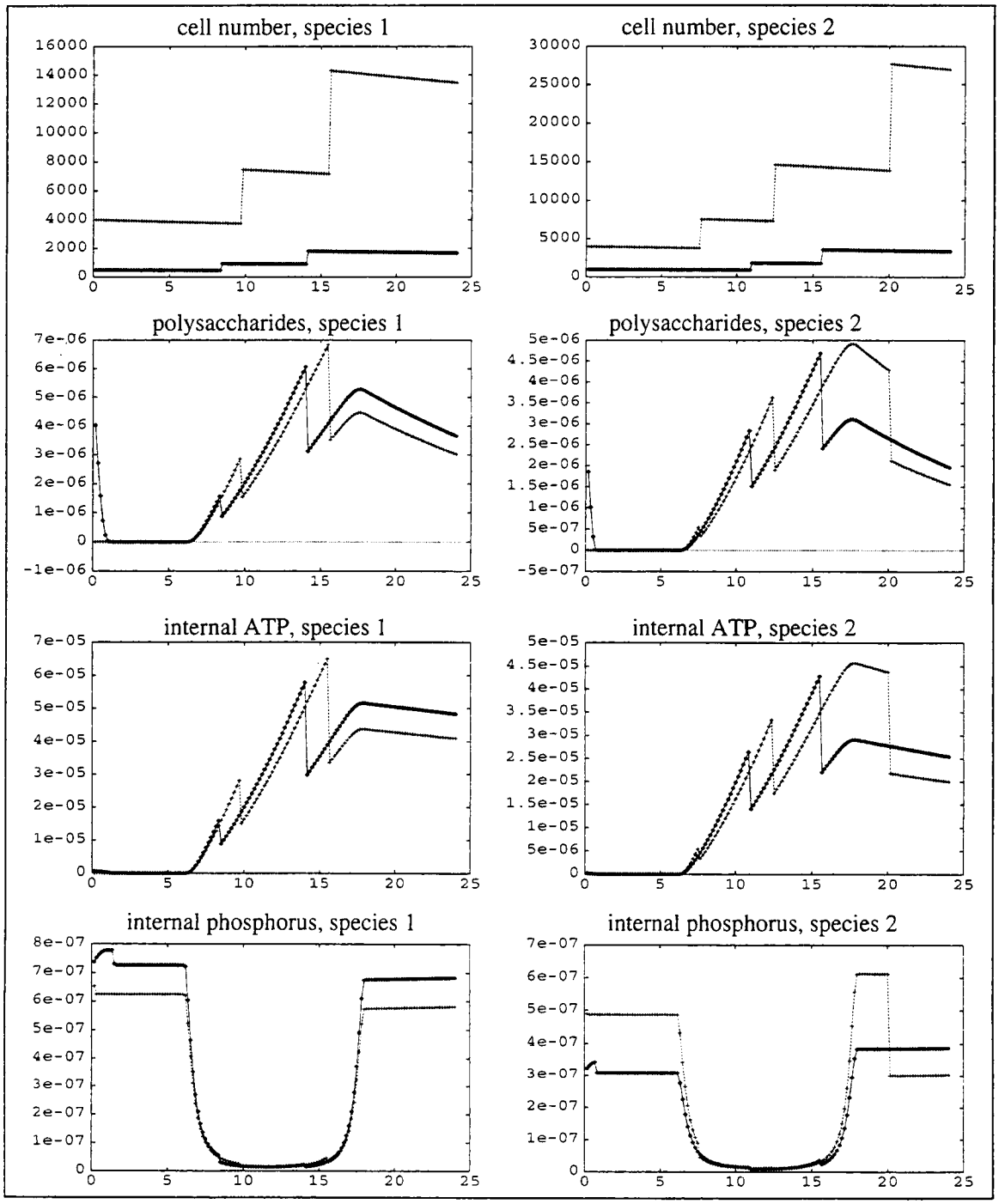

Figure 6.13: Simulation (9a). Cell number in # l^{-1}, other scales μmol, versus time in hours.

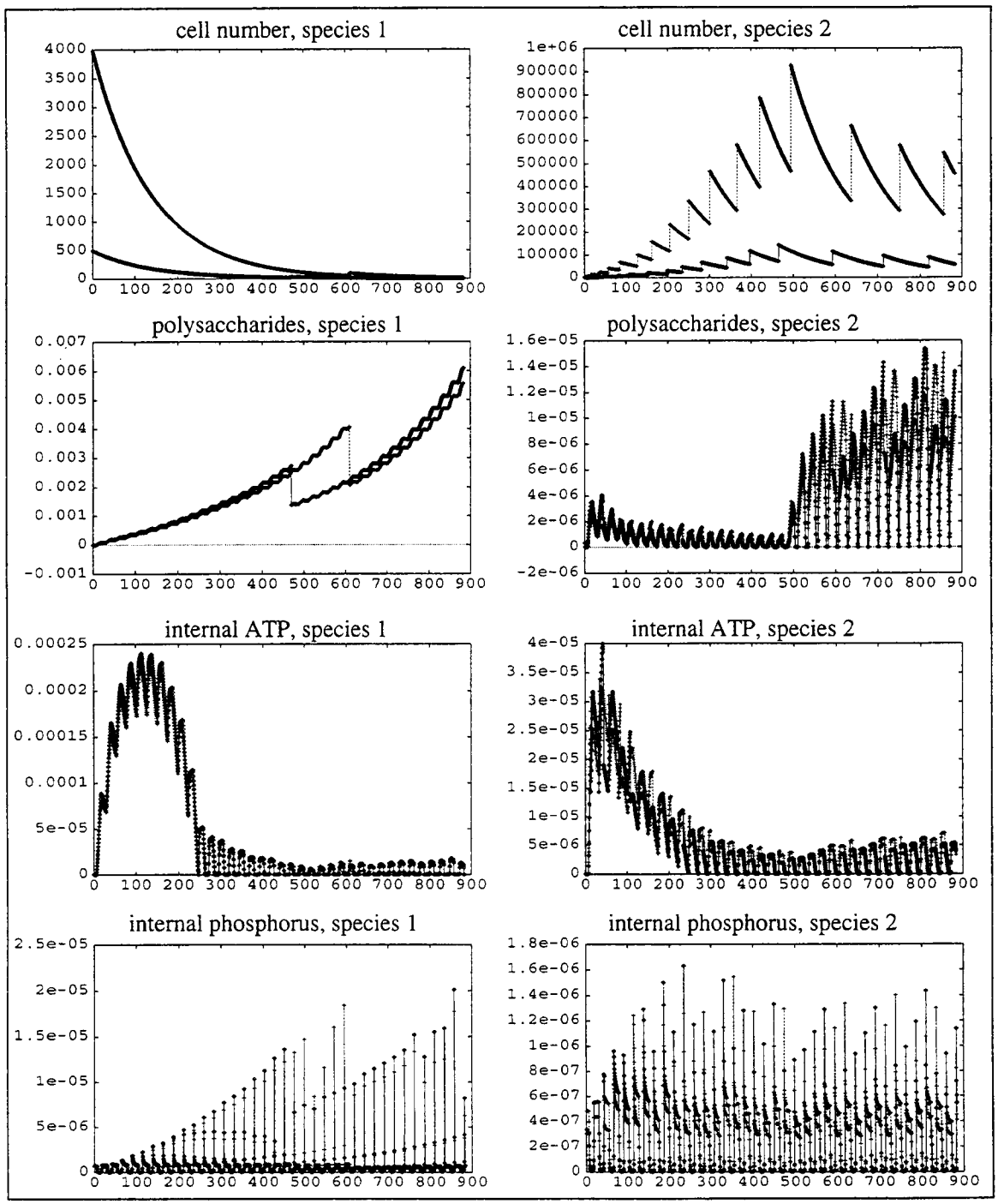

Figure 6.14: Simulation (9b). Cell number in # l^{-1}, other scales μmol, versus time in hours.

quirements.

6.3.11 Simulation (10), Phosphorus Limited

Simulation (10) (Figure 6.15) was performed under the same conditions as Simulations (9a) and (9b), with high silicate and nitrite input, but low phosphorus input. The question, which species performs better in a case where a nutrient required by both species is limiting, cannot be answered in advance. Initially, both species grow fast, and species two clearly outperforms species one. Species two shows about five times the population size of species one. A comparison with Simulation (9a) suggests that under non-limiting nutrient conditions the difference between the two species is not as large. After growth stops (approximately after 16 days), species two can hold its already high population size, whereas species one decreases in cell number.

A possible reason for the different performances is the difference in maintenance costs. Even though species two has a higher maintenance requirement per volume, species one with its large cells needs probably more energy for maintenance. Energy can, however, not be produced in large amounts if phosphorus concentrations are low.

6.4 Sensitivity Analysis

A sensitivity analysis was performed in order to find the parameters that govern the dynamics of the model. Parameters on the individual level as well as on the population level and the habitat level were examined. The following method was used:

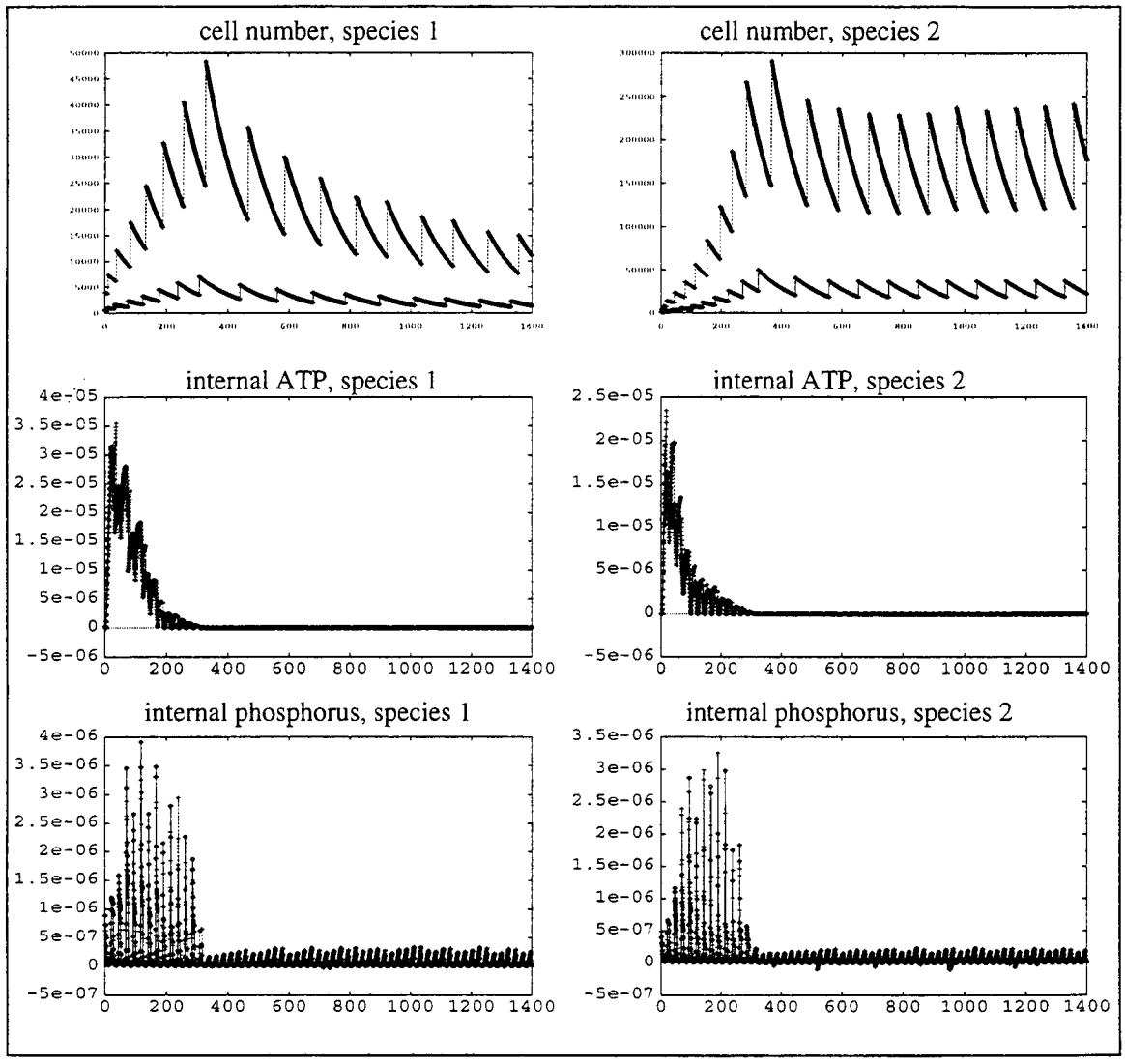

Figure 6.15: Simulation (10). Cell numbers in $\#\ l^{-1}$, other scales μmol, versus time in hours.

Several simulations using the computer code based on Euler's method were performed. During each simulation, the population was divided into four ecotypes, each of them having different parameters. Various parameters were chosen out of an expected range for a specific parameter. Different parameters were changed in the various simulations. All of them lasted for 25 days. Nutrient input in the system was zero during the entire time, allowing cells to feed on initial nutrients only. Results were examined for differences in population size primarily and variations in storage accumulations between the four ecotypes. Populations increased during the first part of the simulations, and growth stopped after nutrients were depleted. Therefore, performance of the various ecotypes could be examined for nutrient abundant conditions (beginning of simulation), as well as for nutrient limiting conditions (end of simulation).

In this section, growth phase means the first part of the simulations (increasing total population size), whereas stationary phase means the second part (nutrients depleted, no growth). During the stationary phase, cell number decreased due to sinking, however, the protein and structure pools showed no variation over time.

First the parameters for the individual are discussed, then some of the global parameters are discussed.

6.4.1 Parameters of the Individual

All parameters on the individual level influence, more or less, the speed of biosynthesis in the individual.

Active Transport, Parameters a, c_{ϕ_e}, and $n_{\phi,A}$

Temperature was assumed to be constant for all simulations. For convenience, $v(T) = 1$ was set all the time, and only the values of a (which plays then the role of a half saturation constant), c_{ϕ_e} and $n_{\phi,A}$ were changed (for phosphorus and nitrogen only).

- A change in a resulted in different growth rates for the ecotypes. A lower value of a allows faster uptake of nutrients, which increases the growth rate.
- A change in the proportionality constant c_{ϕ_e} and the maximum transport rate $n_{\phi,A}$ resulted also in different growth rates. Ecotypes with faster uptake of nutrient grew faster. In addition, these ecotypes are able to adjust their interior phosphorus pools faster. The slow uptake (which is in the model also coupled with a slower excretion rate) of nutrients resulted in large fluctuations for the internal phosphorus pool, because at night catabolism of lipids produced free phosphorus. The advantage for these cells is that they keep more phosphorus in the cell at night.

Maximum Biosynthesis and Functional Response, Parameters m_{0,ϕ_s} and c_{ϕ_e}

Changes in the maximum biosynthesis and functional response term directly influence growth of species.

- The maximum rate of biosynthesis m_{0,ϕ_s} influenced performance of the four ecotypes. Faster biosynthesis resulted in faster growth and larger final cell number.
- Changes in the proportionality constants c_{ϕ_e} in the functional response terms of biosynthesis also had direct effect on growth of species. A larger c_{ϕ_e} yielded a faster growth.

Additionally, more storage in form of polysaccharides and lipids could be produced. This resulted in a higher catabolism at night, and therefore a longer growth phase for these cells (more energy available). During steady state, the higher storage compartments increase the volume and weight of the cell. This can also effect sinking and grazing.

Costs of Protein Synthesis, Parameters $k_{\phi_i,Pr}$ and $mu_{\phi_i,Pr}$

Protein and structure synthesis is one of the most important functions of the cell because they determine the actual growth rate of the population. Higher carbon and nitrogen requirements were coupled with lower ATP requirements and vice versa, suggesting more complicated, but low energy structure on the one end of the scale and less complicated, but high energy structure on the other end. These simulation resulted in different limitations for the four ecotypes. The ecotypes with the more complicated structural materials (high carbon and nitrogen requirement, low energy requirement) were strongly nutrient limited and grew slowly. These ecotypes were, on the other hand, able to accumulate storage materials. Ecotypes with less complicated structural materials were energy limited. They were, however, able to grow very fast under the given conditions, by shifting use of energy from storage production to growth. The results showed that storage production depends on availability of energy, whereas growth is governed by available nutrients.

Photosynthesis, Parameters E_k and L_{max}

Photosynthesis is the only source of energy for the cells. It is therefore not surprising that changes in E_k and L_{max} influence performance of an ecotype strongly. Lower values of E_k and higher values of L_{max} provide the cell with more energy which increases growth and

also production of storage materials.

Maintenance, Parameter M_0

Maintenance rates influenced speed of growth especially at night or during other times of low irradiance. The main source of energy during these times is the catabolism of storage materials. A high maintenance rate did not allow a cell to continue growth at night, whereas a lower maintenance rate allowed growth. Therefore, ecotypes with lower maintenance rates showed higher growth rates.

Respiration, Parameters ζ_C

Changes in the respiration rate ζ_C produced different growth limitations for the ecotypes. Ecotypes with a high ζ_C were carbon limited. A constantly low internal carbon concentration did not allow fast growth. A low value for ζ_C allowed faster growth. Therefore, energy levels for these ecotypes were lower.

Silicate, Parameters c_{Si}, n_{Si}, c_S, and k_{S,P_T}

Changes in the parameters for uptake and incorporation of silicate influenced performance of various ecotypes. Low uptake rate or high silicate requirements for structural materials resulted in a lower growth rate. Lower growth rates increased the size of the storage pools, where the available energy was stored.

6.4.2 Global Parameters

Global parameters determining behavior of the model photosynthetic and sinking parameters. Simulations for sensitivity of the model on global parameters were performed for one ecotype under the same conditions as the individual parameter test (only initial nutrient input).

Depth of Surface Layer, Irradiance, and Daylength

Depth of surface layer, irradiance, and daylength all influence the photosynthetic rate strongly. Depth of surface layer influences the sinking rate.

- Usually in all simulations a surface layer of 15m was assumed. Thinner surface layers of 1 and 10 m did not produce a higher final population size, but higher storage compartments, because more energy is available. A surface layer of 25 m resulted in low ATP levels during growth phase and stationary phase.
- Higher irradiance and longer days increased available energy in the cell. The number of reproductions remained the same for different parameters because limited nutrients allowed only a certain amount of reproductions. Time between reproductions decreased, however, with increasing irradiance or daylength. Internal storage and ATP levels were higher for these scenarios.

6.5 Summary

The model dynamics show realistic results for many environmental conditions. Results are very sensitive to photosynthetic parameters, parameters of nutrient transport, and biosynthesis. In addition, maintenance rate and respiration rate turned out to be important factors.

7 Discussion and Conclusions

Results from the simulations and from the sensitivity analysis examine phytoplankton populations under nutrient and energy limiting conditions. Simulations show that growth of cells can be nutrient limited during the day and energy limited during the night. The simulations showed also many different scenarios where cells shifted biosynthesis from structure to storage, or from one storage material to another. Stored nutrients and energy could then be used for maintenance and growth at night. Under phosphorus limitation, for example, storage in form of polysaccharides was the main reserve. This shows the importance of a storage pool that is divided into several compartments. Other processes that turned out to be very important in determining development of a cell include photosynthetic, maintenance, and respiration rates. For the photosynthetic rate an exact estimation of the cell size is important (which again requires knowledge about the amount of storage in a cell). Maintenance, especially for storage materials, seems also to be a crucial factor, especially during energy limitations. Respiration rates of phytoplankton cells are controversial because they cannot be measured directly. Respiration is, however, an important factor that has to be included in a model. As maintenance, it is important especially during energy limitions.

The uncoupling of growth and storage production and the separate modeling of active nutrient transport allows great flexibility in cell development. This is a major advantage of the model over individual-based models that estimate growth of a cell from exterior nutrient concentrations only. The additional focus on energy flows in a cell includes other abiotic

und biotic constraints of cells in the model. Combined with each other, these formulations are more likely to allow accurate estimates of phytoplankton growth as well as composition of cells. This is important information for effects like sinking and grazing, or toxic effects, that depend heavily on the composition of a cell. It is also not surprising that with the use of the model new relationships between environmental conditions and species performance could be found. Simpler individual-based models often do not allow different compartments to have independent dynamics. Besides, uncoupled dynamics also reveal differences in multi-species simulations and help therefore to explain success of species. Populations of several species, that might look very much the same with a simple model, have in reality big differences in storage and nutrient compartments. Again the uncoupled model can here give new insights.

Many of the rates and flows have been modeled in many ways by various scientists, and there is everything else other than a common opinion about which way is the most accurate. For qualitative behavior of phytoplankton assemblages, the relationships between processes are important. If quantitative results are achieved (exact prediction of population size, amount of storage in a cell), then one has to focus on these different ways of modeling.

Computers provide nowadays an excellent tool to model ecological process in such detail. Graphical tools also allow following the development of a model over time. During computer simulations, the easy numerical methods used were surprising in that they were highly stable. With a time step of 1 second, the system almost never got out of hand by overshooting, for example, to a large negative number. More problems might, however, occur if the system is coupled, for example, with a fish model that operates on a different time-scale. In this case, it might be necessary to implement better numerical methods.

For future times, some analytical results (limits for growth, storage; or equilibria) would

help to answer the question if the model really behaves like a phytoplankton population. Another important task would be to test different formulations for the flows and processes and compare the results. Even more important, but also much more tedious, is the search for parameters for the model. Many parameters can be taken from biochemistry books (chemical compositions of storage, structure and so on), some parameters can be measured in experiments, but some parameters can only be estimated, trying to fit a model to experimental data sets. At the end, this might not be a major drawback, considering the fact that not all cells are exactly the same. Simulations can be performed for many ecotypes (especially with the increasing computer power available), each with a little different parameter values. Diversity and complexity might very well be the tools of the future to build more accurate mathematical models in ecology.

Bibliography

Bibliography

[1] Ackleh, A.S., Hallam, T.G., Smith Jr., W.O., 1994, Influences of aggregation and grazing on phytoplankton dynamics and fluxes: an individual-based modeling approach, *Nonlinear World*, 1:473.

[2] Ackleh, A.S., Hallam, T.G., Muller-Landau, C.M., 1995, Estimation of sticking and contact efficiencies in aggregation of phytoplankton: The 1993 SIGMA tank experiment, *Deep-Sea Research II*, 42:185.

[3] Barker, R., 1971, "Organic chemistry of biological compounds", Prentice-Hall.

[4] Barlow, R.G., 1982, Phytoplankton ecology in the southern benguela current. II. Carbon assimilation patterns, *Journal of Experimental Marine Biology and Ecology*. 63:229.

[5] Brown, M.R., 1991, The amino-acid and sugar composition of 16 species of microalgae used in mariculture, *J.Exp. Mar. Biol. ecol.*, 145:79.

[6] Canziani, G.A., Hallam, T.G., 1994, "Mathematical model for a Phaeocystis sp. dominated plankton community dynamics. I: The basic model", Ph.D. thesis, University of Tennessee, Knoxville.

[7] Chisholm, S.W., Phytoplankton size, in Falkowski and Woodhaed [15]:213.

[8] Conte, S.D., de Boor, C., 1980, "Elementary Numerical Analysis. An Algorithmic Approach", Mc.-Graw-Hill Book Company.

[9] Cook, J.R., 1966, Photosynthetic activity during the division cycle in synchronized Euglena gracilis, *Plant. Physiology*, 41:821.

[10] Darley, W.M., 1974, Silicification and calcification, in Stewart [45]:655.

[11] Dawes, C.J., 1981, "Marine botany", John Wiley & Sons.

[12] De Groot, W.T., 1983, Modeling the multiple nutrient limitation ol algal growth, *Ecological modelling*, 18:99.

[13] Dubinsky, Z., The functional and optical absorption cross-sections of phytoplankton photosynthesis, in Falkowski and Woodhead [15]:31.

[14] Falkowski, P.G., Molecular ecology of phytoplankton photosynthesis, in Falkowski and Woodhead [15]:47.

[15] Falkowski, P.G., Woodhead, A.D., 1992, "Environmental Science Research 43: Primary productivity and biogeochemical cycles in the sea", Plenum Press, New York.

[16] Geider, R.J., Respiration: taxation without representation ?, in Falkowski and Woodhaed [15]:333.

[17] Gilstad, M., Johnsen, G., Sakshaug, E., 1993, Photosynthetic parameters, pigment composition and respiration rates of the marine diatom *Skeletonema costatum* grown in continuous light and a 12:12 h light-dark cycle, *Journal of Plankton Research*, 15v8:939.

[18] Glasstone, S., Laidler, K.J., Eyring, H., 1941, "The theory of rate processes", McGraw-Hill.

[19] Goldberg, J.L., Schwartz, A.J., 1972, "Systems of ordinary differential equations: an introduction", Harper & Row, Publishers.

[20] Hallam, T.G., 1995, "Mathematical Ecology 682, Fall 1995. Notes on structured populations and communities", Lecture notes, University of Tennessee, unpublished.

[21] Handa, N., 1969, Carbohydrate metabolism in the marine diatom Skeletonema costatum, *Marine Biology*, 4:208.

[22] Harding, L.W., Meeson, B.W., Fisher Jr., T.R., 1985, Patterns of photosynthetic carbon metabolism in light-limited phytoplankton, *Marine Biology*, 89:121.

[23] Hellebust, J.A., Extracellular products, in Stewart [45]:838.

[24] Henson, S.M., Hallam, T.G., 1995, Optimal feeding via constrained processes, *Journal of theoretical Biology*, 176:33.

[25] Kirk, J.T.O., 1994, "Light and photosynthesis in aquatic ecosystems, second edition", Cambridge University Press.

[26] Kirk, J.T.O., The nature and measurement of the light environment in the ocean, in Falkowski and Woodhead [15]:9.

[27] Kolber, Z., Zehr, J., Falkowski, P.G., 1988, Effects of growth irradiance and nitrogen limitation on photosynthetic energy conversion in photosystem II, *Plant Physiology*, 88:923.

[28] Konopka, A., 1983, The effect of nutrient limitation and its interaction with light upon the products of photosynthesis in Merismopedia tenuissima (Cyanophyceae), *Journal of Phycology*, 19:403.

[29] Kooijman, S.A.L.M., 1983, "Dynamic energy budgets in biological systems", Cambridge University Press.

[30] Krogmann, D.W., Powers, W.H., 1965, "Biochemical dimensions of photosynthesis", Wayne State University Press, Detroit.

[31] Kuhl, A., Phosphorus, in Stewart [45]:636.

[32] Lalli, C.M., Parsons, T.R., 1994, Biological oceanography: an introduction, Pergamon Press.

[33] Lancelot, C., Mathot, S., 1985, Biochemical fractionation of primary production by phytoplankton in Belgian coastal waters during short- and long-term incubations with ^{14}C-bicarbonate. I. Mixed diatom population, *Marine Biology*, 86:219.

[34] Marsh Jr., H.V., Galmiche, J.M., Gibbs, M., Respiration during photosynthesis, in Krogmann et al [30]:95.

[35] Martin, J.H., Iron as a limiting factor in oceanic productivity, in Falkowski and Woodhead [15]:123.

[36] O'Neill, R.V., De Angelis, D.L., Pastor, J.J., Jackson, B.J., Post, W.M., 1989, Multiple nutrient limitations in ecological models, *Ecological Modelling*, 46:147.

[37] Morris, I., 1974, Nitrogen assimilation and protein synthesis, in Stewart [45]:583.

[38] Parsons, T.R., 1984, "Biological oceanographic processes", 3.ed., Pergamon Press.

[39] Percival, E., McDowell, R.H., Algal Polysaccharides, in Dey, P.M., Dixon, R.A., 1985, "Biochemistry of storage carbohydrates in green plants", Academic Press, 305

[40] Platt, T., Sathyendranath, S., Ravindran, P., 1990, Primary production by phytoplankton: analytic solutions for daily rates per unit area of water surface, *Proc. R. Soc. Lond. B*, 241:101.

[41] Prescott, L.M., Harley, J.P., Klein, D.A., 1993, "Microbiology", 2.ed., Wm. C. Brown Publishers.

[42] Pruppacher, H.R., Klett, J.D., 1980, "Microphysics of clouds and precipitation", Riedel, Boston, 714.

[43] Round, F.E., 1965, "Biology of the algae", St. Martins Press.

[44] Rousseau, V., Mathot, S., Lancelot, C., 1990, Calculating carbon biomass of Phaeocystis sp. from microscopic observations, *Marine Biology*, 107:305.

[45] Stewart, W.D.P., 1974, "Botanical monographs volume 10. Algal physiology and biochemistry", University of California Press, Berkeley and Los Angeles.

[46] Varum, K.M., Ostgaard, K., Grimsrud, K., 1986, Diurnal rythms in carbohydrate metabolism of the marine diatom Skeletonema costatum (Grev.), Cleve, *J. Exp. Mar. Biol. Ecol.*, 102:249.

[47] Vennesland, B., The energy conversion reactions of photosynthesis, in Krogmann et al [30]:48.

[48] Vollenweider, R.A., Calculation models of photosynthesis-depth curves and some implications regarding day rate estimates in primary production measurements, in Goldman, C.R., 1965, "Primary productivity in aquatic environments", Mem. Ist. Ital. Idrobiol., 18 Suppl., University of California Press, Berkeley, 425.

Appendices

Appendix A Future Directions: Population Model

On the population level, aggregation, sinking and grazing are three important factors that govern dynamics. The population model in Chapter 4 does not include aggregation. This chapter introduces a population model that includes aggregation and discusses its possible combination with an individual-based model. For species that form aggregates, sinking and grazing as well as light availability are different.

The population models presented here are derived from Canziani and Hallam [6] and from Ackleh et al, [1] and [2].

A.1 Aggregation

Aggregation is the genesis of larger particles from the collisions of smaller ones. Large aggregates of different species have been found especially during blooms. Aggregates are more likely to be lost from the system due to increased sinking. On the other hand, large aggregates may escape zooplankton grazers.

Only non-flagellated cells produce aggregates. Aggregation depends on the cell-density in the water and on the sticking efficiency, i.e. the probability that two colliding particles or aggregates stick together to form a larger aggregate. Sticking efficiency was estimated e.g. by Ackleh et al [2].

The following assumptions are made:

1. It is assumed that, at the beginning, a fixed portion of the cells are non-flagellated.
2. Sticking efficiency: the sticking efficiency for particles of different species is assumed to be zero, i.e. only particles of the same species can form aggregates.
3. Growth: cells in aggregates follow the same dynamics as single cells. A change in environmental conditions such as light and nutrient availability is not included.
4. Reproduction: following Canziani et al [6] reproduction of cells in aggregates is assumed to occur also after doubling of structural cell mass. However, if a cell division occurs in an aggregate, only one of the two cells remains in the aggregate whereas the second cell is released.

A.1.1 The Aggregation Model

In the following the variable x indicates the volume of an aggregate whereas t is the time. At a given time t the density of aggregates of volume x is denoted by $\delta(t,x)$. The following dynamics for the density $\delta(t,x)$ are assumed:

$$\begin{aligned}\frac{\partial\delta(t,x)}{\partial t} &= F(\delta(t,x)) \\ &= \frac{1}{2}\int_0^x \alpha(x-y,y)\beta(x-y,y)\delta(t,x-y)\delta(t,y)dy \\ &\quad - \delta(t,x)\int_0^\infty \alpha(x,y)\beta(x,y)\delta(t,y)dy\end{aligned} \tag{A.1}$$

where

$\beta(x,y)$ $(\frac{cm^3}{t\,\#})$: rate of collision times contact efficiency of two particles with volume x and y.

$\alpha(x,y)$, nd: sticking efficiency, i.e. probability that two colliding particles of volume x and y stick together.

The first term in Equation A.1 expresses the rate at which collisions occur in the population to form aggregates of the size $x + dx$ whereas the second term expresses the rate of removal of aggregates due to collision with other particles or aggregates which increases their size. The rate of collision β consists of two parts:

1. Rate of collision β^s due to shear: Let d_x and d_y be the diameters of aggregates of volume x and y. Then the contact efficiency due to $(EC)^s_{x,y}$ is assumed to be

$$(EC)^s_{x,y}(d_{min}/d_{max}) = (EC)_0 exp[-\frac{0.1}{d_{min}/d_{max}}] \tag{A.2}$$

where

$d_{min} = \min(d_x, d_y)$ and $d_{max} = \max(d_x, d_y)$ in m

$(EC)_0 = \frac{1}{e^{-0.1}}$, nondim.: constant (Pruppacher and Klett, 1980).

Then the rate of collision due to shear has the functional form

$$\beta^s(x, y) = 0.163(\frac{\varepsilon}{\nu})^{\frac{1}{2}}(d_x + d_y)^3(EC)^s_{x,y} \tag{A.3}$$

where

ε $(\frac{m^2}{s^3})$: dissipation rate

ν $(\frac{m^2}{s})$: kinematic viscosity

$(EC)^s_{x,y}$, nd.: contact efficiency for shear given above.

2. Rate of collision β^d due to differential settling: Ackleh et al [2] used the following formulation for the contact efficiency $(EC)^d_{x,y}$

$$(EC)^d_{x,y} = \frac{(\frac{d_{min}}{d_{max}})^p}{2(1 + \frac{d_{min}}{d_{max}})^u} \tag{A.4}$$

where u is a real number. Pruppacher and Klett [42] used this formulation with $u = 2$. Ackleh et al [2] try to estimate a u which fits experimental data in a better way.

Then the rate of collision due to differential settling has the functional form

$$\beta^d(x,y) = \frac{\pi(d_x + d_y)^2}{4} \mid w_x - w_y \mid EC^d_{x,y} \tag{A.5}$$

where w_x and w_y are the falling velocities for particles of volume x and y, respectively.

Conservation of Volume and Maximum Volume

Equation A.1 describes aggregation only. Therefore, the total volume of all aggregates has to be conserved by this equation. This can be shown using standard integration techniques.

It is biologically reasonable and required for a numerical solution to introduce a maximum volume B for the size of aggregates. The functional form for the density then reads as

$$\begin{aligned} \frac{\partial \delta(t,x)}{\partial t} &= F(\delta(t,x)) \\ &= \frac{1}{2}\int_0^x \alpha(x-y,y)\beta(x-y,y)\delta(t,x-y)\delta(t,y)dy \\ &\quad - \delta(t,x)\int_0^B \alpha(x,y)\beta(x,y)\delta(t,y)dy \end{aligned} \tag{A.6}$$

with the constraints

$$\beta(x,y)\begin{cases} \geq 0 & \text{if } x+y \leq B \\ = 0 & \text{if } x+y > B \end{cases} \tag{A.7}$$

or

$$\alpha(x,y)\begin{cases} \geq 0 & \text{if } x+y \leq B \\ = 0 & \text{if } x+y > B \end{cases} \tag{A.8}$$

where the constraints are needed to keep the volume of aggregates below the maximum B. With these constraints Equation A.6 is equivalent to Equation A.1 and conserves the total

volume of particles in the system. This can be calculated using the same steps as above with the only change being the upper limit of the integral which can be replaced by ∞ because of the constraints.

A sinking and grazing term will be included in the functional form for $\frac{\partial \delta(t,x)}{\partial t}$.

A.2 Sinking

As mentioned above the model distinguishes between flagellated and non- flagellated cells. The non-flagellated cells sink. Speed of sinking follows Stokes' Law. However to calculate the speed of sinking factors like shape, density and surface characteristics (e.g. smoothness, stickiness, surface to volume ratio) need to be known. Canziani and Hallam [6] assumed that particles and aggregates have a spherical shape and do not change their shape and surface characteristics. Given the volume x and assuming a spherical shape the radius of the colony can be estimated as,

$$R = (\frac{3x}{4\pi})^{\frac{1}{3}}$$

For a given radius Ackleh et al [1] assume the sinking velocity to be

$$w(x) = h_p \xi R^{1.17} \tag{A.9}$$

where

h_p: fall scale parameter,

ξ: curve fit parameter.

A.3 Grazing

Ackleh et al [1] introduced a simple population model for a grazer. This will be used as a basic grazer model. Canziani and Hallam [6] use a structured grazer model with different feeding habits. This model would increase the accuracy because grazers of different size feed differently on single cells, small aggregates and large aggregates. Flagellated terms have to be included in the grazer-model. The model given in Section A.3.1 is for one species only.

A.3.1 The Simple Grazer Model

The following dynamics for the zooplankton population are assumed

$$\frac{dZ}{dt} = (MI)\,(AE)\frac{\sum_{species}\left[\int_0^B q(x)(\delta(t,x)+\delta_f(t,x))dx\right]}{\sum_{species}\left[\int_0^B q(x)(\delta(t,x)+\delta_f(t,x))dx\right]+\vartheta_p}Z - \theta\, Z^r \tag{A.10}$$

where

Z in $\frac{\#}{m^3}$: density of grazers

$\delta_f(t,x)$: density of single flagellated cells with volume x at time t.

r, nondim., constant: r is either one for a first order grazing process or 2 for a logistic representation.

(MI): maximum ingestion rate of grazer

(AE): assimilation efficiency of grazer

$q(x)$: probability of an individual grazer to ingest an aggregate of size x.

ϑ_p: trophic response half saturation constant

θ, constant: mortality rate of grazer population

The first term of the equation represents the increase of the grazer population due to grazing on phytoplankton whereas the second term is the mortality term for the grazer population. Ackleh et al [1] choose the function $f(x)$ to be equal zero for a volume $x > 0.04mm^3$ because grazers cannot ingest particles with a larger size.

E.g. Canziani and Hallam [6] present a much more complicated grazer model dividing the grazer population in ciliates, copepod nauplii and other copepod stages.

A.4 Summary

Finally the formulation of the population model for the phytoplankton species takes the form

$$\frac{\partial \delta(t,x)}{\partial t} = F(\delta(t,x)) - \frac{V_x}{z}\delta(t,x) - (MI)\frac{q(x)\delta(t,x)}{\int_0^B q(x)\delta(t,x)dx + \vartheta_p}Z \tag{A.11}$$

for the non-flagellated cells and

$$\frac{\partial \delta_n(t,x)}{\partial t} = F_n(\delta_n(t,x)) - (MI)\frac{q(x)\delta_n(t,x)}{\int_0^B q(x)\delta_n(t,x)dx + \vartheta_p}Z \tag{A.12}$$

for the change in density of the flagellated cells where $F_n(\delta_n(t,x))$ is the change in density of flagellated cells of volume x. Because there is no aggregation for flagellated cells, this function is determined by reproduction only.

A.5 Application to Individual Model

Sections A.1 to A.4 describe the the population model for a phytoplankton and zooplankton community in a continuous manner. The following problems occur if this population model has to be combined with an individual-based model:

1. Because single cells in the individual model grow independently, a calculation of the density of aggregates of a certain volume does not give any information of the composition of the aggregate. Therefore growth of the aggregate cannot be calculated.
2. It is difficult to combine a continuous distribution of a density with a discrete model for the individuals.

However, the importance of the population model has to be recalled. In the presented form, the population model is of importance for losses due to sinking and grazing. If some simplifications and assumptions are made the population model above can be used to fulfill its tasks in a sufficient way.

Assumptions and simplifications:

1. A fixed relation between the number of cells in an aggregate and its size is assumed.
2. Aggregates are assumed to consist of cells of different ecotypes in the same proportion as ecotypes present, i.e. if at a certain time 10% of the total population are of a certain ecotype then in all aggregates 10% of the cells will be of this certain ecotype.
3. Grazers are assumed to feed equally on the different species of phytoplankton relative to their abundance.

Basically the model keeps track of aggregates without consideration of the individual cells. New single cells of a certain volume enter the population model each time reproduction occurs. The total losses due to sinking and grazing can be calculated. However, this calculation of losses is based on volume and the conversion to the number of single cells lost in each ecotype requires the assumptions above.

A.5.1 Individual Losses

As described above we calculate the losses of the population due to sinking and grazing out of the population model. The total losses in number of cells for the non-flagellated cells are given by

$$\int_0^B \left[-\gamma(x)\frac{w(x)}{z}\delta(t,x) - (MI)\frac{\gamma(x)q(x)\delta(t,x)}{\int_0^B q(x)\delta(t,x)dx + \vartheta_p} Z \right] dx \tag{A.13}$$

where

z in m: depth of surface layer.

γ_x: number of cells in an aggregate of volume x.

Total losses in number of cells for flagellated cells are given by

$$\int_0^B \left[-\lambda(MI)\frac{q(x)\delta_f(t,x)}{\int_0^B q(x)\delta_f(t,x)dx + \vartheta_p} Z \right] dx \tag{A.14}$$

The losses in number of cells for each ecotype are calculated according to the assumption above as fractions of the total losses for a species.

Calculation of $\gamma(x)$

Rousseau et al [44] developed the following relationship between the number of cells in a colony and the volume of the colony

$$\log(2^{(i-1)}) = \bar{a} \log x + \bar{b} \tag{A.15}$$

where i is the number of cells in the colony and $\bar{a}$ and $\bar{b}$ are constants.

Equation A.15 can be written as

$$i = 1 + \log_2[x^{\bar{a}}\, 10^{\bar{b}}] = \gamma x \tag{A.16}$$

which allows the computation of the number of cells from the volume of the colony.

A.6 Comparison of the Two Population Models

Table A.1 summarizes the differences between the two population models.

The transition between the individual model and the population model is on solid ground for the Single Cell Population Model. By not taking aggregation into account, this model requires much less simplifications and assumptions. Which population model yields the better result cannot be said. For different simulations a different population model might be favorable. Only simulations allow to decide which model fits better.

Table A.1: Advantages and disadvantages of the two population models

	Population-Aggregation Model	Single Cell Population Model
Aggregation	+ includes aggregation	- does not include aggregation
Sinking	+ includes sinking, dependent on volume of aggregate	+ includes sinking - sinking influenced by aggregate formation which is not modeled
Grazing	+ includes grazing, dependent on volume of aggregate	+ includes grazing - grazing influenced by aggregate formation which is not modeled
Growth dynamics	- no growth of cells in aggregates	+ growth of cells determined by individual model
Cell-composition	- does not keep track of cell composition	+ keeps track of cell composition via combination with individual model
Usage	for simple modeling of losses due to aggregation, sinking and grazing	for estimations of storage and structural products in a population including a death-rate that might depend on this (e.g. due to toxicant)

Appendix B Variables and Units

B.1 Table of Units

The following table summarizes the units and their abreviations used in the model.

Table B.1: Table of units

Symbol	Name	Meaning
$°C$	°Celcius	temperature in Celcius
$°K$	°Kelvin	abolute temperature in Kelvin
g	gram	weight in gram
m	meter	length in meter
$\mu m = 10^{-6}m$	micrometer	length in micrometer
μm^2	square micrometer	area in square micrometer
μm^3	cubic micrometer	volume in cubic micrometer
μmol	micromol	number of molecules
s	second	time in seconds
h	hour	time in hours
$\#$	number	e.g. number of molecules

Units for light intensity:

1 μ mole quanta = $6.02 \cdot 10^{17}$ photons = 1 μ Einstein.

B.2 Abbreviations

The following table summarizes the abreviations used in the text.

Table B.2: Table of Abbreviations

Abreviation	Meaning
ϕ_e	stands for one of the exterior substances
ϕ_i	stands for one of the interior nutrients or ATP
ϕ_s	stands for one of the storage materials or for protein and structure
AM	Ammonium
ATP	Adenosine-tri-phosphate
C	Carbon
CO_2	Carbohydrate
FE	Iron
Lp	Lipids
N	Nitrogen
NI	Nitrate
OP	Orthophosphate
OR	Organic Phosphate
P	Phosphorus
Pr	Proteins and structure
Ps	Polysaccharides

B.3 Table of Variables and Parameters by Name

The following table summarizes the parameters used in the model. Given is also the section were the variable or parameter was used first. Most of the parameter values were estimated from [1], [5], [17], [25], [38].

Table B.3: Table of variables and parameters of the model.

Constant	Units	Description	Section
$\alpha(x,y)$	nd	sticking efficiency	A.1.1
$\beta(x,y)$	$\frac{cm^3}{t\,\#}$	rate of collision times contact efficiency of two particles	A.1.1
γ_x	#	number of cells in an aggregate of volume x	A.5.1
δ	$\frac{\#}{m^3}$	total number of cells	3.4
δ_i	$\frac{\#}{m^3}$	number of cells of ecotype i	4.5
δ_f		density of single flagellated cells	A.3.1
ε	$\frac{m^2}{s^3}$	dissipation rate	A.1.1
θ		constant mortalitiy rate of grazer	4.5
ϑ_p		trophic response half saturation constant	4.5
$\kappa_{\phi_i,*}$		constants for catabolic rates	5.1
λ		fraction of the losses due to grazing	A.5.1
μ_{ϕ_i,ϕ_e}	nd.	number of ϕ_i-molecules in a ϕ_e-molecule	3.9.1
μ_{ϕ_i,ϕ_s}	nd.	number of ϕ_i-molecules in a typical ϕ_s molecule	3.9.2
ν	$\frac{m^2}{s}$	kinematic viscosity	A.1.1
ξ		curve fit parameter	A.2

Table B.3, continued.

Constant	Units	Description	Section
$\rho_{ma,ATP}$	$\frac{\mu mol}{s}$	ATP used during maintenance	3.3
$\rho_{*,*}$	$\frac{\mu mol}{s}$	uptake, excretion, and storage fluxes	3.9.1
$\boldsymbol{\rho}_{*,*}$	vector	vector of uptake, excretion and storage fluxes	3.9.1
σ_{ϕ_s}	$\frac{1}{\mu m^3}$	molecular density of substance ϕ_s	3.10
$\tau(\phi_e)$	s	function for arrival-time of one molecule	3.1.1
ϕ_e	$\frac{\mu mol}{\mu m^3}$	exterior concentration of substance ϕ_e	3.1.1
ϕ_i	μmol	interior nutrient concentration	3.2.4
ϕ_s	μmol	internal storage and protein/structure	3.2.4
$\varphi_i(m)$	$\frac{\#}{s}$	derivetive in McKendrick-Von-Foerster Equation	4.2
a	cm	distance or thickness of cell wall	3.1.1
$\bar{a}$,$\bar{b}$		constants (calcualtion of # of cell in a colony)	A.5.1
A	cm^2	efficient surface area	3.1.1
(AE)		assimilation efficiency of grazer	4.5
c_{ϕ_e}	$\frac{s}{cm^3}$	proportionality constant (uptake function)	3.1.1
c'_{ϕ_i}	s	proportionality constant (functional response)	3.2.4
d_{min}	m	$\min(d_x, d_y)$	A.1.1
d_{max}	m	$\max(d_x, d_y)$	A.1.1
d_x	m	diameter of aggregate of volume x	A.1.1
d_y	m	diameter of aggregate of volume y	A.1.1
$D()$	nd	death-rate function	4.2
D	h	day length	3.4
E_d	$\frac{\mu mol}{m^2\ s}$	surface irradiance	3.4
E_k	$\frac{\mu mol}{m^2\ s}$	light intensity at intersection between linear slope with the height of saturation plaeteu	3.4

Table B.3, continued.

Constant	Units	Description	Section
(EC_0)	nd	constant (aggregation)	A.1.1
$(EC)^d_{x,y}$	nd	contact efficiency for differential settling	A.1.1
$(EC)^s_{x,y}$	nd	contact efficiency for shear	A.1.1
$\bar{E}$	μmol	energy pool (ATP)	3.2.1
f_{ϕ_S}	nd	functional response for production of storage/structure	3.2.1
g_{ϕ_S}	$\frac{\mu mol}{s}$	catabolistic rate of storage/structure	3.2.2
h_p		fall scale parameter	A.2
i	#	number of cells in the colony	A.5.1
I_{m,ϕ_s}	nd.	maximum reaction rate for production of a molecule ϕ_s	3.2.4
j_{ex,ϕ_i}	nd	proportionality constant for excretion	3.6
k_{ϕ_i,ϕ_s}	$\frac{\mu mol}{s}$	number of molecules of type ϕ_i needed for one molecule of ϕ_s.	3.2.4
K_d	$\frac{1}{m}$	total absorption coefficient	3.4
K_p	$\frac{1}{m}$	absorption coefficient for phytoplankton	3.4
K_s	$\frac{1}{m}$	absorption coefficient for seawater	3.4
L_{max}	$\frac{\mu mol\ C}{scm^2}$	maximum photosynthetic rate	3.4
L_α	nd.	nitrogen dependence of photosynthesis	3.4
L_β	nd.	nitrogen dependence of photosynthesis	3.4
L_P	μmol	phosphorus dependence of photosynthesis	3.4
m	vector	vector (m_1, m_2, m_3) or (m_{Ps}, m_{Lp}, m_{Pr})	4.2
m_{ϕ_s}	μmol	ineternal molecules ϕ_s	3.2.1
m_{0,ϕ_s}	$\frac{\mu mol}{s}$	maximum anabolic rate for ϕ_s	3.2.1

Table B.3, continued.

Constant	Units	Description	Section
M_0	$\frac{1}{\mu mol}$	maintenance costs per volume (in ATP)	3.5
$n_{\phi,A}$	$\frac{1}{cm^2}$	number of processors for substance ϕ	3.1.1
$q(x)$		probability of an individual grazer to ingest an aggregate of size x or a single cell	4.5
r	nd	type of grazing process	4.5
R	cm	estimated radius of an aggregate	A.2
$s(T^K)$	$\frac{cm}{s}$	velocity of nutrient transport	3.8
$s(T_1^K)$	$\frac{cm}{s}$	constant (nutrient transport)	3.8
(MI)		maximum ingestion rate of grazer	4.5
t	s	time in seconds	
t_ϕ	s	actual uptake time	3.1.1
$t_{\phi,min}$	s	minimal uptake-time	3.1.1
t_{ϕ_s}	s	time for completion	3.2.4
$t_{\phi_s,b}$	s	building time for one molecule	3.2.4
t_{w,ϕ_i}	s	waiting time for ϕ_i molecule	3.2.4
T	$°C$	Temperature of water	3.1.1
T^K	K	absolute temperature	3.8
T_1^K	K	chosen reference temperature	3.8
T_A^K	K	Arrhenius temperature	3.8
T_{st}	matrix	Transition-Storage-Matrix	3.9.2
T_{up}	matrix	Transition-Uptake-Matrix	3.9.1
u	#	constant (aggreagation model)	A.1.1
$v(T)$	$\frac{cm}{s}$	transport velocity	3.1.1

Table B.3, continued.

Constant	Units	Description	Section
V	μm^3	volume of cell	3.5
w_x,w_y		falling velocities for particles	A.1.1
x, y	cm^3	volume of aggregates	A.1.1
z	m	depth of surface layer	3.4
Z	$\frac{\#}{m^3}$	density of grazers	4.5

Appendix C Notation and Summary of Equations

C.1 Notation

In the computer code, all state variables are stored in arrays for convenience. Each column of an array represents an ecotype. The arrays have therefore as many columns as the total number of ecotypes (sum over all species). The total number of ecotypes will be referred to as n. Tables C.1 and C.2 show the notation used. In this section, indices on parameters specifying to which ecotype it belongs, are usually omitted.

Table C.1: Dynamic variables

Variable	Code	Functional	Meaning
δ_k	$x_{0,k}$	$f_{0,k}$	density of ecotype k
$C_{i,k}$	$x_{1,k}$	$f_{1,k}$	interior carbon of ecotype k
$F_{i,k}$	$x_{2,k}$	$f_{2,k}$	interior iron of ecotype k
$N_{i,k}$	$x_{3,k}$	$f_{3,k}$	interior nitrogen of ecotype k
$P_{i,k}$	$x_{4,k}$	$f_{4,k}$	interior phosphorus of ecotype k
$\bar{E}_k$	$x_{5,k}$	$f_{5,k}$	interior energy pool of ecotype k
$m_{Ps,k}$	$x_{6,k}$	$f_{6,k}$	reserve polysaccharides of ecotype k
user	$x_{10,k}$	$f_{10,k}$	user defined

Table C.1, continued.

Variable	Code	Functional	Meaning
$m_{Lp,k}$	$x_{7,k}$	$f_{7,k}$	reserve lipids of ecotype k
$m_{Pr,k}$	$x_{8,k}$	$f_{8,k}$	proteins and structural material of ecotype k
user	$x_{9,k}$	$f_{9,k}$	user defined, e.g. silicate
FE_e	y_0	g_0	iron concentration in water
AM_e	y_1	g_1	ammonium concentration in water
NI_e	y_2	g_2	nitrite concentration in water
OP_e	y_3	g_3	orthophosphates concentration in water
OR_e	y_4	g_4	other phosphates concentration in water
Z	y_5	g_5	grazer population
I	y_6	g_6	light intensity
T	y_7	g_7	temperature
$\rho_{in,FE}$	y_8	g_8	iron input in water
$\rho_{in,AM}$	y_9	g_9	ammonium input in water
$\rho_{in,NI}$	y_{10}	g_{10}	nitrite input in water
$\rho_{in,OP}$	y_{11}	g_{11}	orthophosphate input in water
$\rho_{in,OR}$	y_{12}	g_{12}	organic phosphate input in water
user	y_{13}	g_{13}	user defined variable on population level (e.g. silicate)
user	y_{14}	g_{14}	orthophosphate input in water
$\bar{\delta}$	y_{15}		total density of cells in number per liter
qu	y_{16}		used for grazer rate
Ed	y_{17}		used for irradiance at time t if not constant

Table C.2: Frequently used terms

Variable	Code	Meaning
$\frac{1}{\frac{a}{v(T)}+\frac{c_{FE}}{FE_e}}$	$z_{0,k}$	active transport for ecotype k
$\frac{1}{\frac{a}{v(T)}+\frac{c_{AM}}{AM_e}}$	$z_{1,k}$	active transport for ecotype k
$\frac{1}{\frac{a}{v(T)}+\frac{c_{NI}}{NI_e}}$	$z_{2,k}$	active transport for ecotype k
$\frac{1}{\frac{a}{v(T)}+\frac{c_{OP}}{OP_e}}$	$z_{3,k}$	active transport for ecotype k
$\frac{1}{\frac{a}{v(T)}+\frac{c_{OR}}{OR_e}}$	$z_{4,k}$	active transport for ecotype k
$V=\frac{m_{Pr}}{\sigma_{Pr}}+\frac{m_{Lp}}{\sigma_{e,Lp}}+\frac{m_{Ps}}{\sigma_{e,Ps}}$	$z_{5,k}$	Volume of cells of ecotype k
$A=(V)^{\frac{2}{3}}$	$z_{6,k}$	Surface area of cells of ecotype k
$f_{Ps}=\frac{1}{max(...)+\frac{1}{I_{m,Ps}}}$	$z_{7,k}$	functional response for polysaccharides, ecotype k
$f_{Lp}=\frac{1}{max(...)+\frac{1}{I_{m,Lp}}}$	$z_{8,k}$	functional response for lipids, ecotype k
$f_{Pr}=\frac{1}{max(...)+\frac{1}{I_{m,Pr}}}$	$z_{9,k}$	functional response for proteins, ecotype k

Table C.2, continued.

Variable	Code	Meaning
$g_{Ps} = \begin{cases} \kappa_{Ps,0}\frac{\frac{m_{Ps}}{E}}{\kappa_{Ps}+\frac{m_{Ps}}{E}} & \text{for} \bar{E} > 0 \\ \kappa_{Ps,0} & \text{for} \bar{E} = 0 \end{cases}$	$z_{10,k}$	function describing catabolism of polysaccharides for ecotype k
$g_{Lp} = \begin{cases} \kappa_{Lp,0}\frac{\frac{m_{Lp}}{E}}{\kappa_{Lp}+\frac{m_{Lp}}{E}} & \text{for} \bar{E} > 0 \\ \kappa_{Lp,0} & \text{for} \bar{E} = 0 \end{cases}$	$z_{11,k}$	function describing catabolism of lipids for ecotype k
$g_{Pr} = \begin{cases} \kappa_{Pr,0}\frac{\frac{m_{Pr}}{E}}{\kappa_{Pr}+\frac{m_{Pr}}{E}} & \text{for} \bar{E} > 0 \\ \kappa_{Pr,0} & \text{for} \bar{E} = 0 \end{cases}$	$z_{12,k}$	function describing catabolism of lipids for ecotype k
$\bar{L}(\delta, E_d(0)$	$z_{13,k}$	photosynthetic activity dependent on light availability
$v(T) = v(T_1^K)\exp(\frac{T_A^K}{T_1^K T^K}(T^K - T_1^K))$	$z_{14,k}$	temperature dependence
user	$z_{15,k}$	user defined (e.g. for silicate)
user	$z_{16,k}$	user defined (e.g. for silicate)

Notes: the functions g_{ϕ_s} in the table are the ones used with Euler's Method. They are replaced by the alternative formulations for Runge-Kutta's Method. In the simulations, $z_{15,k}$ was usually used for uptake of silicate.

C.2 Summary of Model Equations

All equations are summarized in this section. Equations are given in the original notation and in the vetor notation used in the computer code. Changes made for Runge-Kutta's method are not included in this summary.

C.2.1 Equations of Ecotypes

The equations in this section are for each ecotype.

Carbon pool equations:

$$\frac{dC_i}{dt} = \rho_{up,C} - \rho_{st,C} - \rho_{re,C}$$

where

$$\rho_{up,C} = L(I)A$$

$$\begin{aligned}\rho_{st,C} &= \mu_{C,Ps}[m_{0,Ps} f_{Ps}(\bar{E}, C_i, N_i) - g_{Ps}(\bar{E}, m_{Ps})] + [\mu_{C,Lp} m_{0,Lp} f_{Lp}(\bar{E}, C_i, P_i) \\ &\quad - g_{Lp}(\bar{E}, m_{Lp})] + [\mu_{C,Pr} m_{0,Pr} f_{Pr}(\bar{E}, C_i, F_i, N_i, P_i) - g_{Pr}(\bar{E}, m_{Pr})]\end{aligned}$$

$$\rho_{re,C} = j_C C_i$$

Computer code:

$$\begin{aligned}f_{1,k} &= z_{13,k} z_{6,k} - (m_{0,Ps} z_{7,k} - z_{10,k})\,\mu_{C,Ps} \\ &\quad - (m_{0,Lp} z_{8,k} - z_{11,k})\,\mu_{C,Lp} - (m_{0,Pr} z_{9,k} - z_{12,k})\,\mu_{C,Pr} - j_C x_{1,k}\end{aligned}$$

Nitrogen-Pool Equations

$$\frac{dN_i}{dt} = \rho_{up,N} - \rho_{st,N} - \rho_{ex,N}$$

where

$$\rho_{up,N} = \mu_{N,AM} \frac{1}{\frac{a}{v(T)} + \tau(AM_e)} n_{AM,A} A + \mu_{N,NI} \frac{1}{\frac{a}{v(T)} + \tau(NI_e)} n_{NI,A} A$$

$$\rho_{st,N} = \mu_{N,Pr} \left[m_{0,Pr} f_{Pr}(\bar{E}, C_i, F_i, N_i, P_i) - g_{Ps}(\bar{E}, m_{Pr}) \right]$$

$$\rho_{ex,N} = j_N \frac{N_i}{m_{Pr}}$$

Computer code:

$$f_{2,k} = \left[\mu_{N,AM} z_{1,k} n_{AM,A} + \mu_{N,NI} z_{2,k} n_{NI,A} \right] z_{6,k} - \left[m_{0,Pr} z_{9,k} - z_{12,k} \right] \mu_{N,Pr} - j_N \frac{x_{3,k}}{x_{8,k}}$$

Phosphorus-Pool Equations

$$\frac{dP_i}{dt} = \rho_{up,P} - \rho_{st,P} - \rho_{ex,P}$$

where

$$\rho_{up,P} = \mu_{P,OPH} \frac{1}{\frac{a}{v(T)} + \tau(OPH_e)} n_{OPH,A} A + \mu_{P,ORP} \frac{1}{\frac{a}{v(T)} + \tau(ORP_e)} n_{ORP,A} A$$

$$\begin{aligned} \rho_{st,P} &= \mu_{P,Lp} \left[m_{0,Lp} f_{Lp}(\bar{E}, C_i, P_i) - g_{Lp}(\bar{E}, m_{Lp}) \right] \\ &\quad + \mu_{P,Pr} \left[m_{0,Pr} f_{Pr}(\bar{E}, C_i, F_i, N_i, P_i) - g_{Pr}(\bar{E}, m_{Lp}) \right] \end{aligned}$$

$$\rho_{ex,P} = j_P \frac{P_i}{m_{Pr}}$$

Computer code:

$$\begin{aligned} f_{3,k} &= \left[\mu_{P,OPH} z_{3,k} n_{OPH,A} + \mu_{P,ORP} z_{4,k} n_{ORP,A} \right] z_{6,k} - \left[m_{0,Lp} z_{8,k} - z_{11,k} \right] \mu_{P,Lp} \\ &\quad - \left[m_{0,Pr} z_{9,k} - z_{12,k} \right] \mu_{P,Pr} \end{aligned}$$

Energy-Pool Equations

$$\frac{d\bar{E}}{dt} = \rho_{up,ATP} - \rho_{st,ATP} - \rho_{ma,ATP} + \rho_{ex,C}\mu_{ATP,C}$$

where

$$\begin{aligned}
\rho_{up,ATP} &= \mu_{ATP,CO_2}\rho_{up,CO_2} + \mu_{ATP,NI}\frac{1}{\frac{a}{v(T)} + \tau(NI_e)}n_{NI,A}A \\
&\quad + \mu_{ATP,OR}\frac{1}{\frac{a}{v(T)} + \tau(OR_e)}n_{OR,A}A \\
\rho_{st,ATP} &= \mu_{ATP,Ps}\left[m_{0,Ps}f_{Ps}(\bar{E}, C_i, N_i) - g_{Ps}(\bar{E}, m_{Ps})\right] \\
&\quad + \mu_{ATP,Lp}\left[m_{0,Lp}f_{Lp}(\bar{E}, C_i, P_i) - g_{Lp}(\bar{E}, m_{Lp})\right] \\
&\quad + \mu_{ATP,Pr}\left[m_{0,Pr}f_{Pr}(\bar{E}, C_i, F_i, N_i, P_i) - g_{Pr}(\bar{E}, m_{Pr})\right]
\end{aligned}$$

$$\rho_{ma,ATP} = M_0 V$$

$$\rho_{ex,C}\mu_{ATP,C} = j_{ex}C_i\mu_{ATP,C}$$

Computer code:

$$\begin{aligned}
f_{4,k} &= \mu_{ATP,CO_2}z_{12,k} - M_0 z_{5,k} - \left[m_{0,Ps}z_{7,k} - z_{10,k}\right]\mu_{ATP,Ps} + \\
&\quad + \left[\mu_{ATP,NI}z_{2,k}n_{NI,A} + \mu_{ATP,OR}z_{4,k}n_{OR,A}\right]z_{6,k} - \\
&\quad - \left[m_{0,Lp}z_{8,k} - z_{11,k}\right]\mu_{ATP,Lp} - \left[m_{0,Pr}z_{9,k} - z_{12,k}\right]\mu_{ATP,Pr}j_C x_{1,k}\mu ATP, C
\end{aligned}$$

Reserve Polysaccharides Equations

$$\frac{dm_{Ps}}{dt} = \rho_{st,Ps}$$

where

$\rho_{st,Ps} = m_{0,Ps} f_{Ps}(\bar{E}, C_i, N_i) - g_{Ps}(\bar{E}, m_{Ps})$

Computer code:

$f_{5,k} = m_{0,Ps} z_{7,k} - z_{10,k}$

Resrve Lipids Equations

$$\frac{dm_{Lp}}{dt} = \rho_{st,Lp}$$

where

$\rho_{st,Lp} = m_{0,Lp} f_{Lp}(\bar{E}, C_i, P_i) - g_{Lp}(\bar{E}, m_{Lp})$

Computer code:

$f_{6,k} = m_{0,Lp} z_{8,k} - z_{11,k}$

Proteins and Structure Equations

$$\frac{m_{Pr}}{dt} = \rho st, Pr$$

where

$\rho st, Pr = m_{0,Pr} f_{Pr}(\bar{E}, C_i, F_i, N_i, P_i) - g_{Pr}(\bar{E}, m_{Pr})$

Computer code:

$f_{7,k} = m_{0,Pr} z_{9,k} - z_{12,k}$

C.2.2 Substance Concentration Equations

Substances in the water:

Iron Concentration Equations

$$\frac{dFE_e}{dt} = \rho_{in,FE} - \sum_{species} \rho_{up,FE}\delta + \sum_{species} \rho_{ex,FE}\delta$$

where

$\rho_{in,GLU}$: iron input in water

$\sum_{species} \rho_{up,FE} = \sum_{species} \frac{1}{\frac{a}{v(T)}+\tau(FE_e)}\, n_{FE,A}\, A\delta$

$\sum_{species} \rho_{ex,FE} = \sum_{species} j_{FE} \frac{FE_i}{m_{Pr}}\delta$

Computer code:

$g_8 = y_{16} - \sum_{k=1}^{n} x_{0,k} \left[z_{0,k} n_{FE,A} z_{6,k} - j_{FE} \frac{x_{2,k}}{x_{8,k}} \right]$

Ammonium Concentration Equations

$$\frac{dAM_e}{dt} = \rho_{in,AM} - \sum_{species} \rho_{up,AM}\delta + \sum_{species} \rho_{ex,AM}\delta$$

where

$\rho_{in,AM}$: ammonium input in water

$\sum_{species} \rho_{up,AM} = \sum_{species} \frac{1}{\frac{a}{v(T)}+\tau(AM_e)}\, n_{AM,A}\, A\delta$

$\sum_{species} \rho_{ex,AMM} = \sum_{species} j_{AM} \frac{AM_i}{m_{Pr}\mu_{AM,N}}\delta$

Computer code:

$g_9 = y_{17} - \sum_{k=1}^{n} x_{0,k} \left[z_{1,k} n_{AMM,A} z_{6,k} - j_{AM} \frac{x_{3,k}}{x_{8,k}\mu_{AM,N}} \right]$

Nitirte Concentration Equations

$$\frac{dNI_e}{dt} = \rho_{in,NI} - \sum_{species} \rho_{up,NI}\delta$$

where

$\rho_{in,NI}$: nitrite input in water

$\sum_{species} \rho_{up,NI} = \sum_{species} \frac{1}{\frac{a}{v(T)}+\tau(NI_e)}\, n_{NIT,A}\, A\delta$

Computer code:

$g_{10} = y_{18} - \sum_{k=1}^{n} [x_{0,k} z_{2,k} n_{NI,A} z_{6,k}]$

Orthophosphate Concentration Equations

$$\frac{dOP_e}{dt} = \rho_{in,OP} - \sum_{species} \rho_{up,OP}\delta$$

where

$\rho_{in,OP}$: orthophosphate input in water

$\sum_{species} \rho_{up,OPH} = \sum_{species} \frac{1}{\frac{a}{v(T)}+\tau(OP_e)}\, n_{OP,A}\, A\delta$

Computer code:

$g_{11} = y_{19} - \sum_{k=1}^{n} [x_{0,k} z_{3,k} n_{OPH,A} z_{6,k}]$

Organic Phosphate Concentration Equations

$$\frac{dOR_e}{dt} = \rho_{in,OR} - \sum_{species} \rho_{up,OR}\delta + \sum_{species} \rho_{ex,OR}\delta$$

where

$\rho_{in,OR}$: organic phosphate input in water

$\sum_{species} \rho_{up,OR} = \sum_{species} \frac{1}{\frac{a}{v(T)}+\tau(OR_e)}\, n_{OR,A}\, A\delta$

$\sum_{species} \rho_{ex,OR} = \sum_{species} j_{OR} \frac{OR_i}{m_{Pr} \mu_{OR,P}} \delta$

Computer code:

$g_{12} = y_{20} - \sum_{k=1}^{n} x_{0,k} \left[z_{4,k} n_{OR,A} z_{6,k} - j_{OR} \frac{x_{4,k}}{x_{8,k} \mu_{OR,P}} \right]$

C.2.3 Population Equations

There are one difference equation and one differential equation on the population level.

Population Equation

$$\delta(t + \triangle t,\ m_{Ps} + \rho_{st,Ps} \triangle t,\ m_{Lp} + \rho_{st,Lp} \triangle t,\ m_{Pr} + \rho_{st,Pr} \triangle t)$$
$$= \delta(m) - \left[\frac{1}{z} V(m) + q(V(m)) + D(m) \right] \delta(t, m) \triangle t$$

Computer code:

$x_{0,k}(t + \triangle t) = x_{0,k} + \left[\frac{1}{z} z_{5,k} - q(z_{5,k}) \right] x_{0,k}(t) \triangle t$

Grazer Population Equation

$$\frac{dZ}{dt} = (MI)\ (AE) \frac{\sum_{species} \left[\sum_{ecotypes} q(x) \delta(t, x) \right]}{\sum_{species} \left[\sum_{ecotypes} q(x) \delta(t, x) \right] + \vartheta_p} Z - \theta\ Z^r$$

Computer code:

$$g_5 = (MI)(AE) \frac{\sum_{k=1}^{n} q(z_{5,k}) x_{0,k}}{\sum_{k=1} n(q(z_{5,k}) x_{0,k}) + \vartheta_p} y_5 - \theta\ y_5^r$$

Vita

Jochen Hurlebaus was born in Stuttgart, Germany, on September 15, 1971. He attended public elementary school in Urbach, Germany, between August 1978 and July 1982, before entering Gymnasium in Schorndorf, Germany, where he finished his Abitur in May 1991 with a prize for excellent performance. Instead of joining the army for the required year, he has chosen to work for the Munich Wildlife Society in Oberammergau, Germany, as a civil servant, where he had his first contact with mathematics and ecology. He worked there from July 1991 to September 1992. In October 1992 he entered University of Kaiserslautern, Germany, working on a major in Mathematics with a minor in Physics. He achieved his Vordiplom in July 1994. During his three years in Kaiserserlautern he also increased his knowledge in ecology and statistics while working as scientific assistant for the Munich Wildlife Society from August 1993 until October 1993, and for the Forest Research Inistitut in Trippstadt, Germany, from January 1995 until April 1995.

In August 1995, he enterd the Masters program in Mathematical Ecology at the University of Tennessee in Knoxville, Unites States of America. He was working as a teaching assistant and associate between January 1996 and May 1997. In April 1997, he was awarded the Randall Cline Award, which is a yearly award for the best master thesis in the department. He successfully defended his master thesis in Mathematical Ecology in April 1997, and will receive his degree in August 1997.